INDEX

CHAPTER I

Electrochromism

CHAPTER II

Solid thermoplastic laminable electrochromic film

CHAPTER III

Kinetic

CHAPTER IV

Electrical charatterization of electrochromic films extended

INTRODUCTION

The development of large area electrochromic windows is being actively pursued by a number of companies[1-4] and research organisations[5,6]. An extensive review of major contributors and potential markets for electrochromic windows has been presented in a report by SRI[7]. Interest on EC materials has grown during the last decades, especially because of their application in building automation as smart windows[8,9]. The energy savings using them in smart buildings has been established in around 20%[10], but it could reach 50% in cold climates[9]. The promising results in some buildings impel not only their fabrication, but also the research for new materials and drivers, as well as efforts of their electro-optical characterization for new applications like smart glasses or displays [11,12] Electrochromic anti-glare car rear-view mirrors have already been commercialized. The electrochromic materials can be used still in controllable light-reflective or light-transmissive devices for optical information and storage, sunglasses, protective eyewear for the military, controllable aircraft canopies, glare-reduction systems for offices [13,14,15]. More recently they have been used as electroactive layers to modify electrode surfaces[16,17] and as electrode materials for batteries. Generally, there are two kinds of the EC devices: (1) coloration due to the intercalation of small ions into the thin oxide films such as WO_3, NiO and V_2O_5[18], and (2) coloration due to reduction or oxidation of redox chromophores including some organic dye molecules. Since the time for inserting or deinserting small ions into the EC materials is relatively long, type 1 devices are not suitable for application in displays. For type 2 devices, though, a monolayer of redox chromophore can be colored/decolored with relatively rapid switching time is still not sufficient for practical applications[19]. Our device is different from type 1 and 2, it is based on self-standing materials. A new kind of solid plastic EC film has been prepared, were the EC molecules and plasticizers are introduced into preformed

solid thermoplastic polymers. These substances are exposed to a sample thermal blending process. After the mixture is cooled at room temperature, a homogeneous solid film, with EC properties and great adhesion ability to a glassy support, is obtained. This preparation has allowed a particularly easy preparation of ECD suitable for large-scale applications, by simple lamination of the film between conductive glasses. The main purpose of this thesis has been to study this new electrochromic films. In the first chapter will discuss the chemical and physical-chemical properties of the electrochromic molecules in particular bipyridilium systems and will analyze the mechanisms that affect the internal systems electrochromic.

In the second chapter the characterization of the electro optical properties of new ECD is presented. In particularly it will be described the research that has been devoted to analyze the effect of the concentration of the different components and the effect of the thickness on the films EC under object of study. Then chap. 3 will concern about the kinetic study, performed in order to understand the mechanisms underlying the coloration process of the device. The kinetic processes occurring in the EC film is analyzed deriving the equations which describe the coloration processes in the bulk of the film and in the neighbouring of the electrodes.

The coloration and the bleaching of large area electrochromic devices is a complex process, involving electrochemical processes at two electrodes[20] and voltage drops along the transparent conducting electrodes which change the device potential at each point along the device[21-23]. This results in different coloration voltages at each point of the device, whether the device is switched using a constant voltage or a constant current waveform. In chapter 4 the characterization of a large area device, from the electrical point of view, is presented. It is described the schematic electric model compatible with the experimental results, that we have built up with the purpose of finding out the changes in the parameters of the film or the conductive glasses that can minimize the differences of the local potential and allow the film to keep a uniform coloration throughout its extension at any time.

REFERENCES

[1] J. Gallego, Eurosun 96, Pilkington World Wide Web Site: http://www.pilkington.com/custfoco/building/index.htm.

[2] G. Tulloch, Skryabin, G. Evans, J. Bell, *Proc. SPIE* 3136, **1997,** 426-432

[3] J. Nagai, G. D. mcMeeking, Y. Saitoh, *Solar Energy Mater. Solar Cells* 56, **1999,** 309-319

[4] N. Sbar, M. Badding, R. Budziak, K. Cortez, L. Laby, L. Michalski, T. Ngo, S. Schulz, K. Urbanik, *Solar Energy Mater. Solar Cells* 56, **1999**, 321-341

[5] B. Munro, S. Kramer, P. Zapp, H. Krug, H. K. Schmidt, Institut fur nneue Materialien (FRG), *Proocedings of SPIE*, Vol. 3136, p. 470-479, **1997**

[6] A. Azens, L. Kullman, *Solar Energy Mater. Solar Cells* 56, **1999,** 487

[7] Rice Cabiac Smart Glass: seeking a Clear View of the Future, *SRI report* D98-2145, **1998**, 26p.

[8] C.G. Granqvist, A. Azens, P. Heszler, L.B. Kish, L.Osterlund, *Sol energy Mater. Sol. Cells*. 91, **2007**, 355-365

[9] M.L. Persson, *Ph.D.Thesis*, Uppsala University, **2006**

[10] A.Azens, C.G. Granqvist, *Electrochim. Acta* 46, **2001**

[11] E:S: Lee, D.L. DiBartolomeo, S.E. Selkowitz, *Energy Buildings* 38, **2006** 30-44

[12] C.G. Granqvist, *SPIE Newsroom*, 10.1117/2.1200602.0140,**2006**

[13] P.M.S. Monk, R.J. Mortimer, D.R. Rosseinsky, Electrochromism: *Fundamentals and Applications*, VCH, Weinheim, **1995**

[14] M. Green, *Chem. Ind*. 17, **1996**, 641

[15] R.J. Mortimer, *Chem. Soc. Rev* 26,**1997**,147

[16] G.Inzelt, in *'Electroanalytical Chemistry'*, vol.18 (ed. A. J. Bard), Marcel Dekker, New York **1994**

[17] G. S. Ostrom and D. A. Buttry, *J. Chem*. 99, **1995,** 15 236

[18] (a) K.C.Cheng, F.R. Chen, J.J. Kai, *Sol. Energy Mater. Sol. Cells* **2006**,90,1156. (b) A. Ghicov, H. Tsuchiya, R. Hahn, J.M. Macak, A.G. Munoz, P. Schmuki, *Electrochem. Commun*. **2006**, 8, 528. (c) A. Azens, G. Vaivars, M. Veszelei, L. Kullman, C.G. Granqvist, *J. Appl. Phys.* **2001**, 89, 7886. (d) C.C. Liao, F.R. Chen, J.J. Kai, Sol. Energy Mater. Sol. Cells 2006, 90, 1147

[19] R. Cinnsealach, G. Boschloo, S. N. Rao, D. Fitzmaurice *Sol. Energy Mater. Sol. Cells*. **1999**, 57, 125

[20] B. W. Faughnan, R. S. Crandall, i: J. I. Pankove (Ed.), topics in Applied Physics devices, Vol. 40, Springer-Verlag, New York, **1980**

[21] I.L. Skryabin , J.M.Bell, G.B. Smith "optimisation of conductivity of transparent conductor layers in electrochromic device", Paper presented at *BrisPhys'94, 11th Congress of the Australian Institute of Physics*, Brisbane, July **1994**.

[22] D.R. Macfarlane, J. Sun, M. Forsyth, J.M. Bell, L.A. Evans, I.L. Skryabin, Polymer electrolytes for electrochromic windows applications, *Solid State Ionics* 86-88, **1996,** 959-964

[23] I.L. Skryabin, J.M. Bell, G. Volgeman, "Twards a model of large area electrochromic device operation", in: Proceedings of the 3rd Symposium on Electrochromic Materials, International Electrochromic Society, 96-24, **1996**, p. 396

CHAPTER I

Electrochromism

Introduction

An electroactive species often exhibits new optical absorption bands in accompaniment with an electron-transfer or redox reaction in which it either gains or loses an electron. Such colouration was first termed "electrochromism" in 1961 by Platt[1] whose discussions were amongst the first published. Byker has discussed the historical development of electrochromism[2].

Many simple species exhibit electrochromism. To take a laboratory example, the ferrocyanide ion in aqueous solution is pale yellow in colour, but on electrochemical oxidation:

$$\underset{\text{(pale)}}{\left[Fe^{II}(CN)_6\right]^{4-}} \rightarrow \underset{\text{(yellow)}}{\left[Fe^{III}(CN)_6\right]^{3-}} + e^-_{\text{electrode}} \qquad (1.1)$$

a pool brilliant yellow forms around the electrode, and thence diffuses into the bulk. The change in colour is directly attributable to the oxidation of iron(II) to iron(III) in the complex. A somewhat different case is ferrous ion in aqueous solution , in the presence of thiocyanate with

which Fe^{2+} is only weakly complexed. Initially the solution is colourless, but a brilliant blood-red colour appears after oxidation on the formation of electro-generated iron (III). In this case, the colour may not be directly electro-generated, but is possibly due to interaction between electro-generated Fe^{3+} and the electro-inactive CNS^- ion in solution: it is the iron(III) thiocyanate charge-transfer complex that ultimately provides the colour. In this context, a "charge-transfer" species is one in which a photo-effected transfer of charge within the species, sometimes between species, evokes colour, by "optical charge-transfer".

The simplest electrochromic light modulators have two electrodes directely in the path of the light beam. If both electrodes bear an electrochromic layer, then the colour formation within the two must operate in a complementary sense, which can be illustrated here with the example of WO_3 and vanadium pentoxide: WO_3 becomes strongly coloured (blue) when oxidised. By contrast, V_2O_5 is a rich brown/yellow colour when oxidised, yet faintly coloured (blue) when reduced. In an electrochromic device (ECD) constructed with these materials, one oxide layer is present in its reduced form while the other is oxidised; thus the operation of the device is

$$\overbrace{WO_3 + M_xV_2O_5}^{\text{bleached}} \rightarrow \overbrace{M_xWO_3 + V_20_5}^{\text{coloured}} \qquad (1.2)$$

(pale yellow) (pale blue) (blue) (brown)

The tungsten-oxide is termed the *primary* electrochrome since it is the more strongly coloured species and, in this example, V_2O_5 acts as the *secondary*[3].

1.1 Electrochromic parameters

Visible light can be viewed as electromagnetic waves of wavelength 420 nm (violet) to 700 nm (red) or equivalently[4] as particulate photons of energy 4.7×10^{-19} J (violet) to 2.8×10^{-19} J (red). The colors cited refer to light directly entering the eye. However, color is a subjective visual impression involving retinal responses of the eye to particular wavelengths of the impinging light (table 1.1). Light comprising all visible wavelengths appears white. Reflected colors result from absorption by the reflecting material of some of these wavelengths, that is, from subtraction from the full wavelength range comprising incident white light. In with light, the perceived color of a material is the complementary color of the light it absorbs (figure 1.1)[5,6]. A single wavelength of absorption is encountered only with single-atom or single-ion photon absorption, the photon energy being transformed into internal electronic energy by the excitation of an electron between precise energy levels associated with the two orbitals accommodating the electron before and after the photon absorption, or "transition" as it is termed. In molecules the energy levels involved are somewhat broadened by contributory vibrational (and to a lesser extent, rotational) energies. Thus, on light absorption, transitions occur between two "spreads" of energy levels, (of, however, narrow spread) allowing the absorption of photons with a restricted range of energies, that is, of light a restricted range of wavelengths, giving an absorption *band*. The maximum absorption, roughly in the centre of such a band, corresponds to the "average" transition.

The target molecule here is called a *chromophore,* and when the color resulting from absorption is evoked electrochemically, an *electrochromophore* or more briefly, an *electrochrome.* The absorption spectrum of a substance represents the relative intensity (relative number of photons) absorbed at each wavelength.

	λ/nm	λ^{-1}/cm^{-1}	$10^{14}\nu/s^{-1}$	hν/eV	$10^{19}h\nu/J$	LhNkJmol^{-1}
	750	13,300	4.00	1.65	2.65	159
Red						
	635	15,800	4.72	1.95	3.13	1.88
Orange						
	596	16,800	5.03	2.08	3.33	200
Yellow						
	580	17,200	5.17	2.14	3.42	206
Green						
	520	19,200	5.77	2.38	3.82	230
Blue						
	470	21,300	6.38	2.64	4.23	255
Indigo						
	440	22,700	6.81	2.82	4.51	272
Violet						
	390	25,600	7.69	3.18	5.09	307
UV						

Table 1.1 *Wavelength and energy ranges for perceived colours of emitted light. The numbers above and below each colour represent its range.*

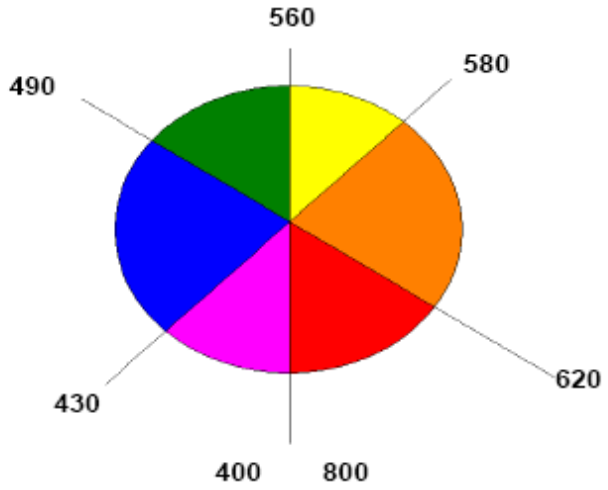

Fig. 1.1 *Approximate wavelength (in nm) of reflected colours. Colours in directly opposite segments are called complementary.*

The Beer-Lambert law[7] for optical absorption relates the absorbance, expressed as log of the ratio of the intensities, to the concentration *c* of chromophore and optical path length *l* through the sample:

$$A = \log\left(\frac{I_0}{I}\right) = \varepsilon c l \qquad (1.3)$$

The proportionality factor ε is the molar extinction coefficient or molar absorptivity of the absorbing species. From the preceding account, it should be clear that ε will vary with wavelength λ since A does, and it is the parameter quantifying the strength of the optical

absorption at each wavelength. ε(λ) (the value at wavelength λ) and ε_{max} (the value at the maximum, often written without subscript) will depend on solvent, or solid matrix, to a greater or lesser extent. When the absorption results from optical CT, Kosower's parameter $Z^{[8]}$, which is the energy (inverse wavelength) for the maximum absorption of a particular chromophore in a given solvent, varies with solvent in a manner followed proportionately by other similar chromophores, Z is a useful indicator of solvation in the chromophore-solvent system involved, which will clearly determine the transition energy, that is, where the absorption maximum occurs. The absorption can thus arise from photo-excitation of an electron from a lower (or ground-state) energy level to a higher one either in the same molecule, which is an *intramolecular excitation*, or within a neighboring moiety, which involves an intermolecular interaction termed *optical charge-transfer*. The redistribution on photon absorption of electron density in the absorbing species is more or less exactly depends on the *transition moment* M. M is measured from the area of the absorption band; the molar absorptivity at the maximum is commonly taken as being proportional to M.

The most intense optical absorptions are often a consequence of optical CT, since like intramolecular electronic transitions these are processes "allowed" by wave mechanical selection rules for spectral transitions. In any electrochromic system, a quantitative measure of the intensity of the color change is required. That commonly used is the contrast ratio CR:

$$CR = \frac{R_0}{R_x} \qquad (1.4)$$

where R_x is the intensity of light diffusely reflected through the colored state of the display, and R_0 is the intensity of light diffusely reflected from the bleached (uncolored) state from a (diffuse) white black plate[9].

In transmission mode, the optical absorption of an electrochromic film is related to the injected per unit area Q (assuming no side reactions) by an expression akin to the Berr-Lambert law, since Q is proportional to the number of color centers:

$$A = \log\left(\frac{I_0}{I}\right) = \eta Q \qquad (1.5)$$

where η is the "coloration efficiency" of the film. A CR of less than 2 or 3 is not easily perceived by eye, and as high a value as possible is desirable. Commonly CR is expressed as ratio, and is best measured at the wavelength of maximum absorption by the colored state.

Where there is a great difference in color between the two redox states, but both are highly colored, then the contrast is not perceived to be great. In this case, the CR is highly wavelength dependent.

The coloration efficiency η is related to an optical absorbance change ΔA via equation (1.5), and to the linear absorption coefficient α, film thickness d and charge injected Q per unit area, by the relationship[10]:

$$\eta = \left(\frac{\alpha d}{Q}\right) = \frac{\Delta A}{Q} \qquad (1.6)$$

In the use of these equations, it is assumed that all optical effects are absorptive, that only a single absorbing species is effective at the wavelength chosen for monitoring, and that the Lambert-Beer law is obeyed. η may be regarded as that electrode area which may be colored to unit absorbance by unit change. η is designated as positive for cathodically induced coloration (by electron gain, or reduction) and negative for anodic color formation (by electron loss, i.e. oxidation).

If η_p is the coloration efficiency of the primary electrochromophore, and η_s that of the secondary, then the coloration efficiency η_o of the complete ECD device is obtained as $\eta_0=(\eta_p - \eta_s)$. For the most intense electrochromism, the parenthesized entity should be maximized, that is, a large change in A is required for injection of a small charge. This may be achieved in two ways, either by using a large η_p together with an η_s of the opposite sign (i.e. complementary electrochromism), or by using a combination of large η_p and small η_s both of the same sign. In other words, both electrodes colorize simultaneously or unwanted color in one electrode is feeble.

In general, organic electrochromes exhibit a greater η than do inorganic species because the molar absorbivities of the former are usually higher.

The write-erase efficiency is the percentage of the originally formed coloration that may be subsequently electro-bleached; it can be conveniently be expressed as a ratio of absorbance changes. For a successful display, the efficiency should closely approach 100%. Species remaining in solution in both colored and uncolored states, such as methyl viologen, diffuse from the electrode surface after electro-coloration. Since bleaching of such an ECD requires all the colored materials to diffuse back to the electrode for electrooxidation, which relatively slow process, the write-erase efficiency on a practical time-scale is poor for all-solution systems.

The time required for an ECD to color from its bleached state to (or vice versa) is termed its response time τ. For most devices, τ values are of the order of few seconds. For ECDs in general, τ is slower than for either LCDs or CRTs, usually because of the necessity for diffusion, either of charged species through the electrode film or, for all-solution systems, of the electrochrome to the electrode. In applications such as electrochromic windows or mirrors, response times of seconds can be tolerated, but if devices such as optical switches or television screen are envisaged, then very fast response times will be necessary.

Unfortunately, there is no consistency in the criteria employed for determining τ: it may be the time necessary for some fraction (arbitrary or defined) of the color to form, such as indicated by a particular increment of optical density, or the time for all or part of the charge to be injected.

Another important electrochromic parameter of ECD is its stability. When an ECD is continually cycled between its colored and bleached states, device failure will eventually occur resulting from physical changes in solid phases or from chemical side reactions. The *cycle life* is a measure of its stability, being the number of cycles possible before such failure. The cycle life is a complicated function of the coloration required in the cycle: the cycle life generally decreases if wide changes in composition are required, that is if the quantity of charge injected or removed is large.

1.2 Electrochemistry and mechanism of electrochromic systems

The electron-transfer process during coloration is denoted by *anodic* or *cathodic:* cathodically coloring materials form color when reduced at an electrode made negative, a *cathode*, and anodically coloring electrochromes are colored at an *anode,* or positive electrode.

The electrode potential for the electrochromic redox couple is related to the ratio of their respective concentrations by a form of Nerst equation:

$$E_{Ox,Red} = E^{0}_{Ox,Red} + \frac{RT}{nF}\ln\left(\frac{[Ox]}{[Red]}\right) \qquad (1.7)$$

where concentrations are denoted by square brackets, *R* is the gas constant, *F* the Faraday constant, *T* the thermodynamic temperature and *n* is the number of electrons involved in the electron transfer reaction. E^{0} is the *standard electrode potential,* and is defined as the electrode potential measured at standard pressure and temperature, with both Ox and Red present at unit concentration (or formally and more accurately, at unit activity[11]).

In an electrochromic cell current flows when appropriate ranges of potentials are applied. Such current will comprise two components, faradaic and non-faradaic. The former current is directly linked with the sum of the electron-transfer reactions effected, and the charge (current-time integrated) indicates directly the extent of the cell reaction, since faradaic current involves that charge which yields product.

Electrochromic operation involves the quantity of electrochrome that changes redox state on passage of current, as governed by Faraday's laws, which are as follows.

1. The number of moles of species formed at an electrode during electrode reaction is proportional to the charge passed;

2. A given charge liberates (or deposits) masses of different species in the ratio of their "equivalent weights" (relative molar masses divided by the number of electrons involved in the electrode reaction).

Non-faradaic current is caused by processes such as charging of the electric double layer at the electrode-solution interface (a local separation of unreactive-solute ions into layers of anion and cation partly governed by application of potential, which results in excess accumulation of ions of one particular charge sign at interfaces). In precise mechanistic descriptions of electrode processes, double layer effects need to be taken into account; this may be complicated.

The rate of electron-transfer at an electrode is a function of the gradient of electric potential applied to the electrode, and follows the Butler-Volmer equation[11,12] which, for a reduction reaction Ox + $ne^- \rightleftharpoons$ Red is

$$i = nFAk_f c_R \left(\exp\left(-\alpha_f n\Theta\eta\right)\right) - nFAk_b c_O \left(\exp\left(\alpha_b n\Theta\eta\right)\right) \qquad (1.8)$$

where, for brevity, Θ = F/RT; c_O is the concentration of the oxidised form of the electroactive species (starting material) and c_R that of the reduced form; α is a fraction termed the transfer coefficient (subscripted f and b for forward and back reaction respectively), itself a measure of the symmetry of the energy barrier to the electron transfer[1]; η is the overpotential, ($E - E_{OC}$),

where E is the potential applied to the electrode and E_{OC} is the zero-current electrode potential. k_f and k_b are the rate constants of electron transfer for the forward and back processes.

1.2.1 Semiconducting electrodes

In the construction of electrochromic display devices, the substrate most commonly used as the optically transparent electrode (OTE) is indium tin oxide (ITO) as a thin film on glass. The thickness of the ITO layer is typically 0.3 μm. Indium(III) oxide, when doped whit *ca.* 8% tin(IV) oxide, is a semiconductor[13] of conductivity *ca.* 8 x 10^{-4} Scm^{-1}, so the thickness and exact conductivity of the ITO layer will affect the ECD response time. The rate of supply (flux *j*) of electrons through the conductor and corresponding current *i* are obtained from the general applicable equations:

$$i = nAve \qquad \text{and} \qquad j = nv \tag{1.9}$$

where *n* is the number density of charge carriers, *A* the cross-sectional area of the conductor, *v* the electronic velocity and *e* the electronic charge. In thin-film indium tin oxide (ITO), the number of charge carriers is relatively small, restricting the rate of charge uptake or loss of the ITO/electrochrome interface. However, some authors believe that the response time of an ECD device with very thin films of ITO depends rather on the rate of electron transport, that is, *v*, through the ITO[14,15].

1.2.2 Mass transport

Before the electron-transfer reaction can occur, of necessity material must move from the solution bulk and approach close to an electrode. This movement is "mass transport", and proceeds via three separate mechanisms: migration, convection and diffusion. Mass transport is formally defined as the flux j_i of electroactive species *i* to an electrode, as defined in the Nerst-Planck equation:

$$j_i = \mu_i c_i \left(\frac{\partial \phi}{\partial x} \right) + c_i \bar{v}_i - D_i \left(\frac{\partial c_i}{\partial x} \right) \qquad (1.10)$$

migration convenction diffusion

where μ_i is the ionic mobility of the species *i*; Φ is the strength of the electric field, *iv* is the velocity of solution, and D_i and c_i are respectively the diffusion coefficient and concentration of species *i*. Convection will not concern us further since it is irrelevant for solid electrolytes and otherwise uncontrolled in other ECDs.

Migration is the movement of ions through solution or solid in response to an electric field, an anode attracting any negatively charged anions, the cathode attracting the cations. For liquid electrolytes containing an excess of unreactive ionic salt, migration may be neglected since the transport number of the electroactive material becomes negligibly small. Migration is an important form of mass transport for ionic movement within solid polymer electrolytes or solid-solution electrochromic layers since transport numbers of the electroactive species become

appreciable[15]. The phenomenon of electrode "polarization" by excess unreactive electrolyte (the buildup of concentration of oppositely-charged electrolyte ions at an electrode) brings about diminution then suppression of migration; diffusion is the only remaining means of approach to the electrode available to a possibly electroactive species, as follows.

Of particular interest to any kinetic study is the diffusion coefficient *D* of the diffusing species, being representative of its spontaneous motion. Diffusive behavior obeys Fick's laws[11,12], the first being for the flux j_i,

$$j_i = -D_i\left(\frac{\partial c_i}{\partial x}\right) \qquad (1.11)$$

where $(\partial c_i/\partial x)$ is the concentration gradient, the change in concentration of species *i* per unit distance. In electrochemical processes, $(\partial c_i/\partial x)$ arises (i.e. is non-zero) because some of the electroactive species is consumed around the electrode; diffusion is evoked by subsequent concentration gradient.

Fick's second law describes the time dependence of diffusion:

$$\left(\frac{\partial c_i}{\partial t}\right) = D_i\left(\frac{\partial^2 c_i}{\partial x^2}\right) \qquad (1.12)$$

The required integration of the second order differential equations often leads to difficulty in the accurate modeling of diffusive systems. However, a useful approximate solution to Fick's second law gives

$$l = \sqrt{D_i t} \qquad (1.13)$$

where D_i is the diffusion coefficient of species *i*, and *t* is the time required for species *i* to move a distance *l*. Another indicator of the rate of ionic movement is the ionic mobility μ (velocity *v* divided by driving field), which is related to the diffusion coefficient D by the Nernst-Einstein equation

$$\frac{D}{\mu} = \frac{k_B T}{ze} \qquad (1.14)$$

where symbols have their usual electrochemical meanings and k_B is the Boltzmann constant.

When the impressed potential of an electrode is stepped from a value giving zero current to one at which the current can reach a maximum, then all the electroactive material at the electrode-solution interface will undergo electrochemical change "instantly". Electroactive material from the solution bulk then diffuses toward the electrode, coming (diffusing) from successively further distances from the electrode. The flux at the electrode therefore decreases with time. The Cottrell equation[16] describes this current/time response as

$$i = nFA\sqrt{\frac{D}{\pi t}} \qquad (1.15)$$

The Cottrell equation is a convenient means of determining diffusion coefficients of solution-phase species[11].

1.2.3 Voltammetry

In electrochemistry of equilibrium (zero-current) the prospect of transfer of electron remains latent and the amounts of electrochrome present do not change, and thus study of the actual electrochromic coloration reaction is precluded. To allow these studies, *dynamic* electrochemistry is used, in which current is passed in a controlled way, by applying a potential E to a particular electrode that is different from the steady value, which we know re-label E_{OC}. The subscript OC means "open circuit" (implying conjunction only to a voltmeter); E_{cell} is equivalently an open-circuit or zero-current value.

Voltammetry is the most common of these dynamic techniques and is useful for discerning rates and mechanism, in addition to the thermodynamic data related to E_{cell} and E^{o} usually obtained at zero current or open circuit. Processes occurring at one electrode are monitored by observing the current change when the potential applied to that electrode (actually between the electrode and the counter-electrode) is varied steadily through a range which evokes an electron-transfer process. The current is recorded as a function of the potential impressed on the electrode. The

potential is varied steadily, the rate *dE/dt* being kept constant know a either the *scan rate* or the *sweep rate, v.*

The electrode at which the electrochemical changes of interest occur is called the *working electrode,* WE. In order that the potential at the WE be known, the potential difference *E* between the WE and a third *reference* electrode, RE, is taken. The saturated calomel electrode (SCE) is usually employed as reference. The scan rate is of course referred to the RE.

In equilibrium (zero-current) electrochemical experiments, voltages between the WE and RE are measured via a voltmeter, and the potential recorded as a function of the externally varied concentration of the electroactive species present, according to the Nernst equation (1.7). by contrast, during voltammetry, compositions at electrodes are perturbed by the passage of charge at electrolyte/working electrode interface when electrode reactions occur; while minimum perturbation occurs in electro-analytical experiments, quite substantial changes generally occur in electrochromic processes. If current were to pass through the RE, then the electrode composition would alter and the electrode potential of the RE would change to give inaccurate potential measurement; in addition, the simple passage of current itself shifts the potential of the electrode. For these reasons, no charge can be allowed to flow through the RE. A third electrode, the *counter electrode,* CE, is therefore used to complete the current-flow circuit, to obviate the apparent paradox of requiring current passage at the WE while using a zero-current RE. As the third electrode is needed only because current must flow at the WE, the nature and composition of the counter electrode are largely irrelevant to the operation of a voltammetric cell. The potential of the CE is not monitored although electrode reactions must clearly take place at the CE if current is to flow; if oxidation occurs at the WE then reduction occurs at the CE, and vice versa, hence current. Figure 1.2 illustrate the connections.

The control of voltage across the working-electrode/counter-electrode pair is achieved using a *potentiostat.* This device adjusts the voltage in order to maintain the potential difference across the working and reference electrodes (sensed using a high impedance feedback loop). The potential is varied in a pre-programmed manner via a function generator. The potentiostat forces current trough the working electrode to achieve the potential desired.

In voltammetric experiment, an electro-inactive electrolyte is required in excess of the reactant species, in order to carry current trough the cell. Its role at the WE is to affect a kind of charge saturation which forces electroactive species to approach this electrode by diffusion rather than any field-effected conduction process (migration). In voltammetric experiments, electroactive species depleted by electrode prior to the electron-transfer reaction. Product if soluble diffuses

back to the bulk after the electron-transfer reaction is complete.

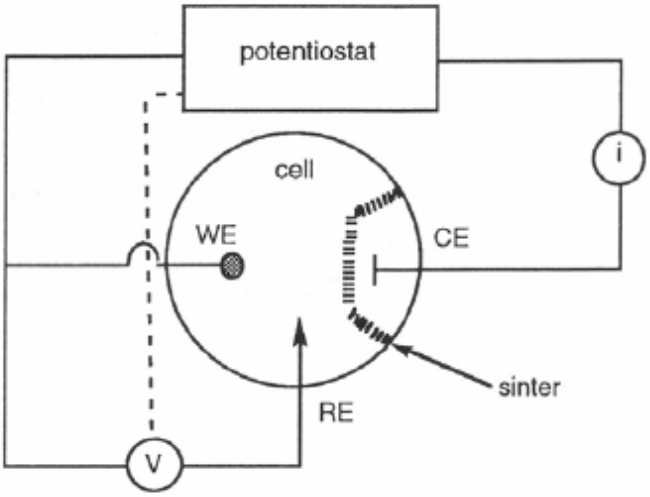

Fig. 1.2 *Schematic representation of a three-electrode cell for voltammetric use. Here the voltmeter V is in practice part of the control circuitry of the potentiostat, as is implied by the dotted line.*

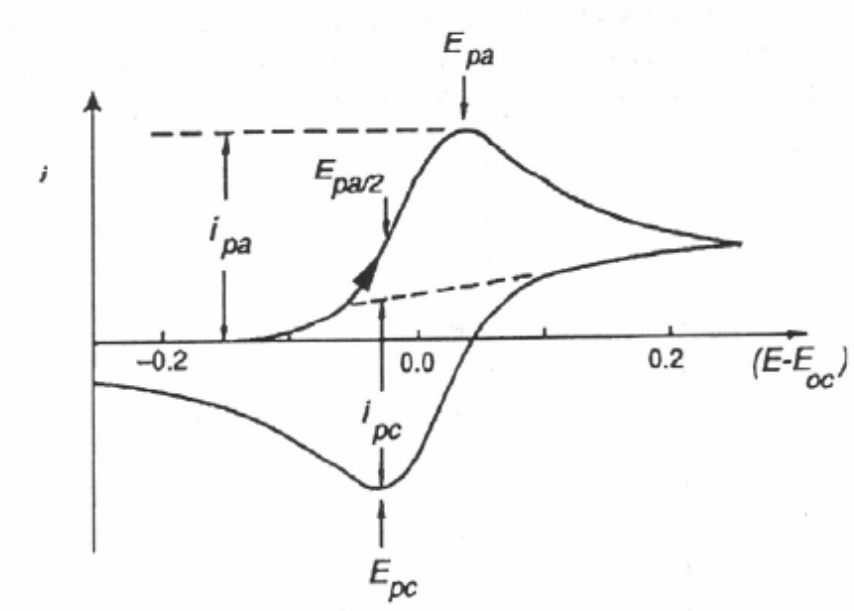

Fig. 1.3 *Typical cyclic voltammogram (CV) obtained for a simple, reversible redox couple in solution, illustrating the key quantities.*

The flux of material at the electrode dictates the shape of the current-voltage curve (voltammogram) obtained.

We shall be concerned only with the equation for the peak current i_p as derived by Randles and Sevcik[16]:

$$i_p = 0.4463 AnF\left(\frac{nF}{RT}\right)^{1/2} D_i^{1/2} \nu^{1/2} c_i \qquad (1.16)$$

where A is the area of the electrode and c_i is the bulk concentration of the electroactive species. D_i is its diffusion coefficient. This equation is applicable to "reversible" all-solution systems (those undergoing rapid electron-transfer at the electrode). Commonly i_{pc} refers to the peak for a cathodic process, while i_{pa} refers to an anodic process.

The peak in the voltammetrically monitored current i_p here is thus proportional to the concentration of the electroactive species, and to the square root of the scan rate. In *cyclic* voltammetry, the potential is ramped twice: the potential of the WE starts at an initial value E_{in} and is ramped to a limit, E_λ known as the *switch potential*, and is then swept back to E_{in}. A plot of current against this potential E is then recorded as a *cyclic voltammogram* or CV. A typical CV for a one electron process is shown in Fig. 1.4. The peak potentials for the anodic and cathodic electron-transfer processes are labeled E_{pa} and E_{pc} respectively. The peak separation is 58/n mV for reversible (i.e. rapid) n-electron reactions[11]. The same general shape but with peak separation greater than 58/n mV indicates "quasi-reversibility" resulting from somewhat slow electron-transfer at the electrode, or from intrusive resistance of electrolyte in a cell comprising less than ideal compositions for voltammetry. Conventionally the sign of v is cited as a positive

number and the range of scan rates commonly employed in cyclic voltammetry is $1< v<500$ mVs^{-1}.

1.3 Classification of electrochrome type

The type of electrochrome used in ECD governs the kinetic behavior evinced. A classification is presented here, borrowed largely from an earlier treatment by Chang *et al.*[17]

For "Always is solution" electrochromes, the electrochemical electron-transfer reaction occurs at the solid-liquid interface. The electroactive species in solution encounters the solid electrode, undergoes an electron-transfer reaction, be it reduction at a cathode or anodic oxidation, and then in its new form moves away from the electrode, returning to the solution bulk. The electrochrome changes color on undergoing the electron-transfer reaction. A simple example of this kind of electrochrome is methyl viologen dication in water. MV^{2+} in the initial solution is colorless (or faint yellow in the presence of some anions), a bright blue radical cation MV^{+*} when the electrode is made cathodic (negative). The rate-limiting process during the (reductive) electron-transfer reaction is the rate at which MV^{2+} dication reaches (diffuse toward) the electrode from the solution bulk, the rate of electron acquisition when MV^{2+} reaches the electrode interface being much faster.

In electrochromic devices on methyl viologen, if a fixed potential, substantially more negative than the (zero-current) electrode potential for MV^{2+} reduction, is applied to the working electrode, then the observed current follows the Cottrell[18] time dependence, $21-\propto ti$. This

dependence follows from the laws diffusion. Hence the absorbance $21+\propto tA$ if the current flow is wholly faradaic, that is, if each electron-transferred generates a color centre. The *t* exponent follows because the amount of $MV^{+\bullet}$ generated depends on the integral of *I* with time.

In "Solution-to-solid" systems the electrochromes are initially soluble and colorless but, following electron-transfer, they form a colored solid film on the surface of the electrode. An example of this kind of electrochrome is heptyl viologen (HV). HV^{2+} dication dibromide is pale yellow is pale yellow in aqueous solution but form a layer of deeply coloured radical cation salt on reduction. The reduction is, in fact, a two-step process (possibly concerted[19]) involving first an electron-transfer reaction

$$HV^{2+} + e^{-} \rightarrow HV^{+\bullet} \qquad (1.17)$$

and subsequent precipitation

$$HV^{+\bullet} + X^{-} \rightarrow HV^{+\bullet}X^{-}_{(s)} \qquad (1.18)$$

The deposit is initially amorphous but becomes more crystalline soon after formation[20]. The morphology, solubility and color of such radical-cation salts depend on the accompanying counter anion[20].

The Cottrell current-time relationship of $21-\propto ti$ together with $21+\propto tA$ is followed fairly closely during short times as soluble HV^{2+} diffuses toward the electrode[21]. At longer times, however, the kinetic response becomes more complicated: $HV^{+\bullet}X^{-}$ is a solid dielectric of relatively poor conductivity, and further coloration involving generation of additional colored product must

proceed via slow electron transport trough the solid deposit at the solution/electrode interface. Again, during electro-oxidative color erasure of the radical cation salt achieved by the reversal of reactions (1.17) + (1.18), complications, in this system become apparent, which necessitate the presence in the electrochemical deposition solution of electron mediators such ferrocyanide ion which acts catalitically to facilitate electron transfer[22,23].

The most commonly used electrochromes for "All-Solid" systems are Rare-earth phthalocyanines, Prussian blue, and metal oxides, for example, of tungsten, molybdenum, nickel or vanadium. For metal oxides and Prussian blue, the electrogenerated color appears as a consequence of an optical charge-transfer transition between metal centers in the solid-state lattice.

The rate-limiting process usually encountered with this type of electrochromes is the ionic charge transport the solid electrochrome. The diffusing species, enters the electrochrome via the electrolyte-film interface and then moves through the film although it does not reach the metal-conductor substrate at the other side of the electrochrome.

Two separate diffusion processes will occur within the solid: both the ion diffusion from the electrolyte/solid interface, and electron from the electrode-electrochrome interface. *Only the slowest, rate limiting, of these diffusion processes will be measurable* in systems in fast electron-transfer in the redox processes.

1.4 Electrochromic devices

Many ECDs comprise a sandwich structure of thin layers, the number and nature of which depend on the intended use. The construction of ECDs will be the same whether a large area cell or one small element (pixel) of a multi-electrode array is required[24].

Electrochromism is used in one of two modes: in adjustment of either reflected or transmitted intensity, Fig. 1.4.

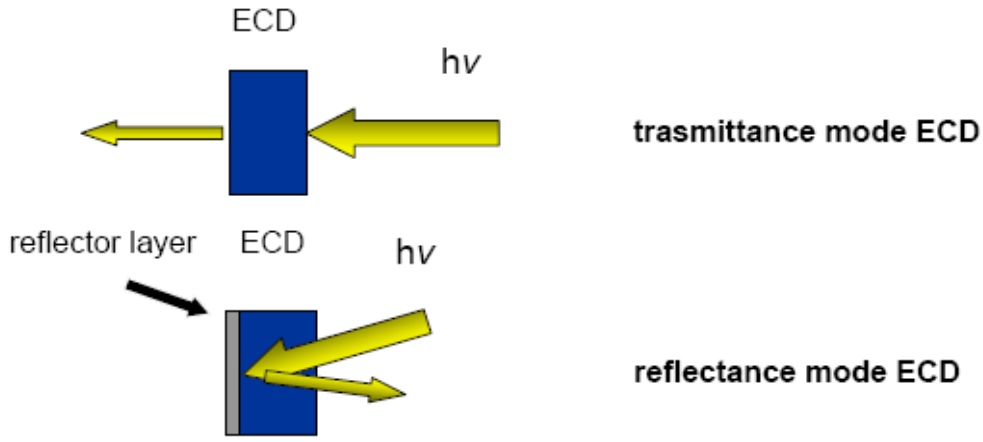

Fig 1.4 *Schematic diagram showing the different modes of ECD operation.*

1.4.1 All-solid cells with reflective operation

For all-solid systems, reflective cells may be assembled according to the schematic diagram in Fig. 1.5. The front panel is an optically transparent electrode (OTE), that is, a solid support, for example glass bearing a thin transparent but conductive film on its solution-facing side. Tin-doped indium oxide (ITO) is commonly employed[25]. Typically about 0.3 μm thick. The glass of chosen thickness may be reinforced to give structural strength. The OTE acts as the conductor of the electrons necessary for the required electron-transfer to take place in the electrochromic material. If the latter is the primary electrochrome, a secondary electrochrome may be deposited on the counter electrode. The layers are deposited by electro deposition,

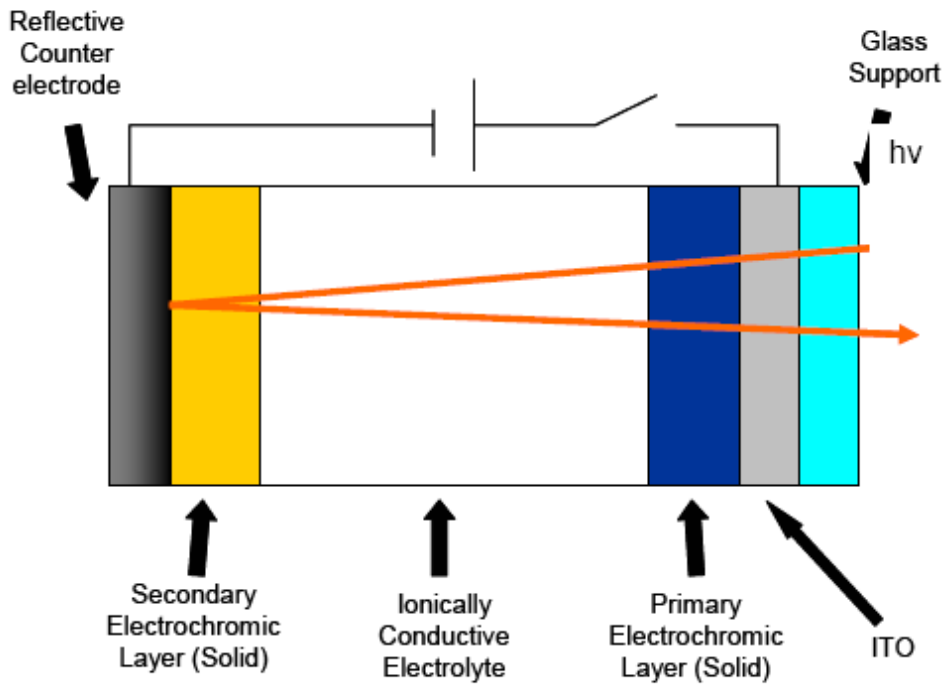

Fig. 1.5 *Schematic diagram of an EC mirror operating in reflectance mode (with the reflector as counter electrode).*

evaporation or some other method directly on to the OTE surface to minimize contact resistances. The use of OTEs for electrochromic applications has been reviewed by Lyman[26] and Granquist[27]. ECDs operating in a reflective mode (Fig. 1.5) employ a reflective material in the path of the light-beam, both the primary and secondary electrochromes being positioned before it. Example of reflector include polished platinum[28] and rhodium alloy[29]. The potential is applied between the front OTE and rear electrode/reflector. Displays may have a metallic (e.g. gold) working electrode on which the electrochrome acts, with transparent ITO as counter electrode and window.

Diffusion is usually the predominant mode of mass transport of counter ions in the electrochromic layer while migration is the transport mechanism in the electrolyte.

ECDs in which a separate reflector is placed before the secondary layer have been described at length by Baucke[28, 30-32]. Although this arrangement this has practical advantages, the counter electrode need not to be electrochromic since it is never in the path of the light beam, the reflector must be ion permeable if charge is to pass across the cell, requiring a porosity which diminishes its reflectivity.

1.4.2 All-solid cells with transmissive operation

Transmissive cells are assembled according to the schematic diagram in Fig. 1.6. Such ECDs are very similar to reflective devices except

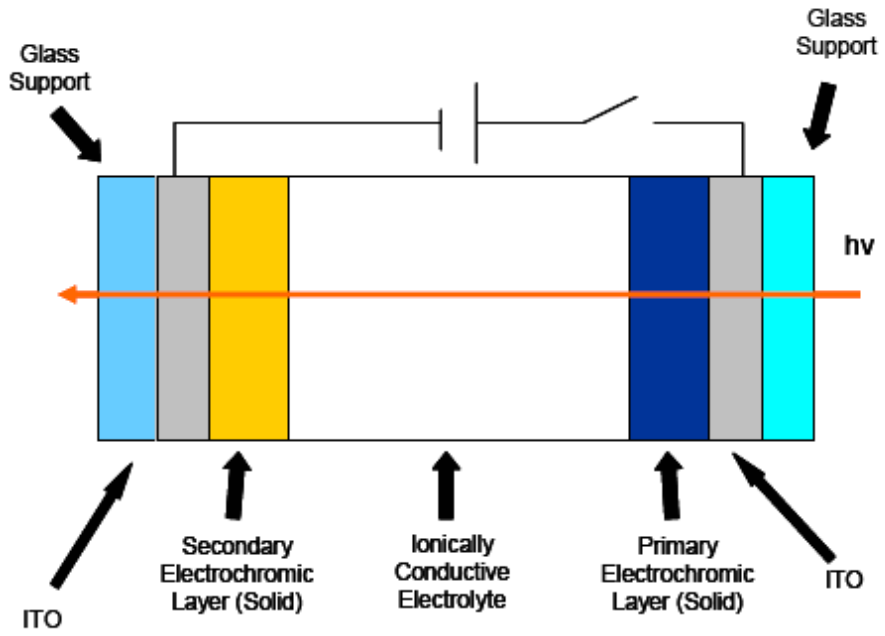

Fig. 1.6 *Schematic diagram of an all-solid ECD operating in transmittance mode.*

that the rear electrode obviously cannot be opaque: all layers must fully transparent in the visible spectral range. The apparent intensity change in a transmissive device is only half that of an otherwise identical ECD acting in a reflective mode. This follows since light passes through the primary electrochrome twice in a reflective device, before and after reflection, but only once in a transmissive cell in which the optical path length is thus, in effect, halved.

1.5 Bipyridilium systems

One of the major group of electrochromes are the bipyridilium species formed by the diquaternising of 4,4'-bipyridil to form 1,1'-disubstituted-4,4'-bipyridilium salts (Fig. 1.7). The positive charge shown localized on N is in general delocalized over the rings. The compounds are formally named as 1,1'-di-substituent-4,4'-bipyridilium if the two substituent at nitrogen are the same, and as 1-substituent-1'-substituent'-4,4'-bipyridilium should they differ. The anion X^- in Fig. 1.7 need not be monovalent and can be part of a polymer. A convenient abbreviation for any bipyridyl unit regardless of its redox state is "bipm" with its charge indicated. The most common name for these salts is viologen which is the color formed when 1,1'-dimethyl-4,4'-bipyridilium undergoes a one-electron reduction to form a radical cation[33,34].

There are three common bipyridilium redox states: a dication ($bipm^{2+}$), a radical cation ($bipm^{\bullet+}$) and a di-reduced neutral compound ($bipm^{0}$). The dication is the most stable of the three and is the species purchased or first prepared in the laboratory. It is colorless when pure unless optical charge-transfer with the counter anion occurs. Such absorbencies are feeble for anions like

chloride but are stronger for CT-interactive anions like iodide[35].

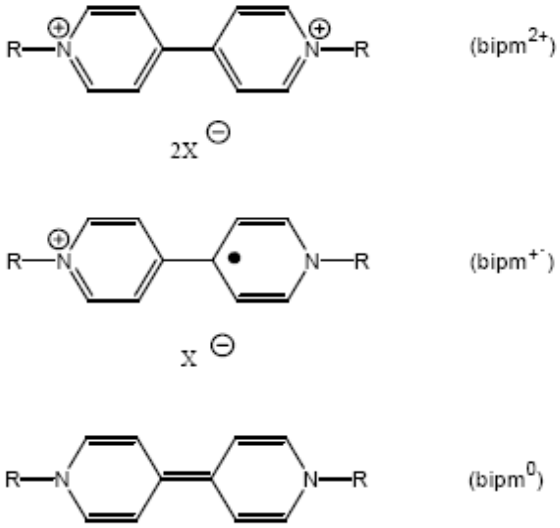

Fig. 1.7 *Bipyridilium salt redox states.*

Reductive electron-transfer to the dication forms a radical cation (equation 1.19). Bipyridilium radical cations are amongst the most stable organic radicals, and may be prepared as air-stable solids[36,37]. The stability of the radical cation is attributable to the delocalization of the radical electron throughout the π-framework of the bipyridyl nucleus, the 1 e 1' substituent commonly bearing some of the charge.

$$\underset{\text{(colourless)}}{\text{bipm}^{2+}} + e^- \rightarrow \underset{\text{(intense colour)}}{\text{bipm}^{+\bullet}} \qquad (1.19)$$

Electrochromism occurs in bipyridilium species because, in contrast to the bipyridilium dications, radical cations are intensely colored owing to optical charge-transfer between the (formally) +1 and zero valent nitrogens, in a simplified view of the phenomenon (in fact, because of the

delocalization referred to, the source of the color is probably better viewed as an internal photo-effected electronic excitation). The colors of radical cations depend on the substituent on the nitrogen. Simple alkyl groups, for example, promote a blue/violet color whereas aryl groups generally impart a green hue to the radical cation. Manipulation of the substituent at N to attain the appropriate molecular orbital energy levels can, in principle, tailor the color as desired.

Comparatively little is known about the third redox form of the bipyridilium series, the di-reduced or so called "di-hydro"[38] compounds formed by one-electron reduction of respective radical cation (reaction 1.20)

$$\underset{\text{(intense colour)}}{\text{bipm}^{+\bullet}} + e^- \rightarrow \underset{\text{(colourless)}}{\text{bipm}^{0}} \qquad (1.20)$$

The same species is formed by a two-electron reduction of the dication. The intensity of the color exhibited by $bipm^0$ species is low since no optical charge-transfer or internal transition corresponding to visible wavelengths is accessible.

Bipyridilium salts are some of the few organic species that undergo the comproportionation reaction in solution, in which two redox states of the same compound react to form an intermediate redox state, equation 1.21:

$$\text{bipm}^{2+} + \text{bipm}^{0} \rightarrow 2\text{bipm}^{+\bullet} \qquad (1.21)$$

the first product of the comproportionation reaction is in fact spin-paired radical-cation dimer[39]. The transition state of reaction 1.21 is thus assumed to have the two redox states lying face to face in a "sandwich"–type configuration.

1.6 The charge transfer equilibrium of bipyridilium species

The bipyridilium dication is a relatively weak electrolyte and almost always evinces some forms of ion association. The association takes the form of ion pairing if the interaction is predominantly ionic, or as charge-transfer complexation if a significant extent of orbital overlap can occur.

The term charge-transfer is used in some of the literature to imply that a discrete electronic charge has transferred from donor to acceptor, i.e. that the wave function for the excited system describes the quantity of charge which transfers as being that of an integral electron. The fraction of electronic charge actually transferred in a ground-state configuration can be small for viologen-donor complexes.

Typically, a charge-transfer complex is detected in UV-visible spectrophotometry. When two compounds in solution are brought together and a new optical absorption band is formed that was not present in the spectrum of either component, then it is likely that a CT complex has been formed:

$$A + D \leftrightarrow AD \qquad (1.22)$$

colourless coloured

The viologens are all excellent electron acceptors (that is, have a high electron affinity *E*): for example, White[40] cites an electron affinity of 120 kj mol^{-1} for methyl viologen.

During complex formation, the orbitals of the approaching molecules overlap, and the resultant distortion causes a movement of charge from the donor to the unoccupied orbitals of the acceptor molecule, this attractive charge-transfer interaction occurs in tandem with the other low-energy interactions always present; a stable complex forms if the attractive interactions outweigh the repulsive energetic forces[40].

CT bands tend to be rather intense owing to the electronic transition being wholly allowed quantum mechanically[41]. The CT band is also quite wide because both acceptor and donor species can have a range of energies and bond separations following a Boltzmann-type distribution. For this reason, the spectroscopic CT band is essentially gaussian[41] when drawn with an energy-related abscissa.

The energy for the electron-transfer reaction is supplied by a photon:

$$AD + h\nu \rightarrow A^{-}D^{+} \qquad (1.23)$$

The CT complex is colored because of the uptake of this photon; and the color seen in the laboratory is the complementary color to that absorbed.

In addition to collision between acceptor and donor followed by photon absorption, equation 1.23, there is also an extensive literature on the formation of CT complexes via redox reactions, as represented here by electron-transfer within an ion pair

$$\left[\text{bipm}^{+\bullet}\text{D}^{n-}\right] \rightarrow \left[\text{bipm}^{2+}\text{D}^{(n+1)-}\right] \qquad (1.24)$$

Photon absorption by the product of equation 1.24 yields the familiar color of a CT complex. Since the viologen dication is almost always involved in some form of CT equilibrium, electro-reduction will involve electron transfer to a $bipm^{2+}$ moiety that is complexed. In fact, complexes of methyl viologen can be relatively electro-inert at solid electrodes and the rate determining step during electro-reduction is the prior dissociation of the complex before electron-transfer: it is thus a CE reaction. This CE reaction (that is, a chemical reaction followed by an electrochemical reaction) is demonstrated in figure 1.8, where the rates of electron-transfer k_{et} and of complex dissociation are plotted together: the correlation is seen to be more than coincidental, which would surely have been the case in the absence of a CE-type process.

The inorganic ion to have received most attention as a CT donor to methyl viologen is hexacyanoferrate(II)[42-46]. The CT of aqueous methyl viologen with ferrocyanide depends[47] on pressure, ε increasing by 35% and λ_{max} shifting by ~ 1700 cm^{-1} when the pressure was increased from 0.001 kBar 10 kBar. The spectral peak width did not alter, although the peak is slightly non-gaussian (too wide) on the low-energy side on the band.

Nitrogen-containing species are represented by amines such as aniline[42, 48, 49], *p*-toluidine[42], *p*-phenylenediamine[50], N,N-dimethyl-aniline[42], benzidine[42]. In passing, it should be noted pyridine or 4,4'-bipyridine also acts as a donor (particularly in organic solution) owing to the lone pairs at nitrogen: when conditions are opposite, the quaternization of 4,4'-bipyridine will proceed with a faintly colored solution since the unreacted bipyridine forms a weak complex with

the newly formed viologen product. No quantitative measurements of association between pyridine or 4,4'-bipyridine and viologens are extant.

The best oxygen-containing donors are the phenols such as *p*-cresol[42], *p*-methoxyphenol[42], and pyrogallol[42]. There is some evidence that a few aliphatic alcohols[51] (such as propan-1-ol and propan-2-ol) can also effect CT with viologens.

Another type of CT is seen when the donor is an aromatic species. Here, it is the π-orbitals of the arene which donates charge to viologens. In this case, it is the (charge) centroid of the arene which is directed toward the nitrogens of the bipyridilium salt acceptor, rather from a specific

donor atom [52-57].

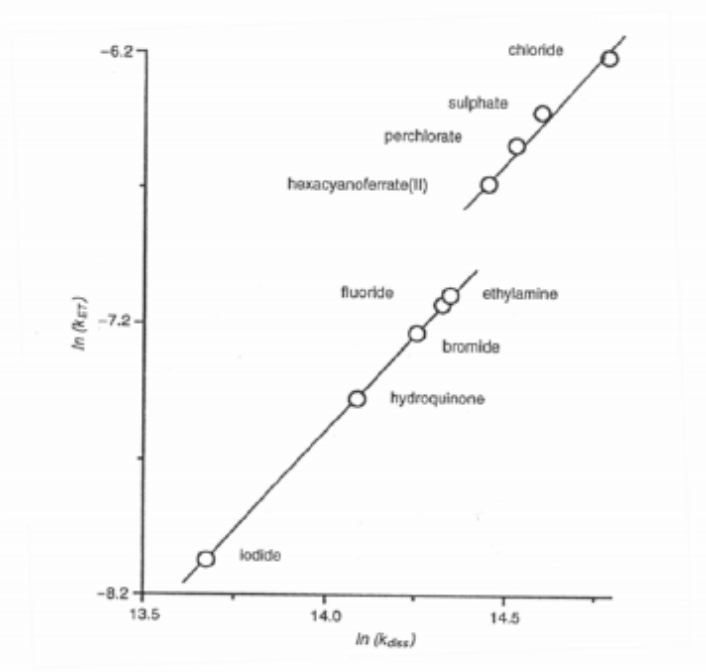

Fig. 1.8 *Plot of lnk_{ET} (k_{ET}=rate constant of electron-transfer to the methyl viologen dication) against lnk_{diss} (k_{diss}=rate constant of the dissociation of methyl viologen charge-transfer complex). Both rates relate to solution-phase complexes in water at 298 K. The lower line relates to a straightforward correlation between k_{et} and k_{diss}; the upper line represents anomalous kinetiks, with adsorption-catalysed electron-transfer (Cl⁻), slow k_{diss} ($[Fe(CN)_6]^{4-}$) and ion pairs without CT (ClO_4^- and SO_4^-). (Electrochim. Acta 1998, vol. 43, P.M.S. Monk and Hodgkinson, page 245).*

The energy of the charge-transfer band in the solid state usually relates to the energy necessary for photo-excitation across the band gap between the valence and conduction bands, although it could still refer to the energy required for electron hopping between acceptor and donor.

The viologen radical cation is comparatively electron rich and can, in the solid state, act as a modest donor. When acting as donor to a viologen dication, the formal oxidation state per viologen moiety is non-integral and the solid is thus deemed to be "mixed valent"[58]. These

mixed-valence species are well-conducting semiconductors or even have metallic electrical properties. It should be recognized that anions are also present in a non-interactive capacity. (The magnitude of anion interactions, hitherto the sole interactions of interest, are probably much smaller here than the other forces in the solid state, so anions can be ignored except insofar as they may influence the resultant crystal structure).

Samples of solid solid-state viologen are held together in a highly stereospecific conformation by charge-transfer-type associatives forces.

REFERENCES

[1] J. R. Platt, *J. Chem. Phys.*, 34, **1961**, 862.

[2] H. Byker, *Proc. Electrochem. Soc.*, 94, **1994**, 3.

[3] S.F. Cogan, T.D. Plante, R.S. McFadden and R.D. Rauh, *Proc. S.P.I.E.*, 823**, 1987** 106.

[4] A.J.M. Rae, "Quantum Mechanics", 2nd Edition, Hilger, Bristol, **1986**.

[5] R.W.G. Hunt, "The reproduction of Colour", Fountain Press, Tolworth, **1987**.

[6] P.W. Atkins and J.A. beran, "General chemistry", 2nd edn., W.H. Freeman, New York, **1992**, pp. 231 and 815.

[7] P.W. Atkins "Physical Chemistry", 5th edn., Oxford University Press, Oxford, **1994**. p. 545.

[8] E.M. Kosower, "An Introduction to Physical Organic Chemistry", Wiley, New York, **1968**.

[9] B.W. Faughnan and R.S. Crandall, in J.I. Pankove (ed.), "Display Devices", Springer-Verlag, Berlin. **1980**. Chap. 5.

[10] S.F. Cogan and R.D. Rauh, *Solid State Ionics,* 28-30, **1988,** 1707.

[11] A.J. Bard and L.R. Faulkner, "Electrochemical Methods", Wiley, New York, **1980**.

[12] The Southampton Electrochemistry Group, "Instrumental Methods in Electrochemistry", Ellis Horwood, Chichester, **1985**.

[13] C. Bohnke and O. Bohnke, *J. Appl. Electrochem.*, 18, **1988**, 715.

[14] H. Kaneko and K. Miyake, *Appl. Phys. Lett.*, 49**, 1986** 112.

[15] P.G. Bruce, in "Polymer Electrolyte Reviews", (eds.) J.R. MacCullum and C.A. Vincent, Elsevier, Amsterdam, **1987**, p. 237.

[16] A. Sevcik, *Coll. Czech. Chem. Commun.,* 13, **1948**, 349.

[17] L.F. Chang, B.L. Gilbert and T.I. Sun, *J. Electrochem. Soc.,* 122**, 1975**, 955.

[18] F.G. Cottrell, *Z. Physik. Chem.,* 42**, 1902,** 385.

[19] R.G. Barradas, S. Fletcher and L. Duff, *J. Electroanal. Chem.,* 100**, 1979,** 759.

[20] J. Jasinski, *J. Electrochem. Soc.,* 124**, 1977**, 637.

[21] J. Bruinik and P. van Zanten, *J. Electrochem. Soc.,* 124, **1977,** 1232.

[22] A. Yasuda, H. Mori and A. Ohkoshi, *J. App. Electrochem.,* 14**, 1984**, 323.

[23] J.G. Kenworthy, *ICI Ltd. British Patent*: 1,314,049 (**1973**).

[24] T.P. Brody and P.R. Malmsberg, *J. Hybrid Microelec.,* II**, 1979**, 29.

[25] R.W. Murray, W.R. Heineman and C.W. O'Dom, *Anal. Chem.,* 39**, 1967**, 1666.

[26] N. R. Lynam, *Proc. Electrochem. Soc.,* 90-2, **1990**, 201.

[27] C.G. Granqvist, *Appl. Phys. A.,* A57**, 1993**, 19.

[28] F.G.K. Baucke, *Rivista della Staz. Sper. Vetro,* 6**, 1986**, 119.

[29] W. Wagner F. Rauch, C. Ottermann and K. Bange, *Nuc. Instr. Meth. Phys. Res.,* B50**, 1990**, 27.

[30] F.G.K. Baucke, K. Bange and T. Bange, *Displays,* October **1988**, 179.

[31] F.G.K. Baucke, *Proc. Electrochem. Soc.,* 90-2, **1990**, 298.

[32] F.G.K. Baucke, *S.P.I.E. Institute Series,* IS4**, 1990**, 518.

[33] L. Michaelis and E.S. Hill, *J. Gen. Physiol.,* 16**, 1933**, 859.

[34] L. Michaelis, *Chem. Rev.,* 16 **, 1935**, 243.

[35] D.R. Rosseinsky and P.M.S. Monk, *J.C.S. Faraday Trans.,* 89**, 1993**, 219.

[36] D.R. Rosseinsky and P.M.S. Monk, *J.C.S. Faraday Trans.,* 90, **1994**, 1127.

[37] B. Emmert and O. Varenkamp, *Chem. Berichte,* 56**, 1923**, 490.

[38] B. Emmert, *Chem. Berichte,* 53**, 1920**, 370.

[39] P.M.S. Monk, R.D. Fairweather, M.D. Ingram and J.A. Duffy, *J. Chem. Soc., Perkin. Trans. II*, ***1992***, *2039.*

[40] B.G. White, *Trans. Faraday Soc.,* 65**, 1969**, 2000.

[41] J.A. Duffy, *Bonding, Energy Levels and Bands in Inorganic Solids*, Longmans, Harlow, **1990**.

[42] A.S.N. Murthy and A.P. Bhardwaj, *Spectrochim. Acta,* 38A, **1982**, 207.

[43] A.M. Kjaer, I. Kristjansson and J. Ulstrup, *J. Electroanal. Chem.,* 204**, 1986**, 45.

[44] L.A.A. de Oliveira and A. Haim, *J. Am. Chem. Soc.,* 104, **1982**, 3363.

[45] J.C. Curtis, P. Sullivan and T.J. Meyer, *Inorg. Chem.,* 19**, 1980**, 3833.

[46] H.E. Toma, *Can. J. Chem.,* 57**, 1979**, 2079.

[47] W.S. Hammach, H.G. Drickamer and D.N. Hendricksen, *Chem. Phys. Lett.,* 151**, 1988**, 469.

[48] A.T. Poulos, C.K. Kelley and R. Simone, *J. Phys. Chem.,* 85, **198**1, 823.

[49] G. Jones and V. Malba, *Chem. Phys. Lett.,* 119**, 1985**, 105.

[50] H. Byrd, E.P. Suponeva, A.B. Bocarsly and M.E. Thompson, *Nature*, 380**, 1996**, 610.

[51] A. Meyerhaus, W. Pfau, R. Memming And P. Margaretha, *Helv. Chim. Acta.,* 65**, 1982**, 2603.

[52] K.B. Yoon, T.J. Huh and J.K. Kochi, *J. Phys. Chem.,* 99**, 1995**, 7142.

[53] S.M. Hubig, *J. Phys. Chem.,* 96**, 1992**, 2909.

[54] K.B. Yoon and J.K. Kochi, *J. A. Chem. Soc.,* 111, **1989**, 1128.

[55] M.E. Wacks and V.H. Dibeler, *J. Chem. Phys.,* 31**, 1959**, 1557.

[56] S.M. Hubig and J.K. Kocji, *J. Phys. Chem.,* 99**, 1995**, 17578.

[57] G. Brigleb and J. Czekalla, *Z. Elektrochem.,* 63**, 1959**, 3**.**

[58] D.B. Brown (ed), *Mixed-Valence Compounds in Chemistry, Physics and Biology*, Reidel Publishing Company, Dordrecht, Holland, **1980**.

CHAPTER II

Solid thermoplastic laminable electrochromic film

Introduction

Electrochromic (EC) technology and EC device are drawing attention for their high potentiality in relation to solar control and display applications. The working principle of EC systems is very simple and is linked to the use of EC molecules which exhibits new optical absorption bands when an electron is gained or lost in a redox process[1,2]. In the most simple EC devices, EC active molecules are dissolved in the some medium interposed, as a single film, between the conductive inner surfaces of two transparent supports (generally glass slabs). The first examples of these EC films are those obtained dissolving anodic and cathodic EC molecules in a fluid electrolyte solvent. In this case the performance of the system is controlled by molecular diffusion of the EC molecules. During the coloration step, when a potential difference between the electrode layers is applied, the EC molecules need to diffuse toward the conductive electrodes, where they are reduced (cathodic process) and oxidized (anodic process). Color across the film is generated by the change of the optical absorption of the cathodic or anodic (or both of these) species[3-5]. When the electric potential is removed, cathodic and anodic molecules diffuse across the medium and the electron-transfer process, between the oxidized and reduced species, takes place. EC molecules will then return to their zero-potential equilibrium state, and the color disappears. The electrochromic fluid film has the advantage of being reasonably fast (operational time less than 1 second) but cannot be used in large solar control window or large display for

several reasons. First of all, it must be mentioned that materials forming the fluid film are subjected to natural convection or to a process known as aggregation[6] or segregation [7], due to the variation of the solvent organization around the EC molecules when they undergo redox processes. Near the anode the solution density increases with respect to the bulk, owing to the oxidation of cathodic material. Polar organic solvents used in EC devices in fact yield a better solvatation of cathions and oxidized species. The motion of solvatation sphere surrounding the anodic material towards the newly formed oxidized species allows the solution to become more dense. At the cathode the effect is reversed. In this way severe color inhomogeneity in large area devices can occur. Other drawbacks phenomena encountered in large EC device where fluid film are sandwiched between glass slabs are due to the onset hydrostatic pressure of the fluid layer which can break or separate from the glass supports. To eliminate the disadvantages of the fluid film EC devices, polymer thickeners have been introduced into the EC fluid solution. Examples of these systems are those described by Tsutsumi et al.[8-10] which contain organic EC redox materials, solvents, and some percentage of a cross-linked polymer, formed by in situ polymerization of some fluid monomers added to the formulation. Other kinds of EC devices involve conducting polymers in which redox molecules are immobilized by providing reactant pendants[11-13]. Our research work is different from EC gelled mobile systems and immobilized systems was devoted to the development of an easy technology based on self-standing materials where redox centre mobility is reduced but not suppressed. Recently we have published a study concerning a new thermoplastic self supported EC film[14,15]. There the preparation of this film, containing wt.40% PVF (poly vinyl formal), 5wt.% ethyl viologen diperchlorate (EV), 1wt.% hydroquinone (HQ) and 55 wt.% propylene carbonate (PC), is described. The absorption data of the device at different pulse voltages are presented as a function of time. The active molecules we have used as cathodic components belong to the class of bipyridinium salts (viologens), which

are a well-known class of EC compounds displaying different colors in dependence of their oxidation state and the nature of the substituents at the nitrogen atoms [16-21]. In this chapter our scope is to study the effect of the concentration of different components and the effect of the thickness on the films EC under object of study.

2.1 Experimental section

2.1.1 Chemicals

All chemical reagents were commercially available and were used as purchased without further purification. Poly(vinyl formal) (PVF), propylene carbonate (PC), hydroquinone (HQ), ethyl viologen diperchlorate (EV) were purchased from Aldrich Chemical.

2.1.2 Samples preparation

Different electrochromic samples with different compositions and different thickness were prepared in order to study their electrooptical parameters and properties. Here we describe the general preparation procedure of an electrochromic solid film; in the following paragraphs the details of the amount of each component will be supplied. Ethyl viologen diperchlorate, hydroquinone and propylene carbonate are mixed in a proper amount, the obtained electrochromic solution is stirred at 100°C for approximately 10 minutes for good homogenization. All solid electrochromic films are produced mixing at 150°C PVF and the electrochromic solution, until an homogeneous perfectly transparent film are obtained (thermal

blending process). After cooling the mixture at room temperature, an homogenous solid film, with EC properties and great adhesion ability to a glass support is obtained. The all solid ECD is then very easily manifactured, by simply heating the electrochromic film to the temperature of softening of the plasticized thermoplastic polymer (100-150 °C), this molted mixture is laminated between two ITO coated conductive glasses. No spacer needed to be added to control the thickness of the cell, because, the control of parameters of the lamination process, as the temperature and the pressure applied to the conductive glasses, allowed us to get an electrochromic cell of the desired homogeneous thickness. This preparation gives the possibility to obtain in a very easy way ECD suitable for large-scale applications, by simple lamination of the film between conductive glasses.

The advantage are:

1) No evaporation of solvent

   Some electrochromic films are obtained dissolving each component of the mixture in a solvent, and then evaporating the solvent to obtain the film. It is not optimal because the production of large area device would ask the disposal of great quantities of harmful solvent.

2) No curing after device obtain

   In some gelled system with the diacrylate monomers it's necessary UV curing of the device after the assemblage to get a self-supported film

3) Mono-layer system
4) Self-consistent
5) Self-supported

2.1.3 Experimental setup

The electro-optical properties of ECD were measured with a YASCO V550 UV-VIS spectrometer. The light intensity with no sample in place was assumed to be the full-scale intensity. Measurements was performed at 25°C, under the application of square voltage pulses. An AMEL 2049 model potentiostat/galvanostat and an AMEL 568 programmable function generator were used to apply a square potential during electrochromic measurements.

2.2 Results and discussion

In order to study the effect of the concentration of the different components and the effect of the thickness on the films EC under object of study, we have prepared six different mixtures containing different amounts of polymer and solvent.

sample name	35%	37%	40%	43%	45%	50%
PVF (poly(vinil formal)	35%	37%	40%	43%	45%	50%
Ev (ethyl viologen diperchlorate)	4%	4%	4%	4%	4%	4%
HQ (hydroquinone)	2%	2%	2%	2%	2%	2%
PC (propylen carbonate)	59%	57%	54%	51%	49%	44%

TABLE N.1

Each mixture has been used for the preparation of films with different thickness

As we can see from the table, in each sample the relative amount of anodic substance (HQ) and cathodic substance (EV) is constant as a study carried out in our laboratory has suggested. This study has shown that the percentage of EC and HQ, published on the table, satisfy the preparation of efficient ECD demands.

The mixture has been prepared mixing and warming the component (PVF, HQ,EV.PC) at 100-150°C. After it was cooled at room temperature, and an homogeneous plastic mixture, with EC properties, has been obtained. The EC film was prepared by laminating the mixture between two glass supports coated with indium tin oxide, in order to apply the dc voltage needed to colour the electrochromic film. Any efforts to delaminate the glass supports at room temperature without breaking the cell was unsuccessful. The system could be delaminated only at 80°C. The film reveals an homogeneous and continuous structure without visible phase separation as reveals the SEM analysis carried out in our laboratory. A complete absence of porosity and channels greatly restricts the migration of the molecules inside the film. In literature ECDs in which redox materials are mixed with a solid polymeric matrix are known [22], but in such systems anodic and cathodic ionic chromospheres are able to migrate in solution phase towards the electrodes when a voltage is applied, because the morphological analysis show the presence of high porosity which contains solvent. EC systems with similar compositions are described as "free-standing gels" [23-28]. A "free-standing gel" is described as " a system of polymer matrix with interspersed EC solution.....". Once again the EC layers are formed by filling devices with a relatively low viscosity solution of monomers, followed by in situ reaction to give a cross linked polymer matrix. A preferred polymer or cross link forming reaction is that of isocyanates with alcohols These gels can be thought as a two phase system in which a continuous phase is interdispersed in

a Three-dimensional matrix formed by a polymer phase. The solution portion of gel is open enough to allow relatively large molecules and ions to diffuse and/or migrate throughout the phase, to and from the electrodes. The morphology of a gelled solution phase EC system is very different from that of our electrochromic solid film which has a continuous structure without visible phase separation, and redox materials are not free to migrate.

The absorption spectrum of the coloured and uncoloured electrochromic cells carried out in our laboratory by another work, reveals at 606 and 413 nm the maximum wavelength of absorption related to the cation of ethyl viologen ($bipm^{+\cdot}$), the resulting colour of the film is blue. This radicalic viologen specie is intensely coloured owing to the presence of the single electron acquired on reduction, which is delocalized extensively over the bipyridilium core. From the spectrum there is no evidence for dimer formation. When viologen is reduced, the colour of radical cation can change from blue to purple, this change in colour of the absorbing molecules being due to formation of viologenic dimeric species. Monomer-dimer equilibration was proposed by Schwarz [29] in 1962, and is outlined in equation 2.1

$$2bipm^{+\cdot} = (bipm)_2^{2+} \qquad 2.1$$

The associated changes in UV-visible spectra are quite marked with absorption bands shifting to lower wavelengths and new bands appearing at right wavelengths for the dimer form how we can see in figure 2.1.

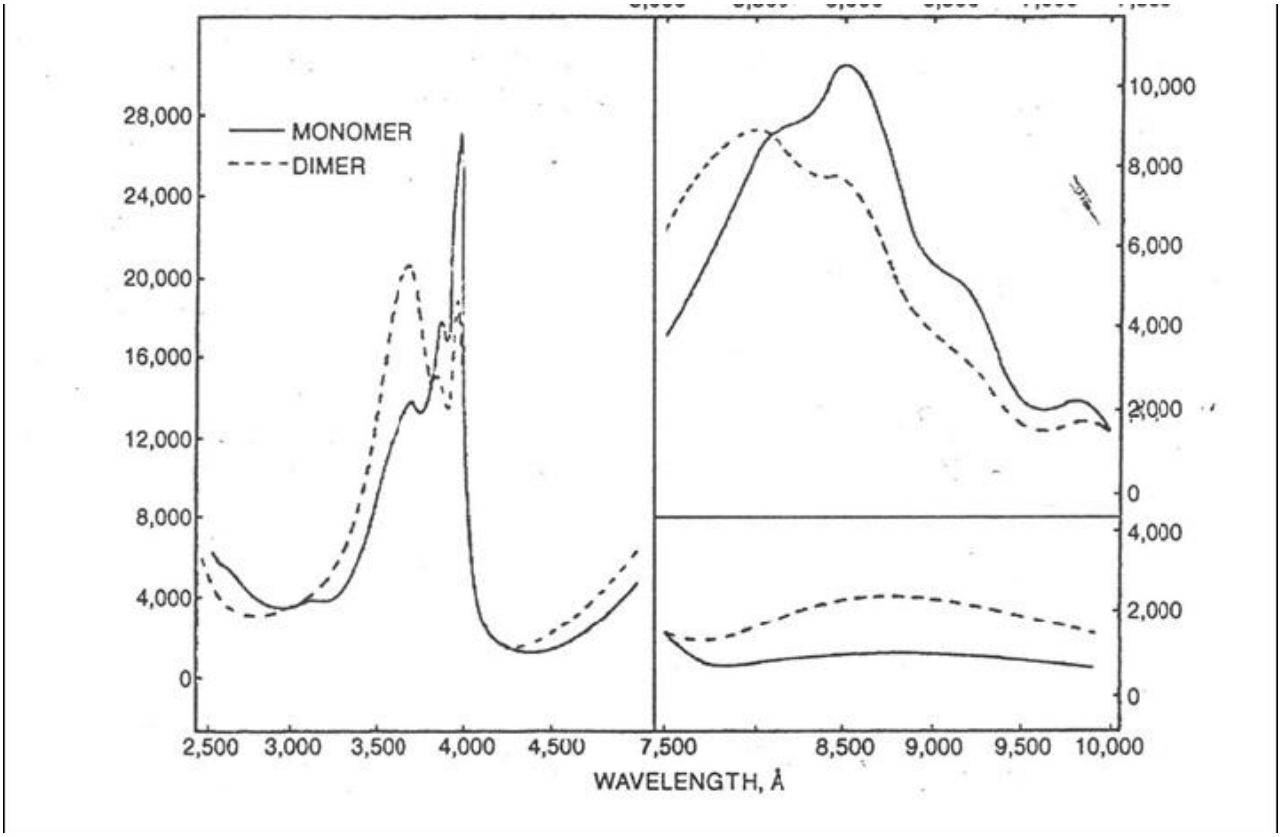

Fig. 2.1 *A comparison of the UV-visible spectra of methyl viologen radical cation as monomer and as dimer* [9].

The shape of the spectrum in the range 400-600 nm (the band for both the monomer and the dimer of the radical cation) does not change, suggesting that the bands arising from the monomer and dimer transitions fall in the same spectral region and exhibit only minimal structural differences. Then we can argue that the dimer is not a complex of dication and di-reduced bipyridilium redox states[(29)]. The new spectral band at high wavelength (at c. 900nm) is best regarded as an allowed transition within the dimer according the energy scheme of Kosower[(29)]. The new band is not a charge-transfer transition, which would be forbidden. Since both dimer and monomer absorb in approximately the same region, and both have similar extinction

coefficients, the colour of the radical cation is not directly attributable to the unpaired radical electron. Comparing the UV-visible spectrum obtained for the ethyl viologen in the solid electrochromic film, with UV-visible spectra of radical cationic methyl viologen and dimer in water reported in work of Kosower and Cotter (Fig.2.1), as said before there is no evidence for dimeric specie existence, in fact spectral profiles of ethyl viologen in our solid polymeric matrix, in range 400-600 nm, 3250-450 nm and 900 nm are very different from that of the dimeric form in the same range of wavelength. In particular the absorption maximum of the dimer was observed at around 530 nm and the colour was violet, while, for the monomeric radical cation the absorption maximum appeared at 606 nm and the colour was blu. Then all alkyl-substituted viologen radical cations in solution have the similar spectra, because the electron resides within the bipyridine core and the electronic interactions beyond the first carbon of the alkyl chain are minimal. The spatial orientation postulated for the dimer[30] is one in which the two radial cations lie face to face in a sandwich-type structure, linked by the two π-clouds overlapping to form a $\pi-\pi'$ bond.

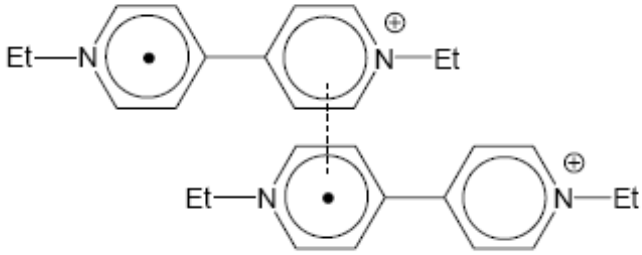

Fig.2.2*: head to head structure of the ethyl viologen dimer with two monomeric molecules having a π-interaction*

Such a dimer would be expected to be unstable with respect to coulombic repulsion as caused by the close proximity of the two positive charges, implying that the spin-pairing of dimer formation is greater than the instability engendered by coulombic repulsion. For our solid film the energy of solvation, in the non aqueous polymeric plasticized system, is probably not great enough to balance the Coulomb repulsion, and so the monomeric species is stabilized, or in other terms the ethyl viologen prefers to interact with some species present in the mixture giving a stable interaction avoiding the formation of dimers. Alternatively another reason which prevents dimerisation could be the strongly limited freedom of motion of bipyridilium molecule inside the polymer matrix of the electrochromic film. Viologen molecules are dissolved in the polymer when they are in the dicationic form, no tendency to dimer formation exists because there is no unpaired electron and molecules are arranged apart because of the Coulomb repulsion. When the coloured radical cation is generated by a suitable voltage, molecules motion is prevented by the hindrance of polymeric chains, thus monomers cannot approach in order to overlap to two π-clouds and to form a π–π' bond making a dimer, this behaviour is outlined in figure 2.3.

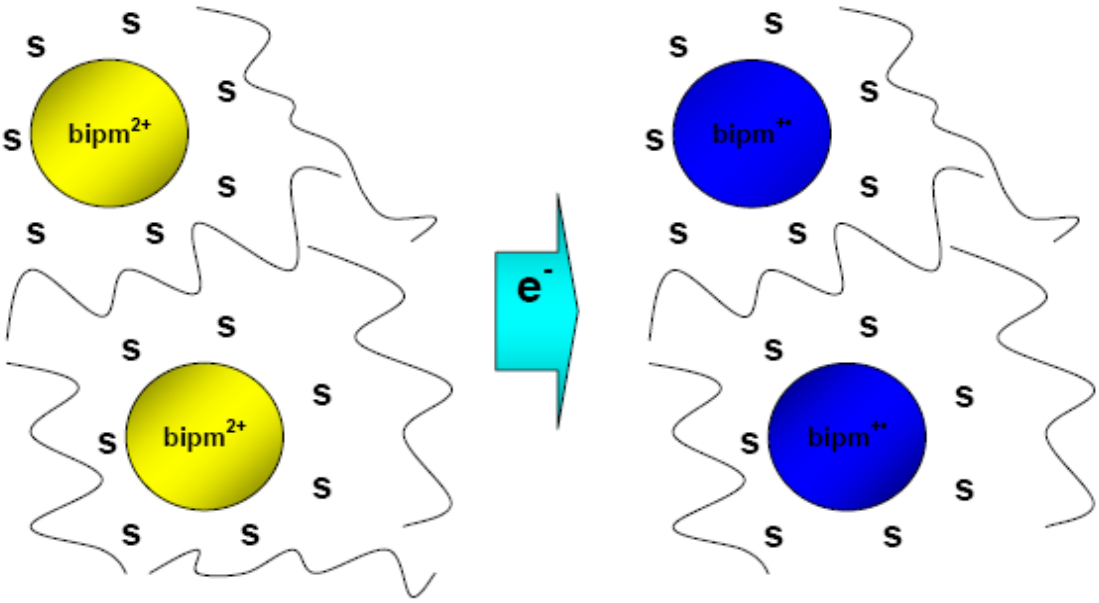

Fig. 2.3: *Dicationic bipyridilium molecules (yellow spheres) and radicalic bipyridilium (blue spheres) inside the plasticized solid matrix. The polymeric chains avoid* $bipm^{+\cdot}$ *radical cations move to each other to form a dimer.*

We have chosen to follow the absorption band centred at 606 nm as a function of the applied voltages and as a function of time to characterize the response of the ECD. A DC square pulse has been applied to the cell.

We have performed measures of transmittance as function of the dc pulse voltage amplitude, for a fixed pulse length of 5 seconds, and then we measured transmittance as function of time for a fixed pulse voltage amplitude.

In figure 2.4 we report the transmittance as a function of time and dc pulse voltage amplitude applied to a cell 90 micron thick, containing 35% of PVF, at a fixed pulse voltage length of 5 sec.

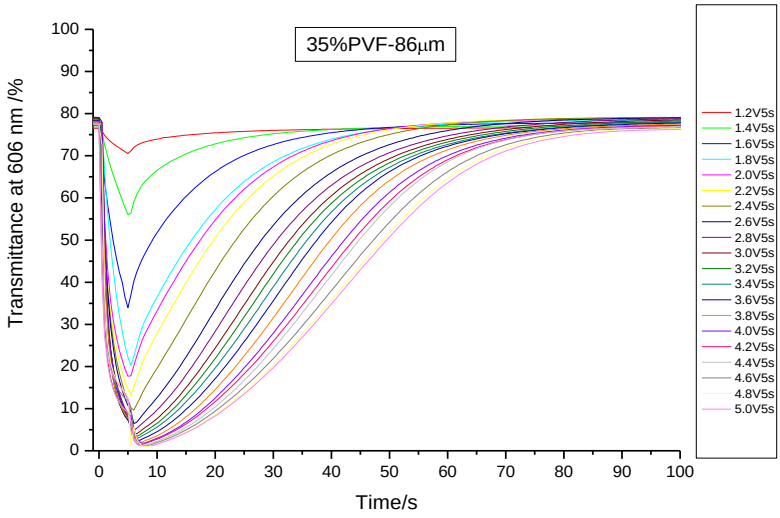

Fig2.4: *Transmittance at 606 nm obtained from an ECD 90μm thick subject to different voltage pulses 5 sec long, as function of time. The EC film has the composition: 35 wt%PVF, 4 wt% ethyl viologen diperchlorate, 2 wt% hydroquinone and 59 wt% propylene carbonate.*

We can observe that the EC response doesn't occur below 1.4 Volt, and it becomes more and more enhanced by increasing the voltage. The transmittance decreases during the dc pulse application since the population of the absorbing $bipm^{+\cdot}$ radical cation gradually increases (eq.2.2), during the electrode charge injection.

$$bipm^{2+} + e^- \longrightarrow bipm^{+\cdot} \qquad 2.2$$

When the voltage applied reaches sufficient values, the second reduction of bipyridinium can occur, according to the following reaction:

$$bipm^{\cdot +} + e^- \longrightarrow bipm^{0} \qquad 2.3$$

so the $bipm^0$ not coloured species start to form. This clearly reduces the population of the red-absorbing $bipm^{+\cdot}$. Once the pulse is removed, two processes must be taken into account: the conversion of the neutral back into the monocation species and the conversion of the latter into the dication form.

$$bipm^0 + e^- \longrightarrow bipm^{+\cdot} \qquad 2.4$$

$$bipm^{\cdot +} \longrightarrow bipm^{2+} + e^- \qquad 2.5$$

If the rate of the first reaction (2.4) is greater than that of the second one (2.5), the population of the absorbing species keeps increasing for a while. In other words, the absorption does not decrease immediately after the removal of the pulse and some increase of coloration can be appreciated instead of the bleaching expected immediately after the voltage removal.

The decade of the neutral species into the monocation form, after the voltage removal, can occur by chemical processes different from that described by eq. 2.4. One of these process is the reaction with the oxidized (1,4-benzoquinone) form of the anodic compound (hydroquinone):

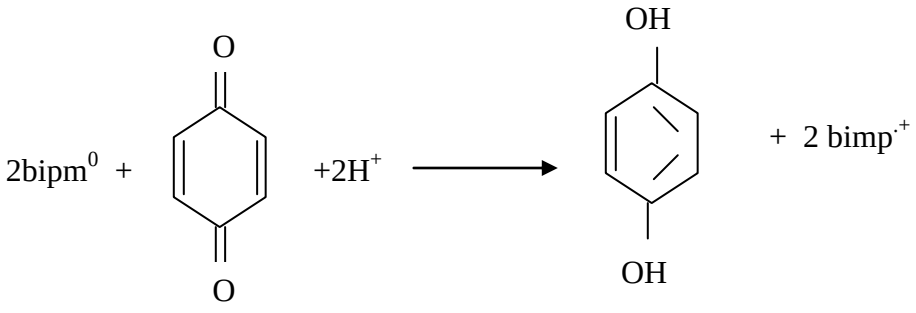

Fig 2.5 : *Redox reduction of neutral bipyridilium to radical cationic form the reducing species is the 1,4 benzoquinone formed at the anode during the charge injection*

Another possible process for the conversion of $bipm^{0}$ into $bipm^{+\cdot}$ is given by the comproportionation reaction 2.6 [31,32]:

$$bipm^{2+}+bipm^{0}=2bipm^{+\cdot} \qquad 2.6$$

This latter mechanism needs more discussions. In fact, evidence for the dimer being the intermediate product of comproportion comes from RRDE (rotated ring-disc electrode) analyses[33] and in situ spectroelectrochemistry [34]. The dimer is thought to have a sandwich-type structure, with two radical cations lying face to face and linked by a π–π'-bond

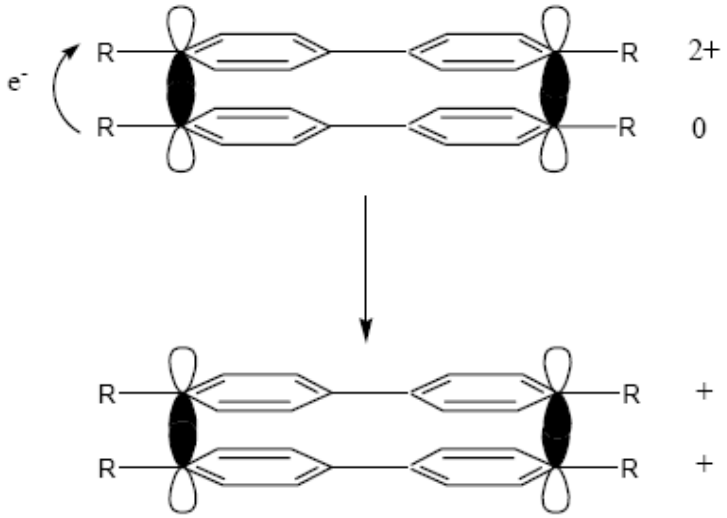

Fig.2.6: *Schematic diagram showing the mechanism of bipyridilium comproportionation: intramolecular electron-transfer yields a radical cation dimer, which dissociates to form monomer units*

The transition state complex (TS) for comproportionation is thought to have the same structure as the dimer (above), with $bipm^{2+}$ and $bipm^{0}$ moieties being parallel to promote the electron transferring through the π–π-bonds. Comproportionation reaction is strictly related to the

dimerization equilibrium. Our results indicate that the dimer is not a stable product in the electrochromic solid film object of this study, but we suppose that factors which prevent the formation of the dimer can also avoid comproportionatin reaction.

This is more evident in Fig. 2.7.

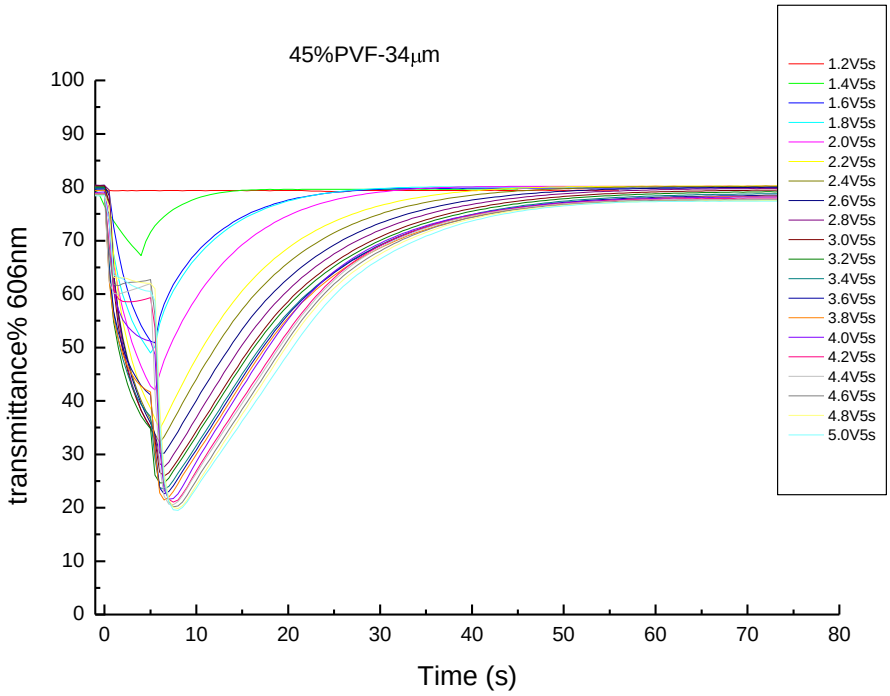

Fig2.7:. *Transmittance at 606 nm, measured as function of time and voltage pulse amplitudes, when voltage pulses having the same pulse length of 5 s have been applied to an EC cell 30 μm thick, containing 45 wt% PVF, 4 wt% ethyl viologen diperchlorate, 2 wt% hydroquinone and 49 wt% propylene carbonate.*

In this figure the transmittance is reported as function of the time and voltage pulse amplitudes, when voltage pulses 5 s long are applied to an EC cell containing 45% PVF and having a thickness of 30 micron. From this figure we can draw that during the dc pulse application the transmittance decreases. After the removal of the pulse the transmittance keep decreasing and we can see the formation of the flex.

In order to analyze the effect of the thickness of the film and the amount of polymer on the operation of our electrochromic device, we have brought back in the diagrams reported in Fig.s 2.8-2.12 the transmittance obtained from different thick devices, where the content of PVF, and then the "hardness", has been progressively increased. In fig. 2.8 we report the response to voltage pulses of various amplitudes (1.8V, 2.2V, 2.4V, 2.6V) and the same pulse length of 5 sec. The voltages have been applied to the cells containing 35% of PVF, 4 wt% ethyl viologen diperchlorate, 2 wt% hydroquinone and 59 wt% propylene carbonate with cell thickness of 30 μm (black line), 60 μm (red line), 90 μm (green line).

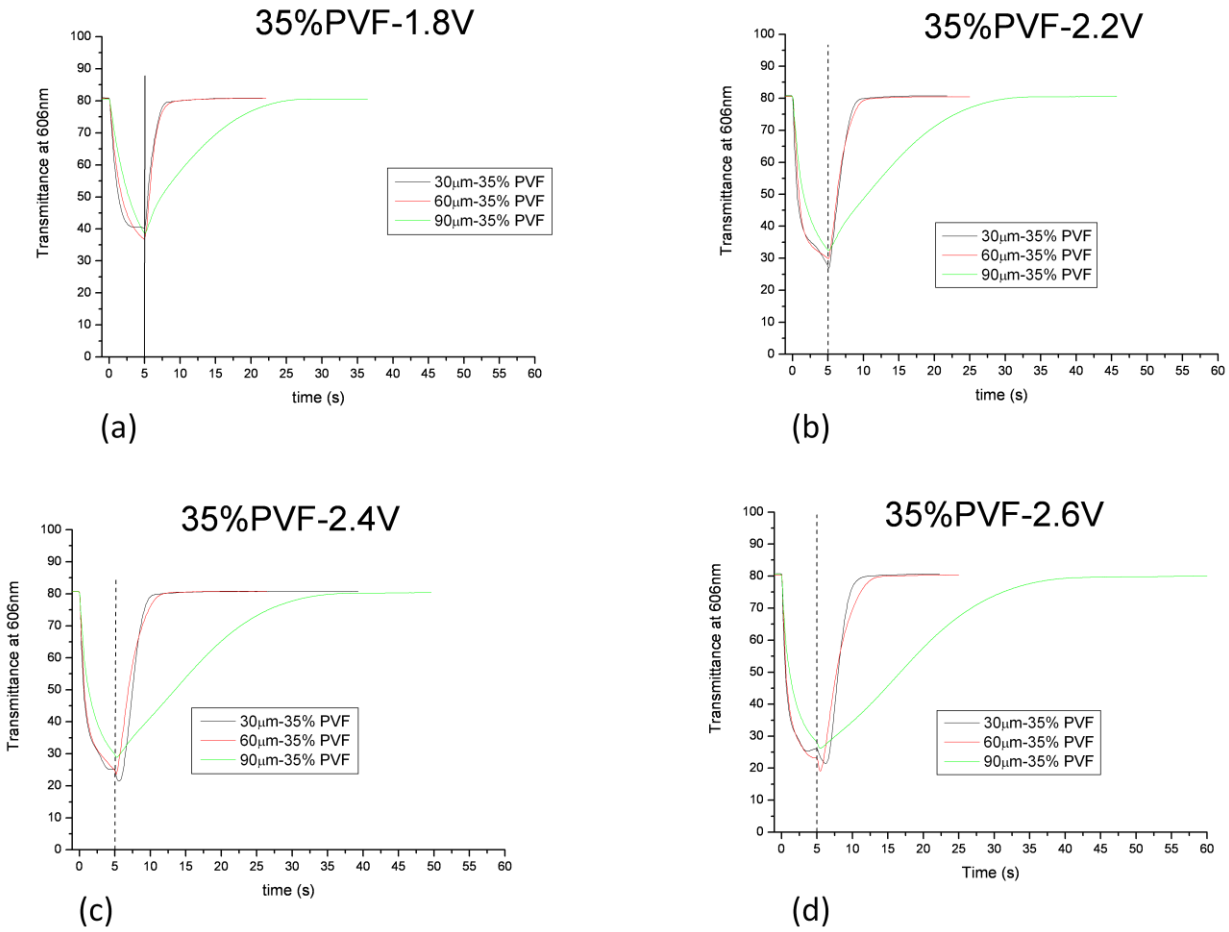

Fig. 2.8: *Transmittance measured at 606 nm as a function of time at different voltage pulse amplitudes (a) 1.8V, (b) 2.2V, (c) 2.4V, 2.6V (d); values obtained for the same pulse length from samples containing 35% of PVF, 4 wt% ethyl viologen diperchlorate, 2 wt% hydroquinone and 59 wt% propylene carbonate, having cell thicknesses of 30μm (black line), 60μm (red line), 90μm (green line). The dashed vertical line indicates the application time of the voltage.*

From figure 2.8 we can observe that the transmittance decreases during the dc pulse application, due to gradual increase of the population of radical cation ($bipm^{+\cdot}$). At 1.8 V (Fig.2.8 a) and 2.2V (fig.2.8 b) the absorption decreases (increased transmittance) immediately after the pulse voltage has been removed (right side of the dotted line). Increasing the pulse voltage to 2.4V (Fig. 2.8 c) the absorption doesn't decrease immediately, after the pulse voltage has been removed, but keeps increasing for a while. This is more evident for the sample with thickness of 30μm. Increasing the pulse voltage to 2.6V (Fig.2.8 d) the decreasing of transmittance is evident, not only in the sample with thickness of 30μm, but still in the sample with thickness of 60μm. The thicker film (90μm), even going to 2.6V, does not exhibit (if not slightly) an increase of absorption (decreased transmittance) after removing the electric pulse.

In figure 2.9 the same experiment presented in Fig. 2.8 is reported, but in this case the voltages have been applied to a cell containing 37% of PVF, 4 wt% ethyl viologen diperchlorate, 2 wt% hydroquinone and 57 wt% propylene carbonate.

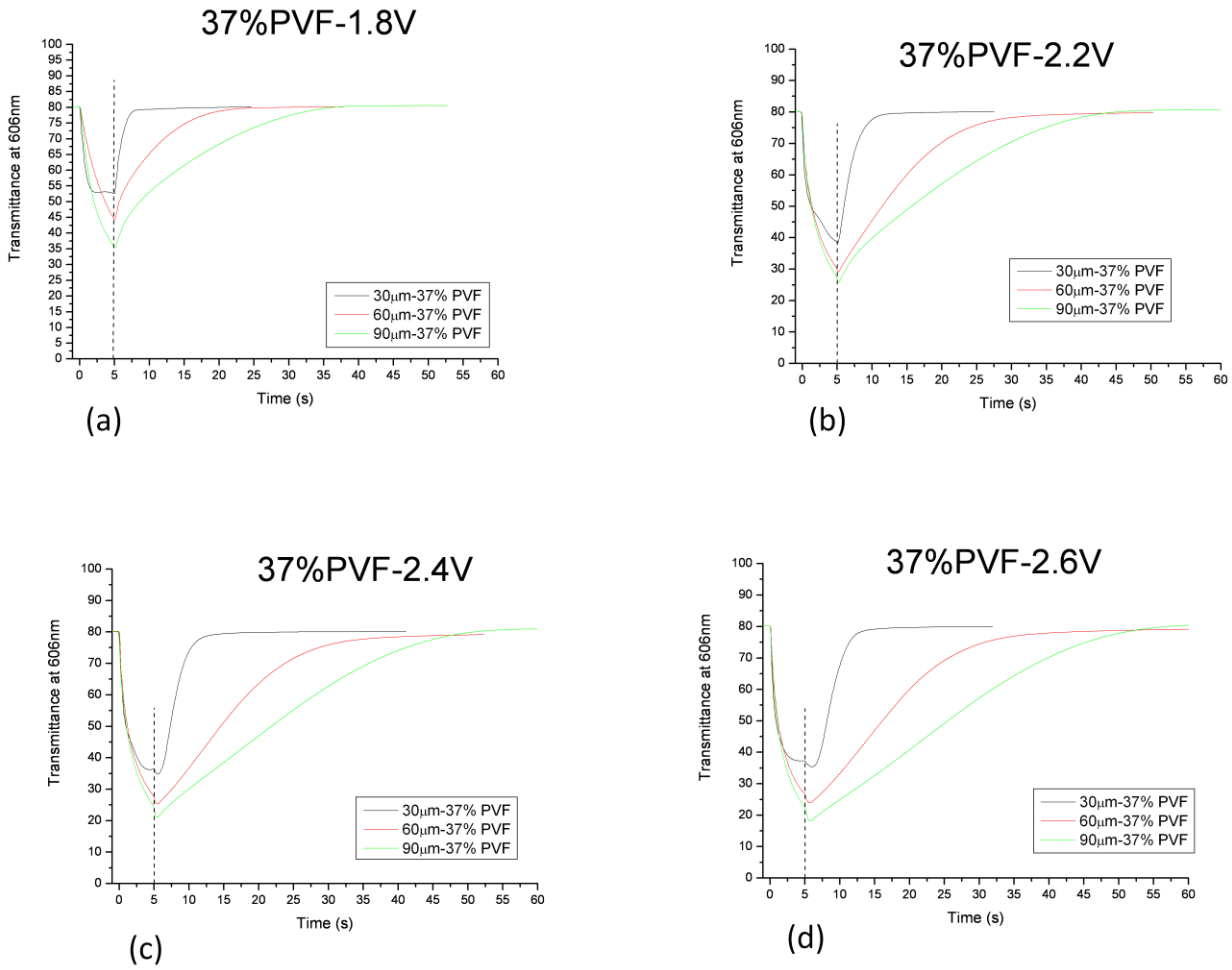

***Fig. 2.9**: Transmittance measured at 606 nm as a function of time at different voltage pulse amplitudes (a) 1.8V, (b) 2.2V, (c) 2.4V, 2.6V (d); values obtained for the same pulse length from samples containing 37% of PVF, 4 wt% ethyl viologen diperchlorate, 2 wt% hydroquinone and 57 wt% propylene carbonate, having cell thicknesses of 30μm (black line), 60μm (red line), 90μm (green line). The dashed vertical line indicates the application time of the voltage.*

An inspection of figure 2.9 evidences that the sample containing 37% PVF behaves as the sample containing 35% PVF. Up to 1.8V (fig.2.9a) and 2.2V (fig.2.9b) transmittance increases (bleaching of the EC film) immediately after removing the electric pulse (at right of the dotted line). Increasing the applied voltage up to 2.4V (Fig. 2.9c) and 2.6V (Fig. 2.9d), the film continues to colour even after the electrical pulse has been removed, as shown by the decrease of transmittance at right of the dotted line in figures 2.9 c and 2.9 d. This is less evident in thicker films (60μm and 90μm).

In the figure 2.10 it is shown the behaviour of the sample containing 40% of PVF, 4 wt% ethyl viologen diperchlorate, 2 wt% hydroquinone and 54 wt% propylene carbonate.

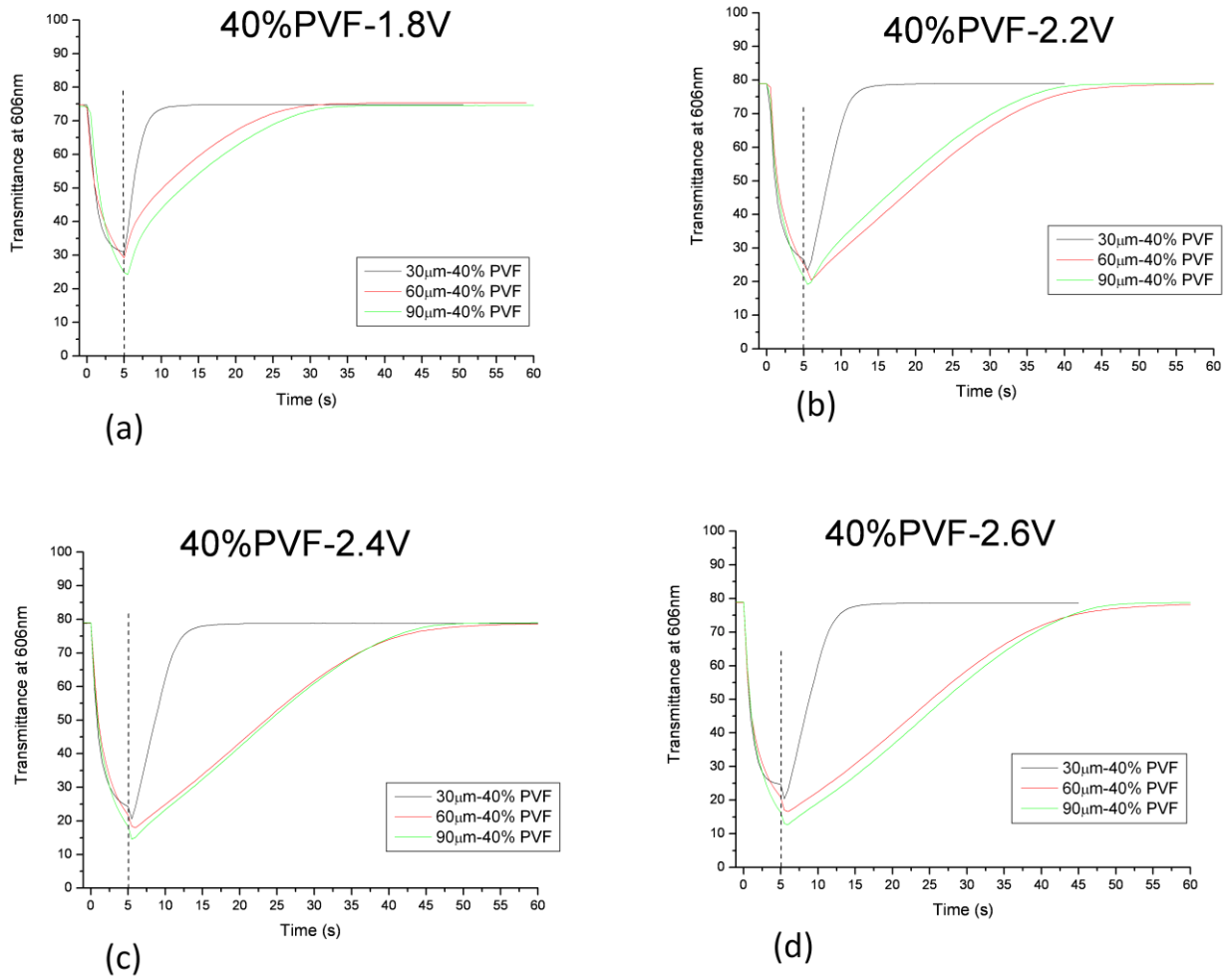

Fig. 2.10: *Transmittance measured at 606 nm as a function of time at different voltage pulse amplitudes (a) 1.8V, (b) 2.2V, (c) 2.4V, 2.6V (d); values obtained for the same pulse length from samples containing 40% of PVF, 4 wt% ethyl viologen diperchlorate, 2 wt% hydroquinone and 54 wt% propylene carbonate, having cell thicknesses of 30μm (black line), 60μm (red line), 90μm (green line). The dashed vertical line indicates the application time of the voltage.*

The increase in coloration of ECD, after having turned off the electrical pulse, occurs at lower voltages than those at which the same phenomenon occurs in softer films (35% and 37% of PVF). From the graphs in figure 2.10 it is evident that at 1.8 V (fig. 2.10a) the sample turns colorless immediately after the electrical pulse has been turned off (increase in transmittance at the right side of dotted line), while already at 2.2V (fig.2.10b), it is evident the increase in coloration (decrease in transmittance) of the film even after the electrical pulse has been removed. This effect is more pronounced in the thinner (30μm) film and is less pronounced in thicker films (60μm, 90μm); it becomes more intense by increasing the applied voltage (fig. 2.10c,d).

For the harder samples, containing 43% of PVF(fig. 2.11) and 45% of PVF (fig.2.12) this trend is confirmed. While at 1.8V, after removing the electrical pulse, the EC film turns colorless immediately, at 2.2 V it keeps a further coloration when the electrical pulse has been switched off (fig.2.11b, 2.12b), as well as we had seen in the sample containing 40% PVF. This phenomenon is even more pronounced at higher voltages: 2.4 V (fig.2.11c, 2.12c) and 2.6V (fig.2.11d, 2.12d).

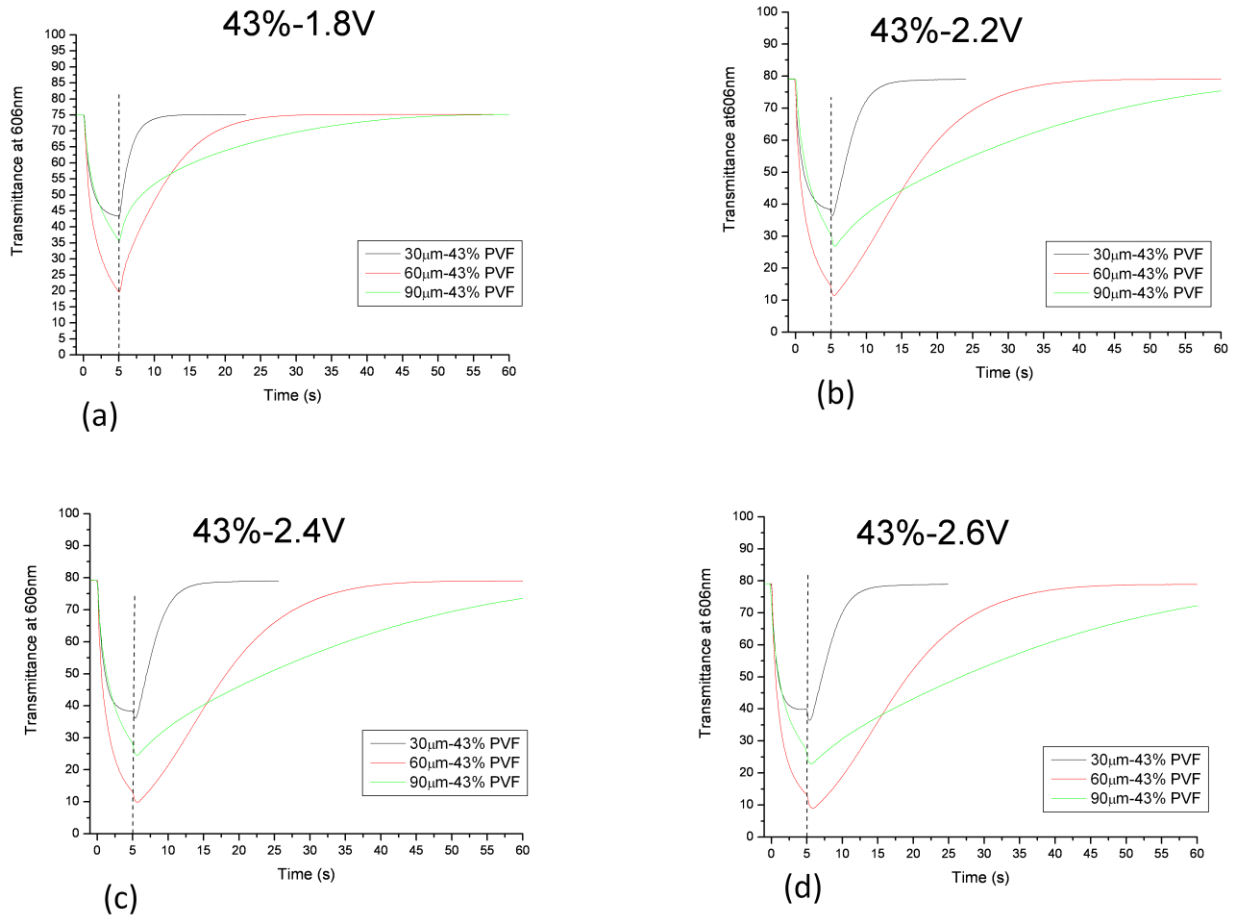

***Fig. 2.11**: Transmittance measured at 606 nm as a function of time at different voltage pulse amplitudes (a) 1.8V, (b) 2.2V, (c) 2.4V, 2.6V (d); values obtained for the same pulse length from samples containing 43% of PVF, 4 wt% ethyl viologen diperchlorate, 2 wt% hydroquinone and 51 wt% propylene carbonate, having cell thicknesses of 30μm (black line), 60μm (red line), 90μm (green line). The dashed vertical line indicates the application time of the voltage.*

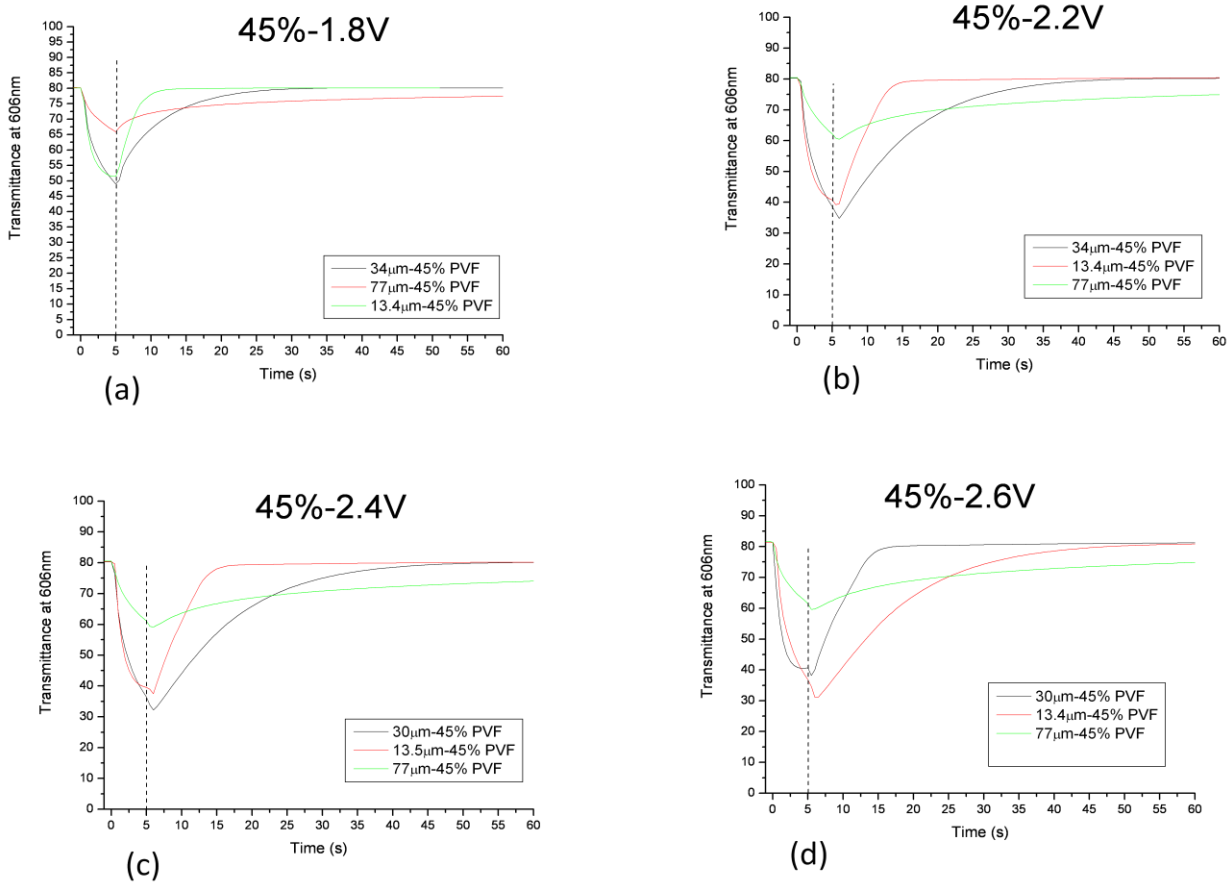

***Fig. 2.12**: Transmittance measured at 606 nm as a function of time at different voltage pulse amplitudes (a) 1.8V, (b) 2.2V, (c) 2.4V, 2.6V (d); values obtained for the same pulse length from samples containing 45% of PVF, 4 wt% ethyl viologen diperchlorate, 2 wt% hydroquinone and 49 wt% propylene carbonate, having cell thicknesses of 30μm (black line), 60μm (red line), 90μm (green line). The dashed vertical line indicates the application time of the voltage.*

The analysis of the graphs presented in Figures 2.8/9/10/11/12, allows us to conclude that the application of voltages greater than 1.8V causes some change in the functioning of the ECD.

In fact at high voltages the ethyl viologen neutral no colored species ($bipm^0$ eq.2.3) is formed. The further increase in staining of the EC film after switching off electrical pulse can be ascribed to the reoxidization (eq. 2.4) of the neutral species into the radical monocation $bipm^{+\cdot}$ colored species, whose population gives rise to an additional film coloration. The bleaching of the film occurs through the oxidization of the radical monocation which is transformed into the not colored dication ($bipm^{2+}$ eq. 2.5).

If our interpretation is correct, transmittance data presented in Fig.s 8-12 will indicate that in our ECD second reduction (eq. 2.3) doesn't occur at voltages lower than 1.8 V, either for the hardest samples. So we have decided to follow the trend over time of the curves of transmittance when voltage pulses of this amplitude have been applied, measuring the transmittance using progressively longer driving times. The figure below (Fig.2.13) shows the results obtained for the sample containing 43% of PVF and cell thicknesses 30-60-90μm. The thinner sample (Fig.2.13a) reaches steady state, where the concentration of the species $bipm^{+\cdot}$ does not change over time, after about 7 seconds. In thicker samples (Fig.2.13b,c) we can see that no stationary region appears, even during the colouring process up to 25-30 sec. of driving time, the absorption keeps increasing only in connection of an increasing of the charging time.

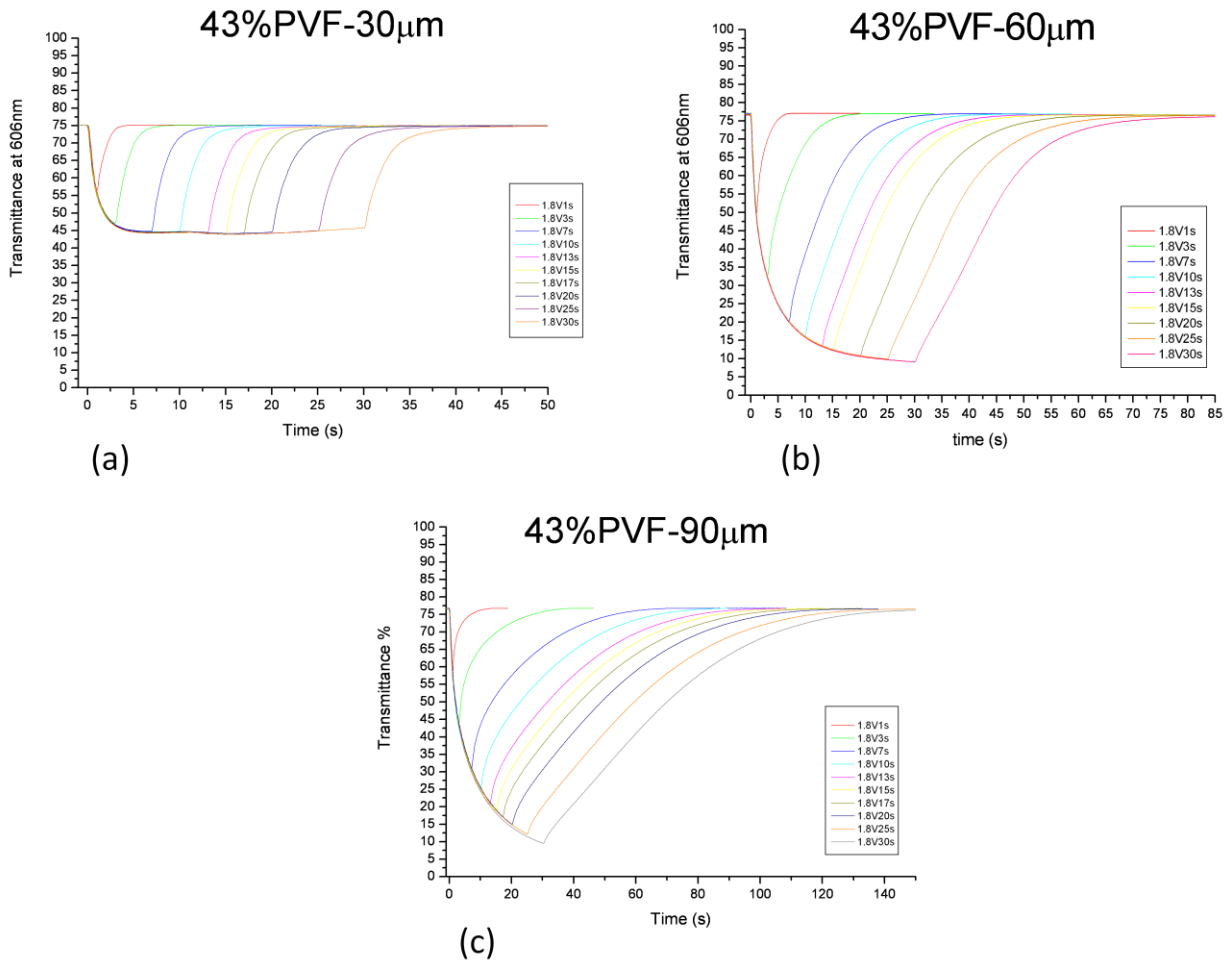

fig2.13: *EC response to different time long voltages. Transmittance of EC cell at 606 nm, as function of time and applied voltage dc pulse of 1.8V. Voltages have been applied to devices containing 43 wt%PVF, 4 wt% ethyl viologen diperchlorate, 2 wt% hydroquinone and 51 wt% propylene carbonate with cell thicknesses of 30μm, 60μm, 90μm.*

The contrast ratio CR is an important parameter to characterize the behaviour of an ECD.

We have defined this parameter in Chap. 1,

$$\mathbf{CR} = \frac{\boldsymbol{R_0}}{\boldsymbol{R_x}}$$

$\mathbf{R_0}$ is the transmittance value before pulse application, $\mathbf{R_x}$ is the transmittance value at the end of pulse; their values are experimentally measured. To study the effect of the second reduction of the bipyridinium ion on the behaviour of **CR** we have reported this parameter, calculated when voltage pulses of a fixed 5s pulse length are applied to different thick cells, as function of the voltage pulse amplitude. Then we have reported **CR** as function of the pulse length, for a fixed voltage pulse amplitude of 1.8 V.

We have performed our calculations on samples with a different content of PVF, that is to say a different softness. Fig. 2.14 refers to the softer sample, containing 35% of PVF, while next figures show the behaviour of CR obtained for the ECD based on films presenting a progressive increase in the content of PVF, that is a progressively increase in the hardness: 40% (Fig.2.15), 43% (Fig. 2.16), 45% (Fig.2.17), 50% (Fig 2.18).

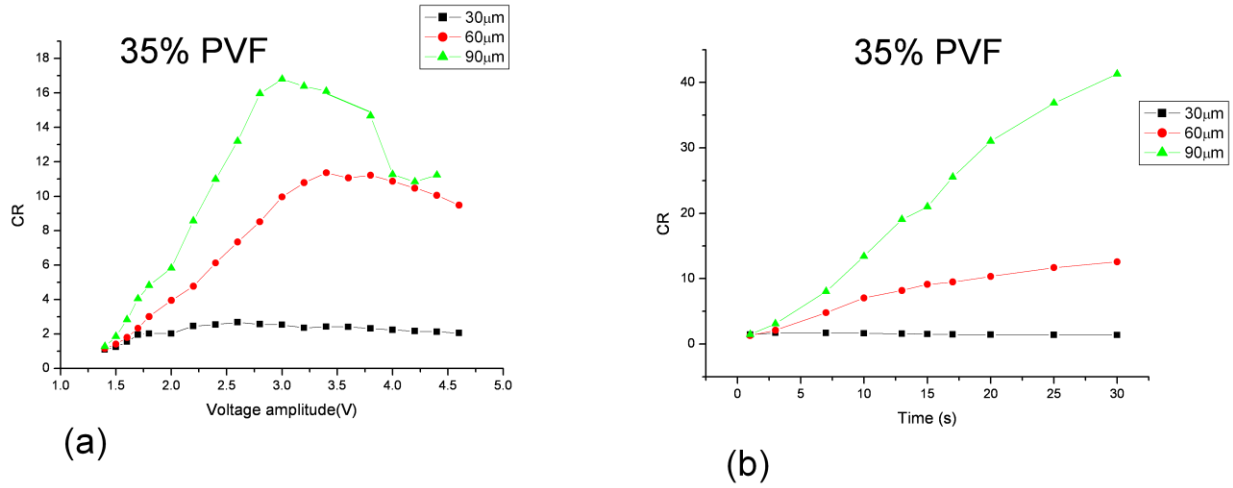

Fig.2.14: *CR ratio as function of pulse voltage, for a fixed application time of 5 sec (a) and as function of the pulse length, for a fixed voltage pulse amplitude of 1.8V (b). Voltage pulses have been applied to devices 30μ (black line), 60 μ (red line), 90 μ (green line) thick. containing 35% PVF, 4% ethyl viologen diperchlorate, 2% hydroquinone , 59% propylene carbonate.*

Paying a deep attention to observing Fig. 2.14a, we can say:

1) The values of CR are enough high (at least for the samples with thickness of 60 and 90 micron) that can allow the human eye to perceive the colour variation induced by application of the voltage pulse.
2) The contrast ratio, under the same voltage pulse, becomes more and more enhanced by increasing the thickness, probably since increasing the thickness the number per surface of active electrochromic molecules increases.
3) For the same thickness, the contrast ratio becomes more and more enhanced by increasing the voltage pulse amplitude up to 3.0-3.5 volt. If the voltage pulse amplitude is greater

than 3-3.5 volt the CR values decrease. This is probably due to the formation of the not coloured bipm^0 species, occurring at high voltages, which reduces the coloured radical monocation concentration. The formation of the neutral species, according to the observation of Fig. 2.8, already starts at 2.4 V, but its effect on the CR ratio, which is directly connected to the human eye perception, is observed at higher voltages, when the population of bipm^0 has reached considerable values.

From the analysis of the figure 2.14b we can argue that:

1) for pulse lengths higher than 5 sec. (Fig.2.14b) the thicker samples have the better CR ratio
2) the increase of the charging time allows the enhancement of the number of coloured molecules per surface unit. This effect is more evident for the thicker sample, in with CR drastically increases in time.

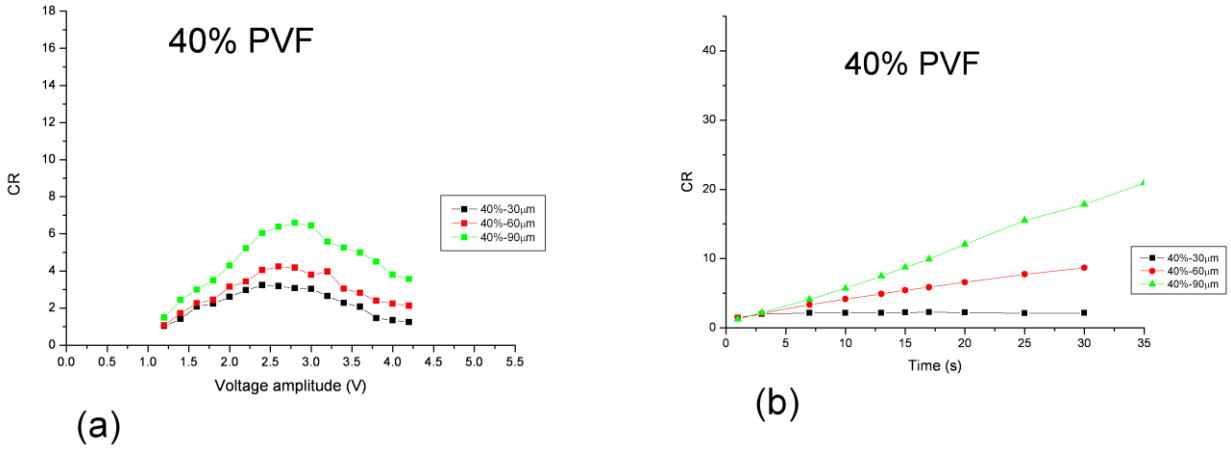

Fig.2.15: *CR ratio as function of pulse voltage, for a fixed application time of 5 sec (a) and as function of the pulse length, for a fixed voltage pulse amplitude of 1.8V (b). Voltage pulses have been applied to devices 30μ (black line), 60 μ (red line), 90 μ (green line) thick. containing 40% PVF, 4% ethyl viologen diperchlorate, 2% hydroquinone , 54% propylene carbonate.*

From the qualitative analysis of graphics presented in Fig. 2.15-2.18 we obtain the same results of precedent sample containing 35% PVF. In Fig. 2.15 CR data obtained from ECD device containing 40% PVF can be inspected. It is possible to notice that the CR values are smaller than the values of the sample containing 35% PVF. The number per surface of coloured molecules decreases, probably owing to the greater amount of polymer The film is very hard, with respect to previous one, and hinders both the mass transport to the electrode and the redox hopping,(process probably involved in the coloration kinetic).

Moreover the pulse voltage corresponding to maximum CR (2.5-3.0V) is smaller than the pulse voltage corresponding to maximum CR of sample containing 35%PVF. Indeed from the analysis of Figure 2.10, we deduced that at 2.2V is formed species $bipm^0$ not colored. Probably, its quantity increases with the applied field

Figures 2.16 reports CR data obtained from the sample containing 43% PVF.

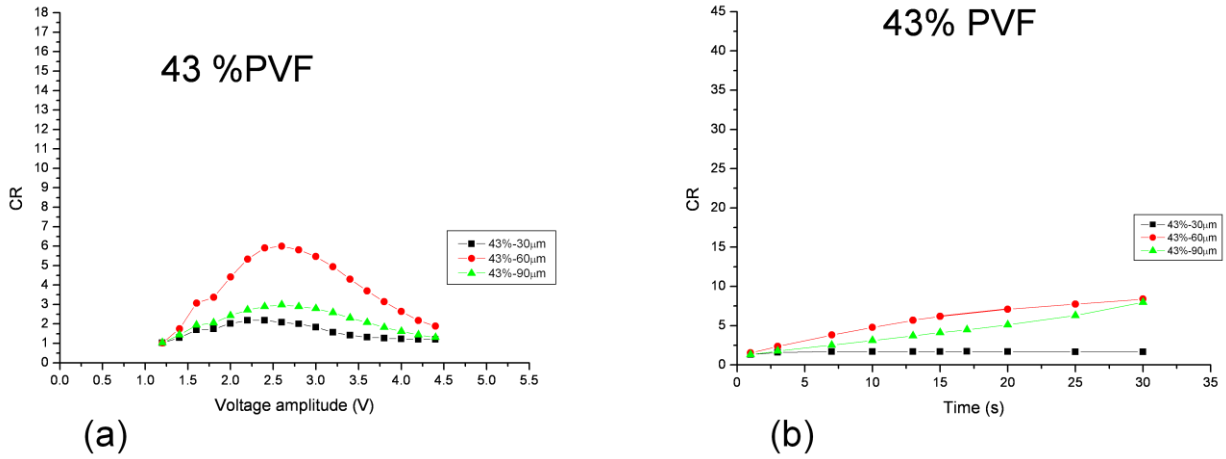

Fig.2.16: *CR ratio as function of pulse voltage, for a fixed application time of 5 sec (a) and as function of the pulse length, for a fixed voltage pulse amplitude of 1.8V (b). Voltage pulses have been applied to devices 30µ (black line), 60 µ (red line), 90 µ (green line) thick. containing 43% PVF, 4% ethyl viologen diperchlorate, 2% hydroquinone , 51% propylene carbonate.*

Looking at the graph reported in Fig. 2.16a, we can draw out these conclusions:

1) Under the same pulse voltage, the behaviour of the sample with thickness of 30 and 60 μm is the same of that seen for the previous concentrations 35-40% of PVF, but the thicker sample has CR values lower than the less thick samples, probably owing to the higher stiffness of this sample with respect to the stiffness of the previous one. The reason of this effect can probably ascribed to the greater amount of polymer which slows down the injected charge diffusion towards the inner layers of the film. This slowing down causes the lowering of CR values , with respect to sample containing 35% and 40% PVF, and, besides a certain thickness there is an inversion of the curve trend: the values of CR corresponding to the 90 μ thick sample are lower than those for the 60 μ sample. Probably by increasing the thickness of the film, for the same stiffness (quantity of PVF), the charge injected spreads with greater difficulties to the inner layers and then the display is colored less intensely.
2) The curve trend is the same to that previously seen when samples having the same thickness are considered. In this case the values of CR increase with the voltage applied, reaching the maximum at about 2.5-3.0 V

From the analysis of the figure 2.16b we can tell:

1) When samples having the same thickness are compared considering their behaviour as a function of the charging time, it must be noticed that the CR value of the 90 μ thick sample increases very quickly when the charging time is increased, with respect to the CR value of the 30 μ thick one. This confirms that the increasing of pulse voltage dc and increasing the time of charge have different effect on the ECD.

Figures 2.17 and 2.18 report the CR values of the samples containing 45% PVF (fig.2.17) and 50%PVF (Fig.2.18) with the cells of different thickness. Increased rigidity of the film causes a

drastic decrease of the values of CR, in particular those corresponding to the thicker films. The curves for the three different thicknesses are gathering to the point that it isn't possible to distinguish from each other.

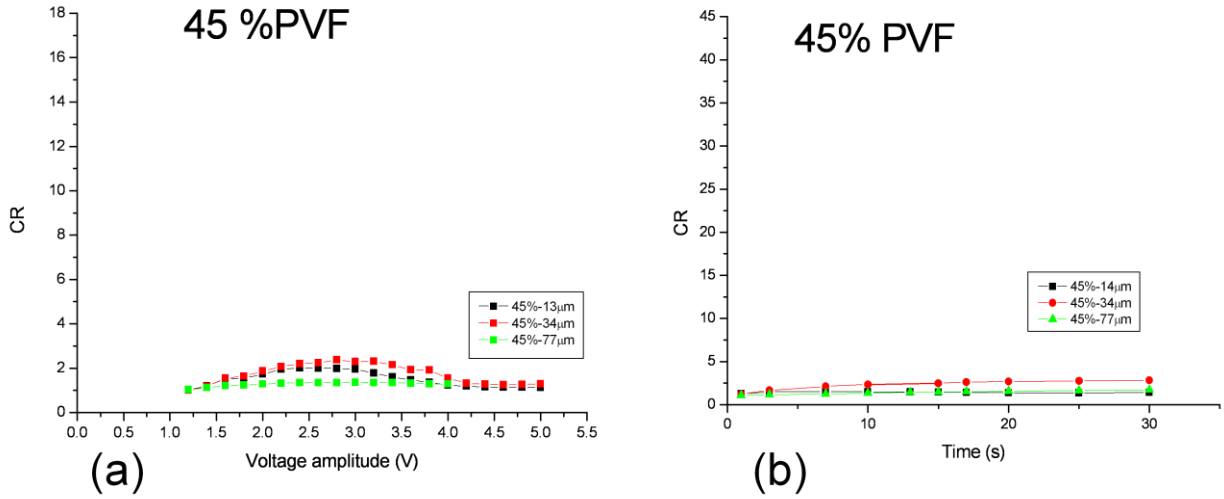

Fig.2.17: *CR ratio as function of pulse voltage, for a fixed application time of 5 sec (a) and as function of the pulse length, for a fixed voltage pulse amplitude of 1.8V (b). Voltage pulses have been applied to devices 30µ (black line), 60 µ (red line), 90 µ (green line) thick. containing 45% PVF, 4% ethyl viologen diperchlorate, 2% hydroquinone , 49% propylene carbonate.*

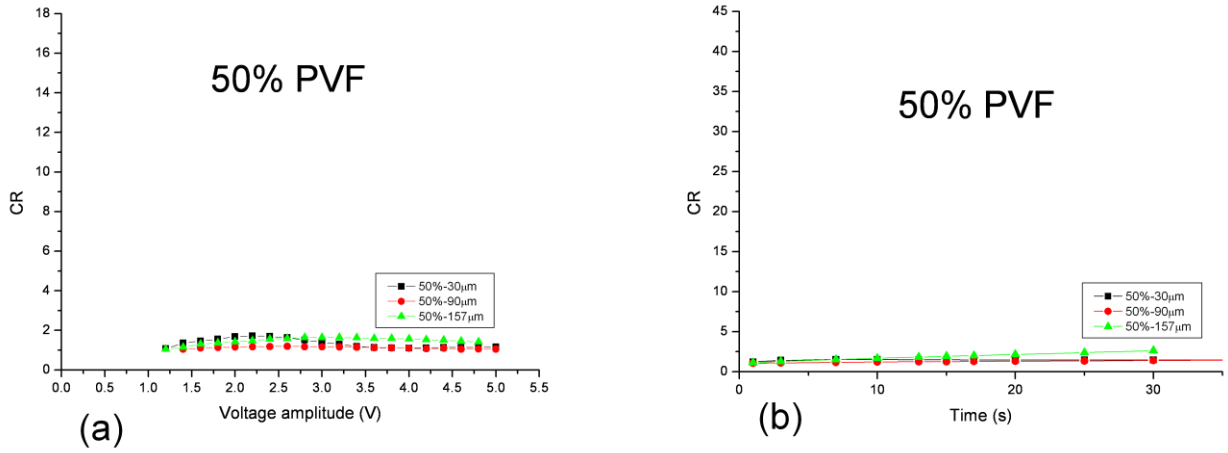

Ffig.2.18: *CR ratio as function of pulse voltage, for a fixed application time of 5 sec (a) and as function of the pulse length, for a fixed voltage pulse amplitude of 1.8V (b). Voltage pulses have been applied to devices 30μ (black line), 60 μ (red line), 90 μ (green line) thick. containing 40% PVF, 4% ethyl viologen diperchlorate, 2% hydroquinone , 44% propylene carbonate.*

Another important parameter that must be considered in order to understand the operation of the ECD is the response time.

- T_{on} is the time required for an ECD to achieve 95% of the colour

- T_{off} is the time required for on ECD to achieve 95% of the maximum transmittance value starting from the minimum transmittance value. This minimum was not always reached as the pulse was turned off, because for high voltage values reaction 2.5 was occurring.

In this figure we report T_{on} and T_{off} as a function of voltage pulse amplitude, for samples containing 35%PVF (Fig.2.18a), 40% PVF (Fig.2.18b) and 45% PVF (Fig.2.18c).

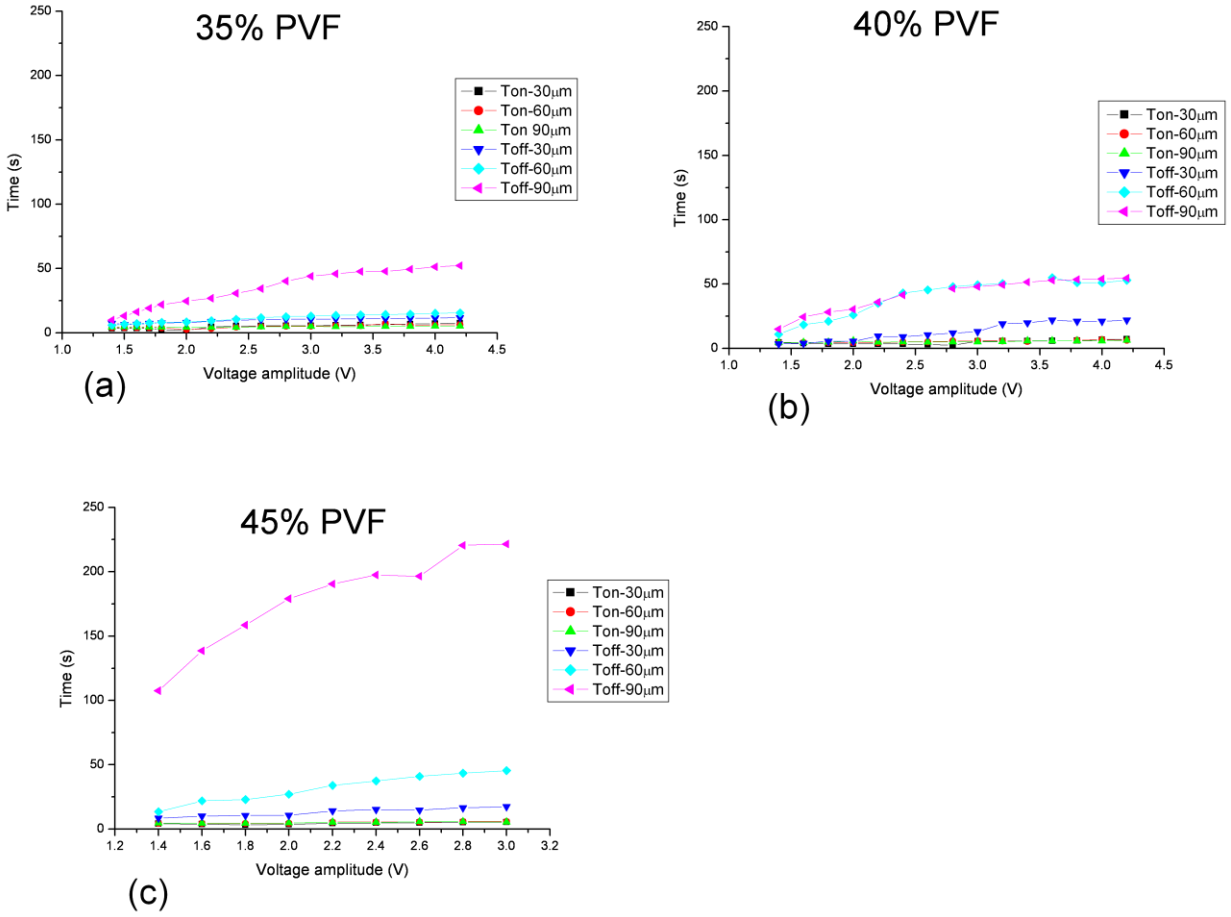

Fig.2.19: *T_{on} (line black, red, green) and T_{off} (line blue, cyan, magenta) value as function of different voltages dc pulse of 5 sec. applied to the films containing: 35% of PVF (a), 40% of PVF (b), 45% of PVF (c); and cells thickness of: 30μm , 60μm , 90μm .*

From the analysis of the above figures we can argue that:

- The values of T_{on} are not dependent on the thickness of the film and the applied voltage; they fall within a range of values between 3 and 5 seconds for whatever content of PVF.
- The values of T_{off} increase with the thickness of the film and the applied voltage. This increase is even more evident by increasing the hardness of the film EC (higher concentration of PVF). Probably the reduced mobility of the EC molecules produces a negative effect on the process of bleaching, but also the amount of $bipm^0$ in the EC mixture can influence the rate of the spontaneous discoloration of the device.

REFERENCES

[1] J.R. Platt *Chem. Phys*. **1961**, 34,862

[2] P. M. Monk, R. J. Mortimer, D.R. Rosseinsky *Electrochromism: Foundamentals and Application*; VCH: Weinheim,**1995**

[3] R. Srinivasa, D. Lin. R. French, T.F. Guarr, H.J. Byker, K.L. Baumann, D.A. Theiste *U.S. Patent 6037471,* **2000**

[4] . Srinivasa, D. Lin. R. French, T.F. Guarr, H.J. Byker, K.L. Baumann, D.A. Theiste *U.S. Patent 6037471,* **1999**

[5] K.L. Baumann, H.J. Byker, T.F. Guarr, K.E. Seigrist, D.A. Theiste, D.D. Winkle *US Patent 6020987,* **2000**

[6] I.V. Shelepin, V.I. Gavrilov, V.A. Barechevskii, N.I. Karpova *Elektrokhimiya* **1997**, 13, 404

[7] H.J. Byker *US Patent 4902108,* **1990**

[8] H. Tsutsumi, Y. Nakagawa, K. Tamura *Sol. Energy Mater. Sol. Cells* **1995**, 39, 341

[9] H. Tsutsumi, Y. Nakagawa, K. Miyazaki, M. Morita, Y. Matsuda *J. Pol. Sci* **1992**, 30, 1725

[10] H. Tsutsumi, Y. Nakagawa, K. Miyazaki, M. Morita, Y. Matsuda *Eletrochim. Acta* **1992**, 37, 369

[11] N. Leventis, Y. Chung *US Patent 5818636*, **1998**

[12] N. Leventis, Y. Chung *US Patent 5457564*, **1995**

[13] M.S. Wrighton, D.C. Bookbinder *US Patent 4473695*, **1984**

[14] G. Chidichimo, D. Cupelli, M. Be Benedittis, G. De Filpo, J. Lanzo, F.P. Nicoletta, B. Gabriele, G. Salerno, L. Veltri *European Patent WO 2006008776*, **2006**

[15] G. Chidichimo, M. De Benedittis, J. Lanzo, B. C. De Simone, D. Imbardelli, B. Gabriele, L.Veltri, and Giuseppe Salerno,*Chem.Mat*.,**2007**,19,353-358 (a). M. De Benedittis *Ph.D. thesis* "Solar Control Solid Organic Electrochromic Films" Calabria University, **2006** (b).

[16] P. M. S. Monk, *The Viologens: Physicochemical Properties, Synthesis and Applications of the Salts of 4,4'-Bipyridine* John Wiley & Sons, **1998**.

[17] E. Kosower, J. L. Cotter, *J. Am.Chem.Soc.* **1964**, *86*, 5524.

[18] N. J. Goddard, A.C. Jackson, M.G. Thomas, *J. Electroanal. Chem.* **1983**,159, 325.

[19] J.E. Downes, *J.Chem.Soc.* **1967**, *C*, 1491.

[20] H. Sato, T. Tamamura, *J. Appl. Polym. Sci.* **1979**, *24*, 2075.

[21] M. S. Simon, P. T. Moore, *J.Polym. Sci. Chem. Ed.* **1975**, *13*, 1.

[22] I.V. Shelepin, et al., *Elektrokhimia (English Transaction),* 13, **1977**, 346.

[23] R.S. Becker and W.E. Wentworth, *J. Am. Chem. Soc*.,85**, 1963**, 2210.

[24] D.B. Brown (ed.), *Mixed-Valence Compounds in Chemistry, Pysics andBiology,* Reidel Publishing Company, Dordrecht, Holland, (**1980**).

[25] M. Macchione, G. De Filpo, A. Mashin, F.P. Nicoletta, G. Chidichimo**,** *Advanced Materials,* 15, **2003**, 327.

[26] W.L. Tonar et al., *United States Patent, 5679283,* **1987**.

[27] W.L. Tonar et al., *United States Patent,* 5888431, **1999**.

[28] W.L. Tonar et al., *United States Patent,* 5928572, **1999**.

[29] E. Kosower and J.L. Cotter, *J. Am. Chem. Soc.,* 86, **1964**, 5524.

[30] S. H. Kim, J. S. Bae, S. H. Hwang, T. S. Gwon and M. K.Doh, *Dyes and Pigments,* 33, **1997**, 167.

[31] D.R. Rosseinsky, P.M. S. Monk *J.Chem. Soc. Faraday Trans* **1993**, 89,219

[32] D.R. Rosseinsky, P.M. S. Monk *J.Chem. Soc. Faraday Trans* **1990**, 86,3597

[33] D.R. Rosseinsky and P.M.S. Monk, *J. Chem. Soc. Faraday trans.*, 86**, 1990,** 3597..

[34] P.M.S. Monk, R.D. Fairweather, M.D. Ingram and J.A. Duffy, *J. Chem. Soc. Perkin Trans. II*, 86**, 1992**, 2039.

CHAPTER III

KINETIC

Introduction

In our device (presented in previous chapter) the operational times required for maximize the optical contrast of the order of 5-10 sec, considerably longer than those required for applicative aims. We suppose that that the shortening of these times can be achieved through a deeper analysis of the kinetic mechanisms acting on the film during the colouration and bleaching steps.

The introduction of anodic compounds that can act as donors, shorten the bleaching time of the presented EC films, as it was expected. The shortening is more marked for particular anodic molecules, such as hydroquinone. Without these molecules it has been observed that the film works as a memory device (ref. 15b cap2) The role of the anodic substances will be elucidated in a future publication where the kinetics of the bleaching process will be analysed.

In the present study the chemical reactions occurring in the bulk of the film and in the neighbouring of the electrodes during the colouration process are written and the kinetic equations are derived. Two important points have supported us in tackling the problem of kinetics. The first one has been the observation that a satisfactory colouration of the film can be reached only when samples are exposed to the air. When oxygen is removed our device gains a poor colouration in very long times. Another important point is connected to the fitting of the

experimental absorption curves obtained at different amplitudes of the voltage pulses for a sample of well defined composition and thickness. We observed that the fitting of the data is given by a single exponential equation when the voltage is kept under a threshold value, while it is necessary to add a quadratic exponential term when the voltage exceeds this value.

3.1 Fit of the experimental data

In order to define the kinetic mechanism acting on our film during the stage of coloration, we decided to analyze, for reasons to be discussed below, the one containing 35% PVF and thickness of 90 microns. On this sample we performed kinetic studies, and later electrical studies as will be discussed in the next chapter, disregarding the second reduction, to which are subject bipyridilium species. It was possible because for this particular sample (see chapter 2, Fig.2.7), the second reduction doesn't occur if the voltage is not sufficiently high. This allowed us to simplify the kinetic treatment and is therefore one of the reasons that led us to choose a sample with the above composition.

Indeed, as discussed in chapter 1 (eq. 1.19-1.20) and in chapter 2 (eq. 2.3-2.4), the bipyridilium species follow the following redox process:

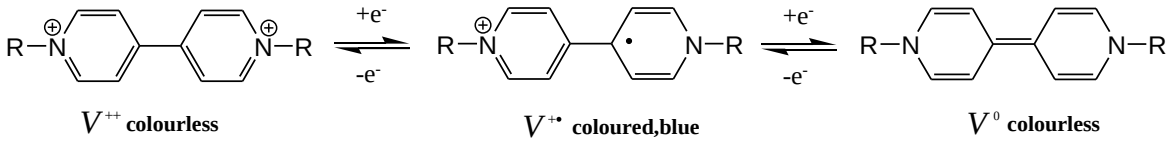

(1)

Fig. 3.1: *Redox processes determining colour changes of the viologen dication.*

In the sample containing 35% PVF and thickness 90 micron, as it can be seen in Fig. 2.8 chapter 2, still at 2.6 volts it is not observed an increase in staining of the EC film after turning off the electrical pulse. This means that neutral ethyl viologen, coming from the second reduction, is not formed or at least its quantity is so small that it cannot be detected by our measures. Having used voltages not higher than 2.6 Volt during our kinetic studies, we assume that only the first reduction of the viologen species can be considered. One other reason that led us to choose the film to 35% PVF for our kinetic studies is the high values of contrast ratio (Fig. 2.14 chapter 2), compared to those of other samples, which allowed us to see by unaided eye color changes of the film due to the application of different electric fields.

In Fig. 3.2 and Fig. 3.3 the absorbance data of a sample containing percentage of polymer (PVF) equal to 35% and a thickness of 90 micron are presented as a function of the pulse length. Data of Fig. 3.2 have been collected when the device was being opened to air, while those presented in Fig. 3.3 have been obtained when oxygen had been removed. It is possible to distinguish between two different behaviours: data recorded at applied voltages lower than 1.8 V (Fig.3.2a,3.3a) and data recorded at applied voltages higher than 1.8 V (Fig.3.2b, 3.3b). For the data related to the aerated sample it is possible to point out that at high voltages (Fig. 3.2b), the absorbance increases with pulse length more rapidly than it was observed at low voltages (Fig. 3.2a). The initial slope of the curve presented in Fig. 3.2b is considerably higher than that observable in Fig.3.2a.

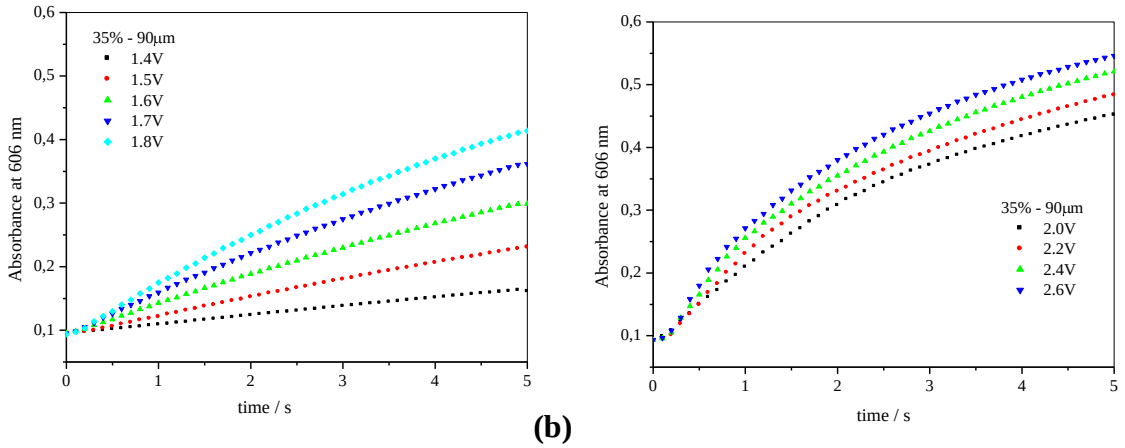

(a) **(b)**

Fig. 3.2 (a),(b): *Absorbance data obtained for the sample in presence of oxygen at various voltage amplitude as a function pulse length. a) behaviour at low voltages: 1.4 V (black squares),1.5 V (red rhombs),1.6 V (green triangles),1.7 V(blue triangles), 1.8 V turquoise rhombs ; b)high voltages: :2.0 V (black squares),2.2 V (red rhombs),2.4 V (green triangles),2.6 V(blue triangles)*

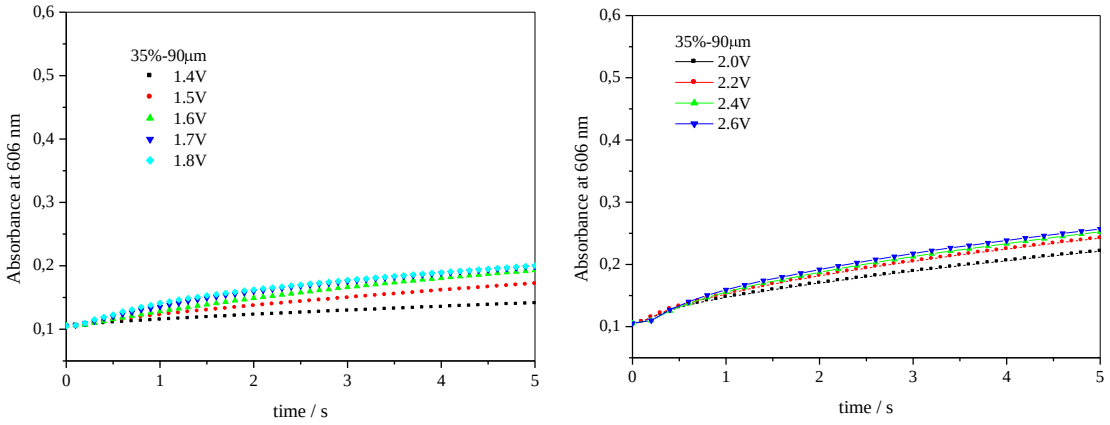

(a) **(b)**

Fig.3.3(a),(b): *Absorbance data obtained for deoxygenated sample at various voltage amplitude as a function pulse length. a) behaviour of low voltages: 1.4 V (black squares),1.5 V (red rhombs),1.6 V (green triangles),1.7 V(blue triangles), 1.8 V turquoise rhombs ; b)high voltages: 2.0 V (black squares),2.2 V (red rhombs),2.4 V (green triangles),2.6 V(blue triangles)*

It is evident that the absorption (corresponding to a more intense blue coloration) is noticeably increased in presence of oxygen. Moreover, while the aerated sample shows a more intense colouration correspondingly to the voltage increase, either beneath or above the threshold value, in the degassed sample the voltage effect is very poor or almost absent, especially for V>1.8 volt. In Fig.3.4 the contrast ratio (CR) obtained from the device at air and in absence of oxygen is reported at various voltages (Fig.3.4a) and different pulse lengths (Fig.3.4b). As it can be seen, the CR exhibited by the degassed device is very poor when compared to that obtained from the device exposed to oxygen. The set of the experimental data presented in Fig.s 3.2-3.4 allowed us to hypothesize that the reduction of oxygen is a relevant step for the kinetic mechanism associated to the operative cycle of the device.

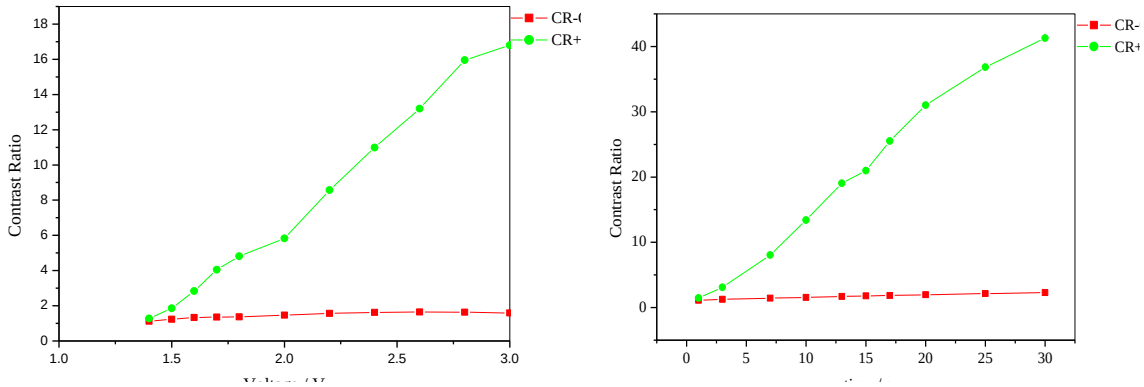

(a) **(b)**

Fig.3.4 a),b): *Comparison between contrast ratios (CR) obtained for aerated (red) and deoxygenated (green) sample as a function of a) Voltage; b) Time.*

Taking into account the experimental data presented, our aim was to study the kinetic processes underlying the functioning of the EC films during the coloring process. For this purpose a fitting procedure was performed on the experimental data presented in Fig. 3.2. We didn't perform the

fitting of the data taken from the degassed sample, which have been shown in Fig. 3.3, because the dependence exhibited by this sample on the applied voltage was very poor and resulted inside the limits of the experimental error. The fitting procedure on the aerated sample gave different results depending on the value of the applied voltage and the equations giving the best fit are different for applied voltages lower than 1.8V and higher than 1.8 V. In the figure 3.5 we presented the fitting performed on experimental data obtained at 1.6 V, presented in fig. 3.2, for the device containing 35% of PVF and thickness 90 μm. For values lower than or equal to 1.8 V, as it is shown on Fig. 3.5, which is obtained at an applied voltage of 1.6 V, the equation giving the best fit was a single exponential equation:

$$y_1 = y_0 + C\left(-e^{-k_1 t}\right) \qquad 3.1$$

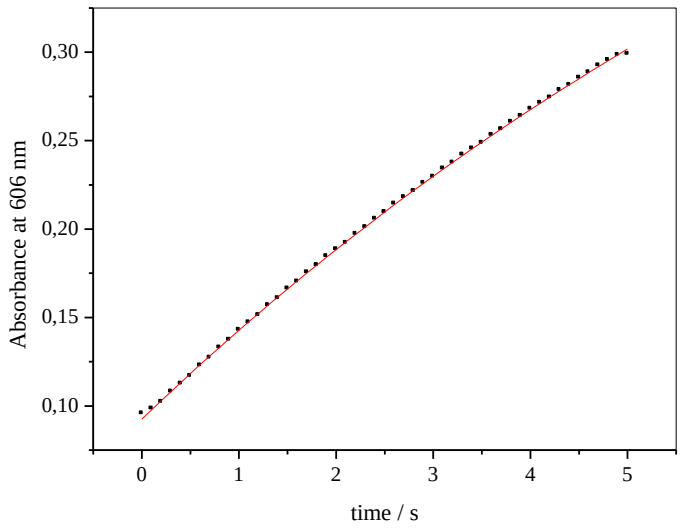

Fig. 3.5: *Fitting of the absorbance data obtained from a sample subjected to a pulse amplitude of 1.6V and pulse length progressively increasing until 5 sec. The black squares describe the experimental data curve, while the red continuous line is the single exponential fitting curve expressed by eq.3.1.*

Table 3.1 presents the values of the parameters governing the single exponential equation (eq. 3.1) giving the best fit of the experimental data shown in fig. 3.2a

The constant term y_0 represents the fraction of absorbance which is present in all the devices and that cannot be related to any active redox species. The term C, which doesn't considerably vary when voltage is increased, is in some way the "weight" of the single exponential mechanism governed by the time constant k_1. In the Kinetics section we will give an interpretation of this parameter k_1 in terms of kinetic mechanisms describing the coloring process occurring inside the film. Table 3.1 shows that this parameter (having the dimension of a time), increases with the applied voltage.

Table 3.1

Values of single exponential curve fitting parameters for various voltages. The percentage error for k_1 kinetic constant ranges from 2 to 7 %. For the lower voltage (1.4V) the presence of a certain amount of noise in the electrooptical measurements didn't allow to get the determination of k_1 by the fitting of the adsorbance data with an error less than 13%.

V	y_0	C	k_1
1.4V	**0.09**	**0.53**	**0.029**
1.5V	**0.09**	**0.59**	**0.054**
1.6V	**0.09**	**0.55**	**0.095**
1.7V	**0.09**	**0.59**	**0.123**
1.8V	**0.09**	**0.60**	**0.159**

For values of the electric potential higher than 1.8 V (data of Fig. 3.6 refer to a potential of 2.4V) the fitting requires the addition of another term. The results obtained employing only a single exponential equation, on experimental data obtained at 2.4 V, are shown on Fig. 3.6a, while on Fig. 3.6b it is possible to appreciate the visible improvement of the fit reached through the addiction of a quadratic exponential term.

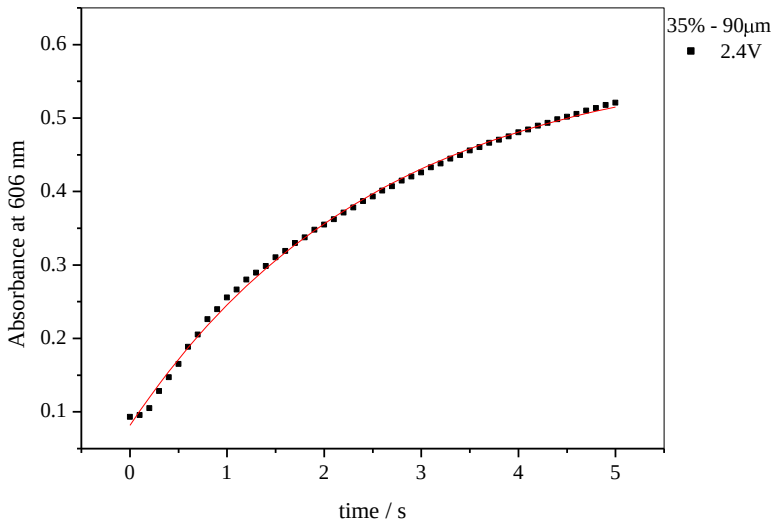

Fig. 3.6a : *Fitting of absorbance data obtained from a sample subjected to a pulse amplitude of 2.4V and a pulse length progressively increasing from 0 to 5 sec. The black squares identify the experimental data points, while the red continuous line is the single exponential fitting curve obeying to eq.3.1*

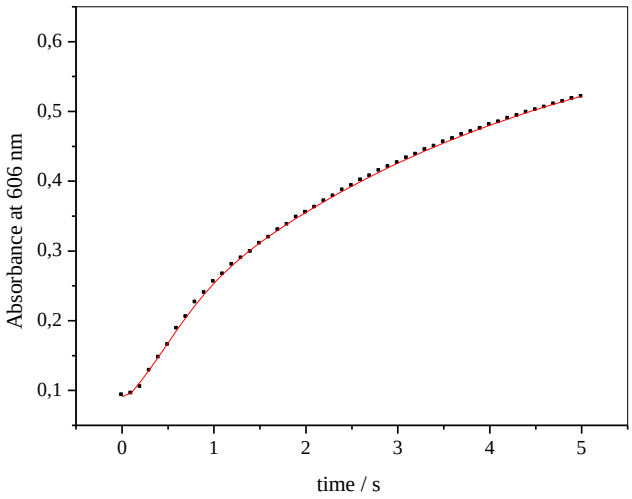

Fig. 3.6b: *Fitting of absorbance data obtained for a sample subjected to a pulse amplitude of 2.4V and a pulse length of 5 sec. The black squares represent the experimental data, while the red continuous line is the fitting curve described by eq.3.2(single exponential function combined with a quadratic exponential term) .*

So the final fitting equation for voltages higher than 1.8 V is:

$$y_2 = y_0 + C\left(-e^{-k_1 t}\right) + B\left(-e^{-k_2 t^2}\right) \qquad (3.2)$$

Table 3.2 presents the values of the parameters governing the y_2 equation (eq. 3.2) giving the best fit of the experimental data presented in Fig. 3.2b. The constant term y_0, as it was expected, has the same magnitude that in the case of the fit presented in Fig.3.5. Also C and k_1 have values and behaviours similar to those obtained from the fit performed by eq.3.1. The parameter B, measuring the weight of the quadratic exponential term, is almost an order of magnitude smaller than C, and is slowly decreasing while the applied voltage is increased. When we are concerned with time constant k_2, it is possible to notice that it exhibits an increase with the higher voltages that is more sensitive when compared to that undergone by the single exponential time constant

k_1. The meaning of k_2 will be given in the Kinetics Section, where this constant will be connected to a particular kinetic mechanism acting on our system.

Table 3.2

*Values of single exponential (***C**,**k_1***) and quadratic exponential (***B**,**k_2***) curves fitting parameters for various voltages. The percentage errors for the* **k_1** *and for the* **k_2** *kinetic constants range respectively from 4 to 7% and from 5 to 10%.*

V	**y_0**	**C**	**k_1**	**B**	**k_2**
2.0V	**0.09**	**0.45**	**0.203**	**0.074**	**0.542**
2.2V	**0.08**	**0.49**	**0.224**	**0.075**	**1.188**
2.4V	**0.08**	**0.52**	**0.259**	**0.064**	**1.780**
2.6V	**0.08**	**0.51**	**0.322**	**0.055**	**2.215**

3.2 Kinetics

In the followings, we will derive the kinetic equations describing the coloration processes in the bulk of the film and in the neighbouring. We will use the letter A to indicate the anodic substance (in this specific case we have used the hydroquinone molecule), V^{++} and $V^{+\cdot}$ to indicate the viologen dication and radical cation respectively. As we have seen from the experimental data presented in the previous paragraph, the oxygen plays an important role in the functioning of the EC film. We assume that at the cathode, near the electrode, the oxygen is reduced and carries

the charge acquired in the EC film where reduces both viologeno that hydroquinone. In both redox reactions the oxygen is transformed into its neutral form by acting as a charge carrier.

We assume that the reduction reactions in our system are:

$$O_2 + e^- \xrightarrow{k_0} O_2^- \qquad \text{at catode} \qquad (3.3)$$

$$O_2^- + 2V^{++} \xrightarrow{k_v} 2V^{+\cdot} + O_2 \qquad \text{in the bulk of the film} \qquad (3.4)$$

not coloured coloured

Eq.s 3.3 and 3.4 allow us to write the kinetic equation for $V^{+\cdot}$ as:

$$\frac{dV^{+\cdot}}{dt} = k_v [V^{++}][O_2^-] \qquad (3.5)$$

The oxidation reactions are:

$$A \xrightarrow{k_3} A^+ + e^- \qquad \text{at anode} \qquad (3.6)$$

$$A^+ + O_2^- \xrightarrow{k_4} A + O_2 \qquad \text{in the bulk of the film} \qquad (3.7)$$

According to eq.s 3.3-3.7 the diffusion equation for the O_2 molecule can be written as :

$$\frac{d[O_2^-]}{dt} = k_0 [O_2] + k_v [V^{++}][O_2^-] + k_3 [A^+][O_2^-] + \vec{\nabla} \cdot \vec{J}[O_2^-] \qquad (3.8)$$

The first term at the right-hand of eq. 3.8 has be written in the hypothesis that application of the pulsed voltage supplies a constant electronic distribution on the surface of the device, and then a

constant electronic concentration (included in the constant k_0). The last term at the right-hand side has added to take into account the diffusion of the small (O_2^-) reduced oxygen molecule.

From the experimental data and from the procedure for fitting these data presented in the previous section, we know that the EC film which is object of study behaves differently depending on the applied voltage. So to solve the equations 3.5 and 3.8 we distinguish two cases: caseI $\phi < \phi_c$(1.8Volt), caseII $\phi > \phi_c$ (1.8Volt).

Case 1: Φ < Φc

Absorbance measurements have been performed under the application of square pulsed voltages of various amplitudes. In the followings, we will use the term voltage and the symbol **Φ** referring to the amplitude of the pulses.

The usage of low voltages prevents any accumulation of the species undergoing reduction (O_2^-), for any pulse length.

In the particular case in which the applied voltage is less than a critical value (**Φ< Φc),** which has been found to be 1.8 V, the fitting curve for the absorbance data is a single exponential function (fig.3.3). According to our findings eq. 3.8 must be drastically simplified; so we assume that O_2^- concentration reaches a stationary state across the whole sample:

$$\frac{d[O_2^-]}{dt} = 0 \qquad (3.9)$$

$$[O_2^-] = const = a_0\Phi \qquad (3.10)$$

Eq. 3.10 has been written assuming a proportional relation, expressed through the constant a_0**,** between the amount of the reduced oxygen and the applied voltage **Φ.**

Then, eq. 3.5 can be rewritten:

$$\frac{d[V^{+\bullet}]}{dt} = -k_1([V^{+\bullet}] - [V^{++}]_0) \qquad (3.11\text{-a})$$

Where $[V^{++}]_0$ is the value of the initial concentration of V^{++} inside the film and k_1 is related to the voltage:

$$k_1 = k_v a_0 \Phi \qquad (3.11\text{-b})$$

The integration of eq. (3.11-a) leads to

$$[V^{+\bullet}](t) = [V^{++}]_0(1 - e^{-k_1 t}) \qquad (3.12)$$

Case 2: Φ >Φc

When the potential exceeds the critical value **Φc** of 1.8 V, eq. (3.12) cannot give a satisfactory fit of our experimental data (fig.3.6a,b), so we hypothesized that in our samples two regions, where different potentials and different reduction mechanisms are acting, can be identified (fig.3.7).

The applied voltage is given by the sum of the two potentials acting on regions I ($\mathbf{\Phi_I}$) and II ($\mathbf{\Phi_{II}}$).

(see Fig. 3.7)

$$\Phi = \Phi_I + \Phi_{II} \qquad (3.13)$$

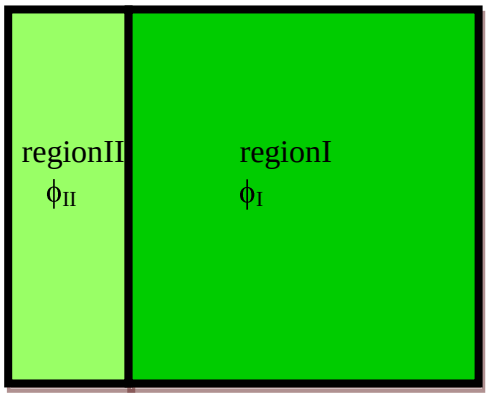

Fig. 3.7: *Subdivision of the voltage inside a device: region I (bulk) where is acting a voltage* $\mathbf{\Phi_I}$, *region II (neighbouring of the electrode) undergoes a voltage* $\mathbf{\Phi_{II}}$

Region I is the region in the bulk of the film and is characterized by a stationary concentration of O_2^-. The behaviour of the system resembles that already described as Case 1:

$$\frac{d[V_I^{+\bullet}]}{dt} = -k_1 [V_I^{++}] a_0 \Phi_I \qquad (3.14)$$

$$\text{where } k_1 = k_v a_0 \phi_I$$

$$[V_I^{+\bullet}] = [V_I^{+\bullet}]_0 (1 - e^{-k_1 t}) \qquad (3.15)$$

In region II, that is in the neighbouring of the cathode, the concentration of the reduced oxygen varies with a linear dependence in time:

$$\frac{d[D_2^-]}{dt} = const = a_2\Phi_{II} \tag{3.16}$$

Where a_2 is a constant, allowing us to rewrite eq. (3.3) as:

$$\frac{d[Y_{II}^{+\bullet}]}{dt} = k_v[Y_{II}^{++}][D_2^-] = k_v[Y_{II}^{++}]a_2\Phi_{II}t \tag{3.17}$$

Integrating eq. (3.17) and making the substitution:

$$k_2 = \frac{1}{2}k_v a_2\Phi_{II} \tag{3.18}$$

the expression that gives the concentration of the coloured species in the bulk is derived:

$$[Y_{II}^{+\bullet}] = [Y_{II}^{++}]_0(1 - e^{-k_2t^2}) \tag{3.19}$$

Then the equation that describes the kinetics of coloration is:

$$[Y_I^{+\bullet}] = [Y_I^{+\bullet}]_0(1 - e^{-k_1t}) + [Y_{II}^{++}]_0(1 - e^{-k_2t^2}) \tag{3.20}$$

3.3 Test of the model

Here we propose a test to check the consistency of our model. More precisely, we want to show that our assumptions have not only a consistency on a simply numerical basis (evidenced by the numerical fit of our data), but also on a physical point of view.

Starting from Case 1, which has been defined for **Φ** < **Φc,** and identified with one kinetic mechanism acting in the whole sample, we have found a linear equation connecting the kinetic constant k_1 and the applied voltage **Φ.** It cannot be done in the particular situation described as Case 2, characterized by an applied voltage subdivided into two contributions not determinable "a priori".

Fig. 3.8 reports ***k₁*** data presented in Table I as a function of the applied voltage.

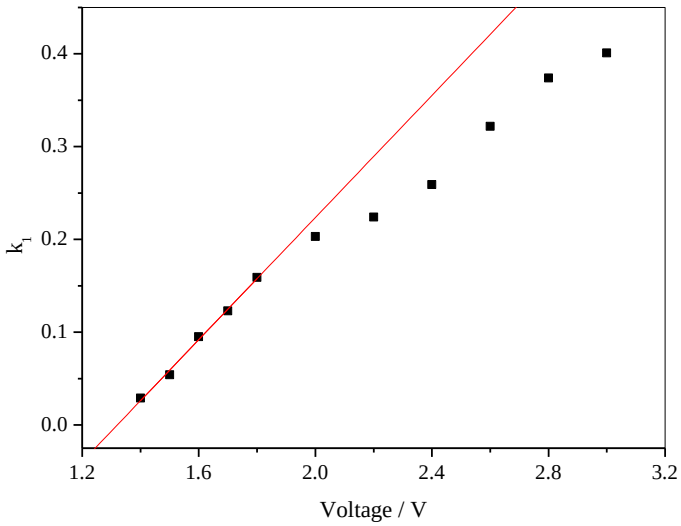

Fig. 3.8: *k_1 kinetic constant determined values as a function of the applied voltage.*

The linear fit made to these data allows us to write the equation

$$k_1 = -0.4344 + 0.329\Phi \qquad (3.21)$$

Here $\phi \leq 1.8\text{V}$

The constant -0.4344, determined by a linear fitting procedure with a % error of ± 4.6, represents a "shift term", while the angular coefficient 0.329, reminding eq. (3.11-b) and taking into account the error affecting the fitting, can be expressed as:

$$k_v a_0 = 0.329 \pm 0.013 \qquad (3.22)$$

Eq. 3.21 is still valid in Case 2 (**Φ > Φc),** but only for the bulk region, where the concentration of the reduced oxygen doesn't change in time, and where the voltage is equal to $\mathbf{\Phi_I}$

We have supposed a linear variation of the voltage across the thickness of the film. In the figure 3.9 we show the subdivision of the voltage inside a device of thickness l, d is the thickness of region I (bulk) where is acting ϕ_1 voltage. The region II (in the neighbouring of the electrode) undergoes a voltage ϕ_{II} and its thickness is Δx.

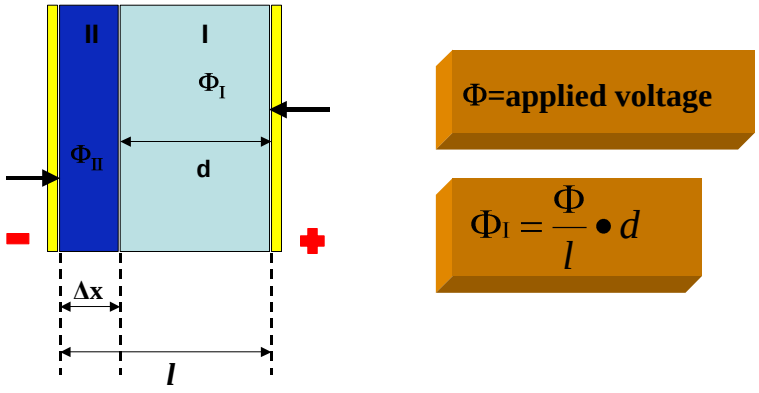

Fig. 8: *Subdivision of the voltage inside a device of thickness* ***l*****= d+Δx.** ***d*** *is the thickness of region I (bulk) where is acting a voltage* $\mathbf{\Phi_I}$ *varying across this portion of the film according to 3.23-b.. Region II (neighbouring of the electrode) undergoes a voltage* $\mathbf{\Phi_{II}}$ *related to its thickness* **Δx** *by eq. 3.23-c.*

Here:

$$l = \Delta x + d \qquad (3.23\text{-a})$$

$$\Phi_I = \Phi \cdot \frac{d}{l} \qquad (3.23\text{-b})$$

$$\Phi_{II} = \Phi \cdot \frac{\Delta x}{l} = \Phi\left(1 - \frac{d}{l}\right) \qquad (3.23\text{-c})$$

Now the equation 3.21 becomes:

$$K_1 = -0.4344 + 0.329\phi\frac{d}{l} \qquad (3.24)$$

Applying eq. (3.24) to the particular case of a sample with a thickness ***l***=90 μm subjected to an applied voltage Φ =2.4 V and taking into account the data reported in Table II, it is possible to write:

$$0.259 = -0.4344 + 0.329 \cdot 2.4 \cdot \frac{d}{l} \qquad (3.25)$$

Straightforward calculations lead to:

$$d = 79\mu m \qquad (3.26\text{-a})$$

Substituting this value in equation 3.23a we get:

$$\Delta x = 11\mu m \qquad (26\text{-b})$$

If we repeat this calculations for the other values of the applied voltages we find that the extension of the region Δx near the electrodes is strictly connected to the value of the voltage. For low values of the applied voltage the extension of the zone in which reduced oxygen is accumulated is quite restricted (Δx is ~ 3 μ, in the case of Φ =2.0 V). When the voltage is increased, the concentration of reduced oxygen gets higher values and it is possible to find this species accumulating in a zone which extends from the cathode to 11 μ inside the film. Correspondingly, the bulk of the film, where the reduced oxygen concentration keeps a constant value, reduces its extension with the voltage increase.

CHAPTER IV

Electrical characterization of electrochromic films extended

Introduction

The coloration and bleaching of large area electrochromic devices is a complex process, involving electrochemical processes at two electrodes[(1)] and voltage drops along the transparent conducting electrodes which change the device potential at each point along the device[(2-4)]. This results in different coloration voltages at each point of the device, whether the device is switched using a constant voltage or constant current waveform. If we could know the potential actually "experienced" in the different positions of the sample, we might try, when possible, to make some change to one or more parameters of the film or of the glass conductive to minimize the difference of the local potential and then the film keep a uniform coloration throughout its extension. Consequently, it is important in large devices to understand the factors in order to optimise device design and develop control strategies which will lead to optimum performance[(5)]. In the present we study the electrical characterization of our system leading to the experimental curve potential according to the position. Our research activity was then addressed to the study of an electrical model that could supply an interpretation of the inner potential curve and to build a schematic model in agreement with the experimental results. The novelty lies in the fact that the electric information was obtained using measurements of optical transmittance through the film. Indeed in literature are present many publications having the aim to describe the kinetics of the

studied systems in by analyzing the electrical information obtained from experiments of impedance spectroscopy.[6-12]

4.1 Electrical characterization

When the films are confined within large electrochromic conductive glass plates, the transition from colorless to colored state occurs with modes that strongly depend on the spatial location of the electrodes. In particular, in qualitative terms, it is noted that the staining is more intense at the edges (or small areas close to the regions where the electrodes are applied) and is attenuated as we proceed into the internal (and therefore more distant from the electrodes) areas. Moreover, the intensity of staining in any particular region of the film reaches its maximum value over time according to the kinetic laws previously studied (cap. 3). Analyzing the phenomenon from another point of view, we could say that parts of the sample with different geometric coordinates "do not feel" the same potential applied.

It's obvious that if we could know the potential actually "tested" in the different positions of the sample, we might try, when possible, to change one or more parameters of the film or of the conductive glass to minimize the differences in the local potential and then we could color the film in a more uniform way throughout its extension, with the same T_{on}.

With this goal in mind, we sought to characterize from an electrical point of view our system and to study the propagation of the color. We made two samples of different sizes, but containing the same electrochromic mixture (35% PVF, 4%EV, 2%HQ, 59%PC) and having the same thickness (90 μm). The surface of the first sample (sample A) was equal to cm1 x cm1 while that of the second (sample B) was equal to cm20 x cm1 (fig.4.1).

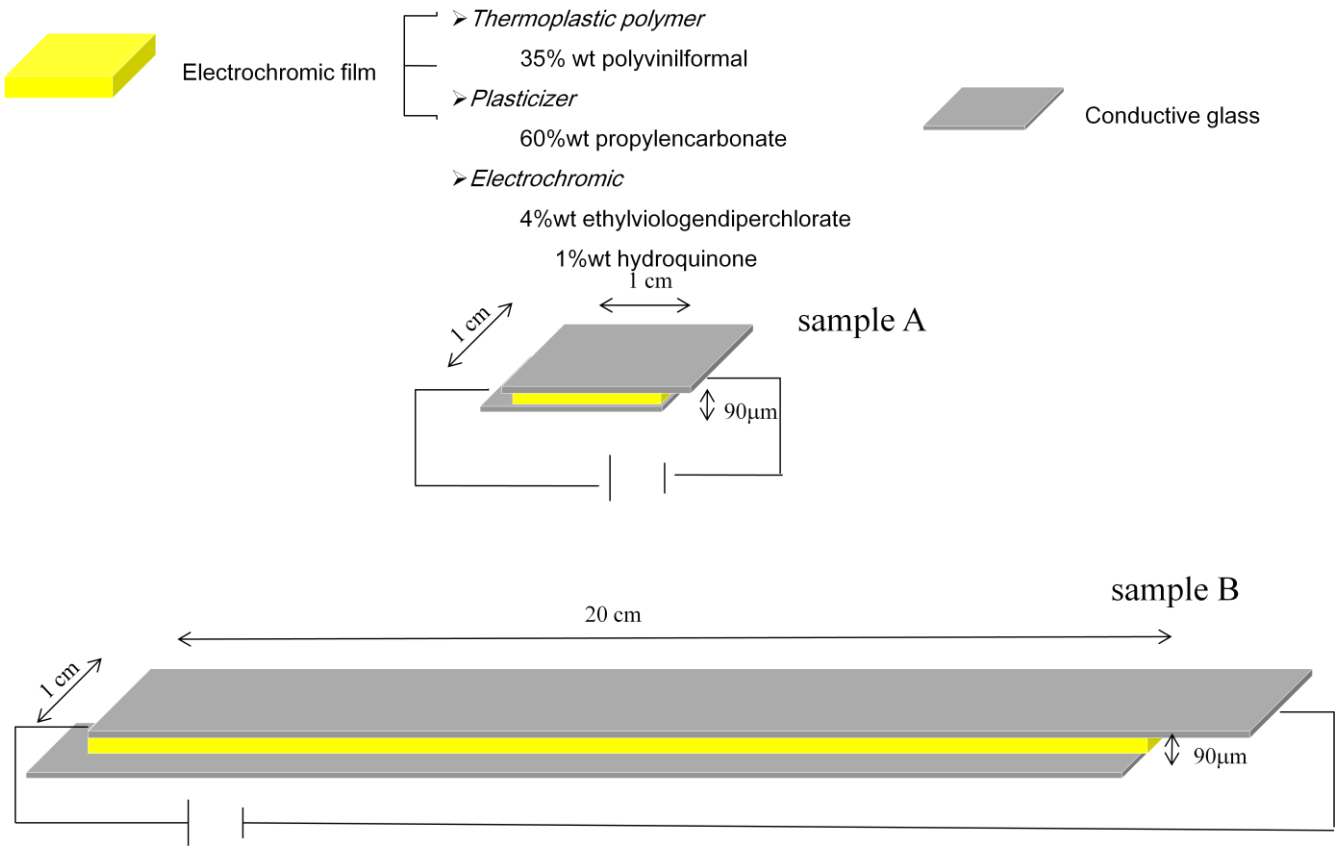

Fig.4.1: *composition of the film under objet of study and sizes of samples A and B*

It wasn't possible to make measurements of transmittance on sample B using the spectrometer, as described in chapter 2 section 2.2.3, because its dimensions were such that we couldn't place the sample inside the instrument itself, so we decided to get the optical information needed through the use of optical line following this schema:

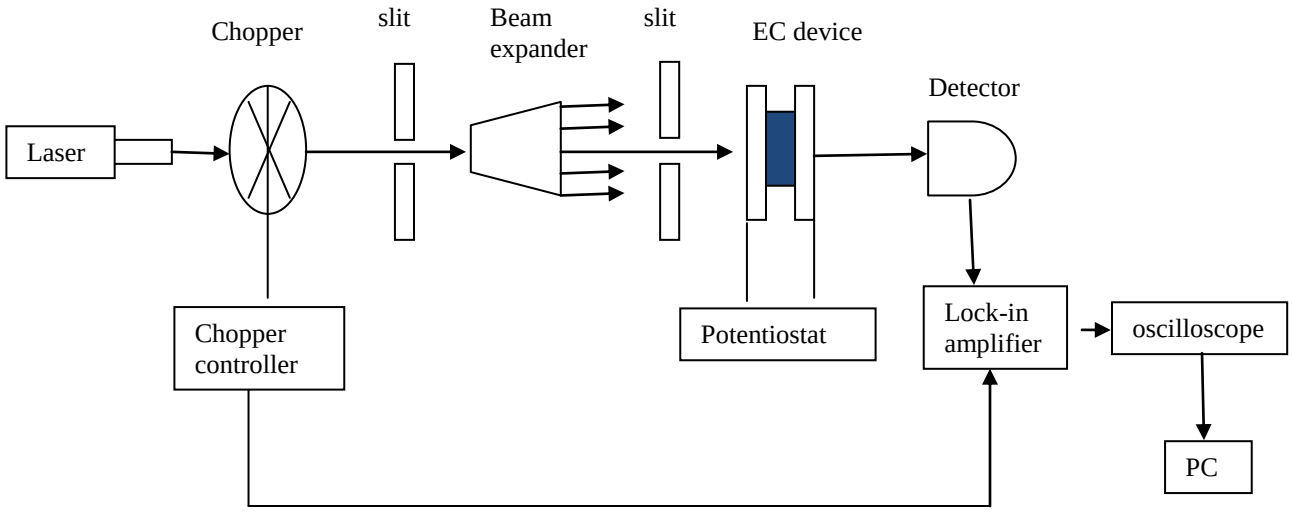

***Fig. 4.2**: schema of optical line used for measuring of trasmittance*

The beam of bright light emerging from a He-Ne laser passes through a chopper, whose rotation frequency controls the reference signal of the lock-in. The light leaving the chopper through a slit which avoids any reflections. The presence of a beam-expander, increasing the size of the beam, and a slit, reducing the size of the beam, produces a perfectly collimated beam of light, which reaches the sample on which an electric field is applied through a power generator. The sample is placed on a device that allows us to move it along the direction perpendicular to that of incidence of light, so measurements of transmittance as a function of distance from the point of application of the electric field can be made. The light leaving the sample is incident on a detector: a photodiode that collects light and converts it into an electrical signal. The signal is then directed to a lock-in amplifier, sent to a reader, digital oscilloscope, and recorded on a PC. The software for recording and processing the optical data has been made in our laboratory.

To have comparable data, both samples A and B underwent transmittance measurements through the same optical line above schematized.

All the measures of reference were made on sample A, which turns on almost uniformly.

Figure 4.3 shows the transmittance of sample A after applying voltage pulses with a duration of 5 seconds and amplitudes varying between 1.2 and 3.0 Volts.

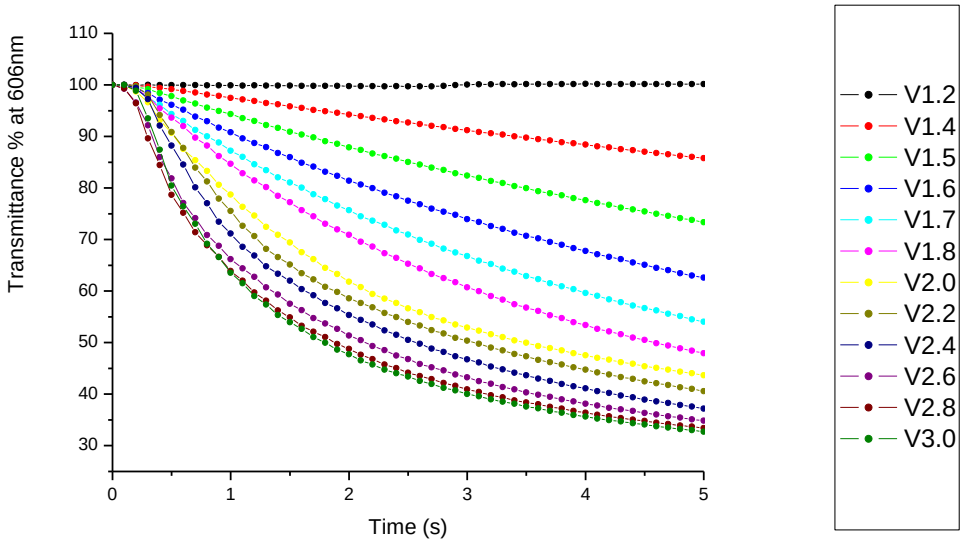

***Fig. 4.3**: EC response to different pulse voltages. Transmittance of the sample A as function of the time for pulse voltages of various amplitudes and a fixed pulse length of 5s.*

Transmittance data of sample B, to whose ends a pulse of 3 V has been applied, were recorded at various distances from the point of application of the electric voltage.

Assuming x = 0 at one end of the sample, the transmittance was recorded at positions x = 0.1 cm, 1cm, 2cm, 3cm, 4cm, 5cm, 7cm, 10cm, 11cm, 14cm, 16cm, 17cm, 18cm, 19cm. Before taking each new measurement we waited until the sample returned to the not colored state. Only the value of the transmittance recorded in the immediate vicinity of the electrode (0.1cm) was comparable with that recorded on the sample A, when the same pulse (3.0 V for 5sec) was applied.

For the other positions the values given in figure 3 were obtained. In this figure we have reported only the curves obtained from the first half sample, having verified that the other half part has a specular behavior.

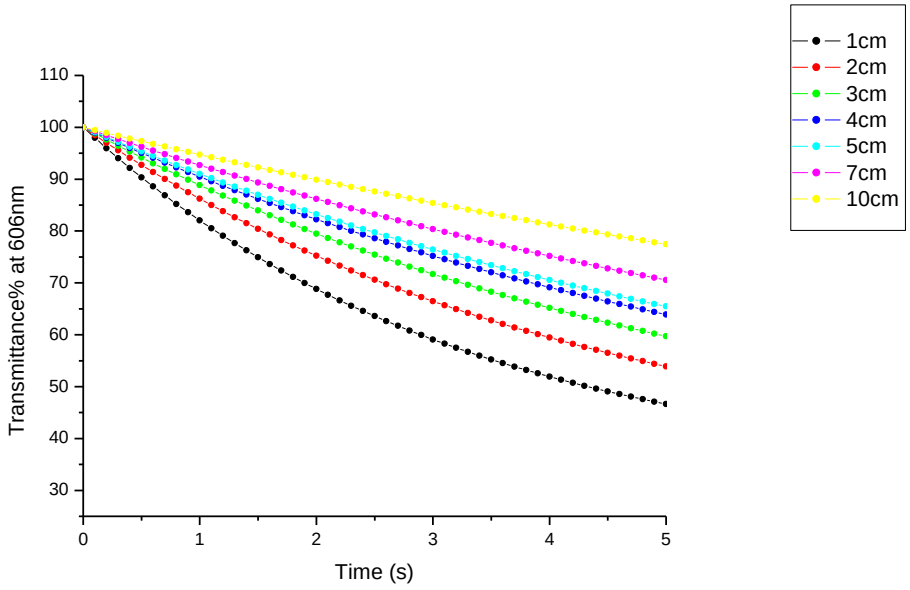

***Fig. 4.4**: EC response to different distances from the point of application of pulse voltage. Transmittance of the sample B as function of the time using voltage pulses of 3V and a fixed pulse length of 5 s.*

A comparison of the value of transmittance at the time (arbitrarily chosen) of 4 seconds, obtained for both samples, allowed us to obtain, indirectly, the potential actually experienced at the various positions of sample B. The comparison was done by overlaying each curve in Figure 4.4 (transmittance of the sample B) to the curves of Figure 4.3 (transmittance of sample A). Figure 4.4 shows the comparison between the curves of transmittance of sample A and the transmittance of sample B at 2 cm from the point of application of electric voltage.

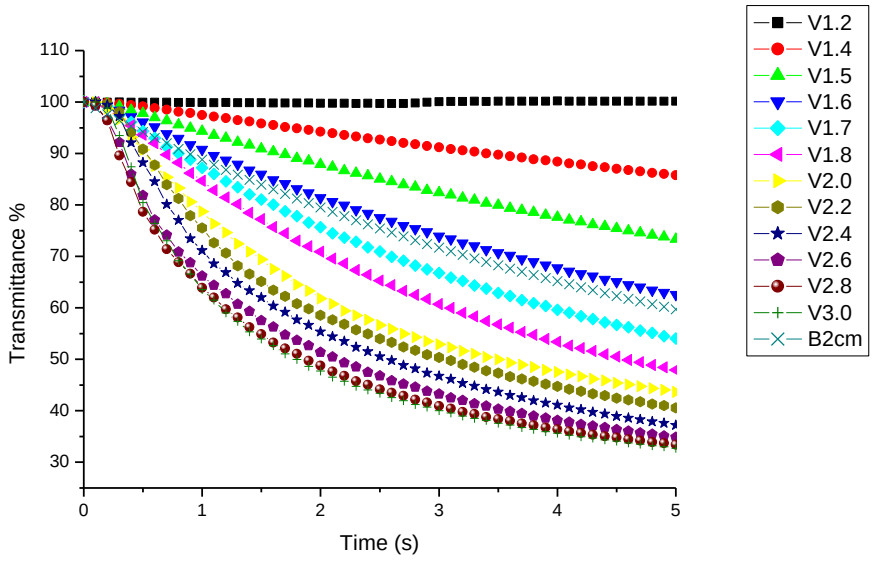

***Fig. 4.5**: Comparison of the transmittance curves of sample A and the transmittance curve of sample B (20cm) determined at 2 cm from the point of application of the electric voltage. At the ends of sample B a 5 sec long pulse of 3 V has been applied.*

Fig.4.5 shows that after 4 sec the value of the transmittance of sample B falls between the values obtained at 1.6 and 1.7 volts for sample A. A linear fit (fig. 4.6) of the latter ones allows us to determine the value of the voltage acting, after 4 sec, on the portion of sample B which is 2 cm distant from the point of application of electrical voltage.

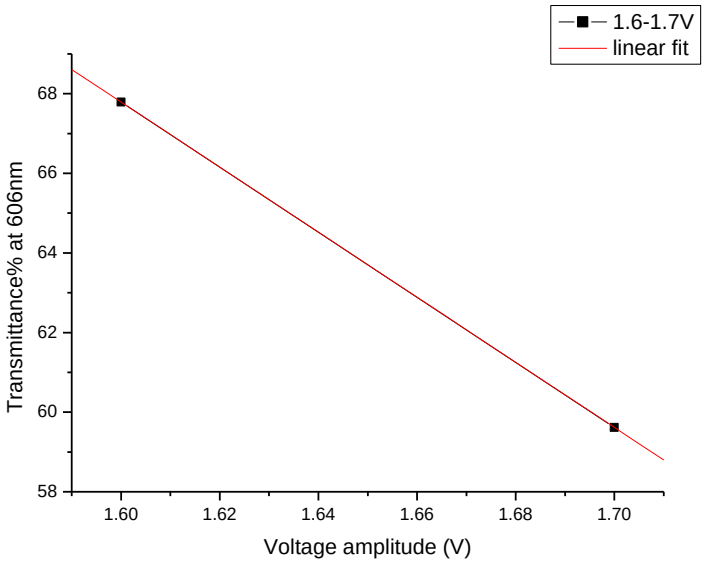

Fig. 4.6*: linear fit of the values determined 4 sec after 5 sec of application of electric field of 1.6 and 1.7 volts for 5 sec to the sample A,*

Repeating the operation of interpolation for all the curves of transmittance of sample B we have been able to provide the value of the inner potential at each position and to built, indirectly, the experimental curve of the potential along the film (Figure 4.7).

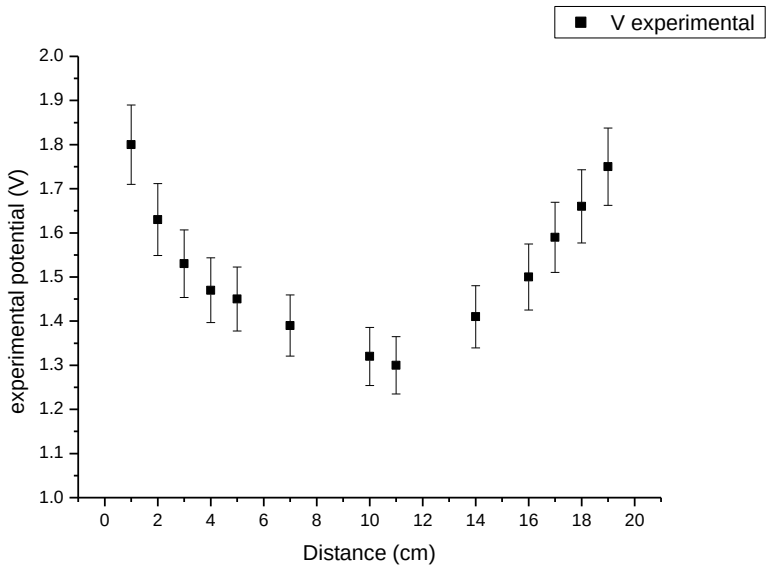

***Fig. 4.7**: Potential inside the sample B as a function of the distance from the point of application of electrical voltage*

It is important to notice that the internal potential does not exceed the value of 1.8Volt

4.2 Electric schematic model

The experimental potential curve reported in Fig. 4.7 on the one hand gives us the possibility of tuning the voltage to be applied to our system, on the other hand suggests an electric schematic model consistent with our experimental results. Since our measures were at taken at 1 cm interdistant positions, while reference cell extension was equal to 1 cm^2, it seemed useful and convenient to build a model comprising up to 20 cells, each one associated with a 1 cm^2 of film. The schema we have adopted is the following one:

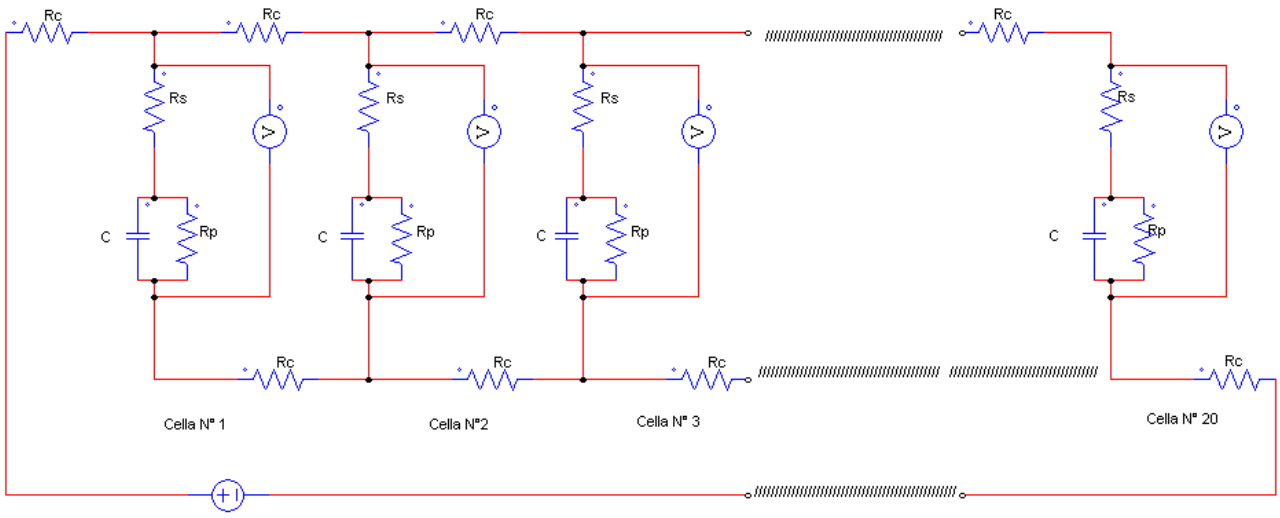

***Fig. 4.8**: Schema of 20 cells model, used for calculation the potential at different points along the extension of the large area device*

Here Rc is the resistance of the conductive glass, Rs is the impedance in the region of contact between the glass and the film, Rp is the resistance of the film while Cp is the capacity of the double layer. The study was carried out through a simulation step (commercial program. PSIM 7.1-Powersim Inc.- Simulation Softwer). Voltmeters were also placed inside each cell and a DDP of 3 V was applied for 5 seconds. In the adopted simulation program the values of the electric parameters could be varied at will and the best fit was obtained for the following values:

- Rc = 55 Ω
- Rs = 100 Ω
- Rp = 15 kΩ
- C = 50 μF

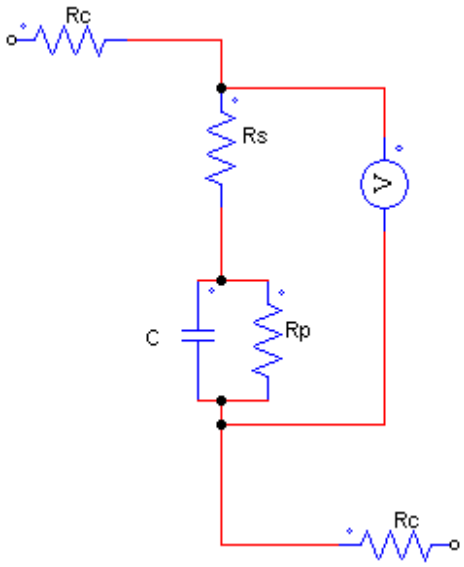

Figure 4.9 *: The elementary cell used to build the 20 cells model*

This is basically a Randles cell. Moreover Vergaz and al. [6] have shown, through impedance spectroscopy techniques, applied directly on our system, that the device acts as a cell Randles up to 1.8 V, a value in perfect agreement with the results of our fit (Fig.4.7).

With these values, the DDP calculated during the pulse at the heads of the cells numbered from 1 to 10 follow this pattern (there is also symmetry in the middle of the circuit) :

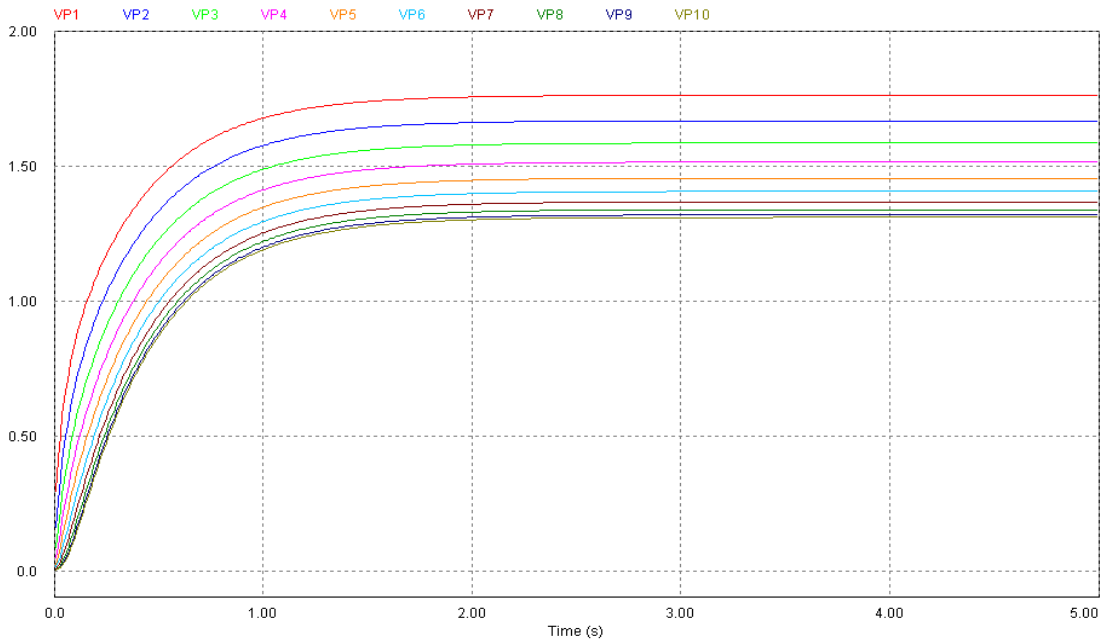

***Figure 4.10**: DDP calculated during the application of 5 sec long voltage pulses of 3 V, at the heads of the cells numbered from 1 to 10*

Figure 4.11 shows the values of equilibrium (asymptotic) of DDP at the heads of individual cells according to the sequence number of the cell. For comparison, the same figure shows the experimentally obtained data. Each cell is associated with a portion of linear dimension equal to 1 cm. And therefore the number of cells corresponds to the distance from the electrodes in cm. Thus we see that within an error of 5% of the potential curve is tested in good agreement with that produced by our model.

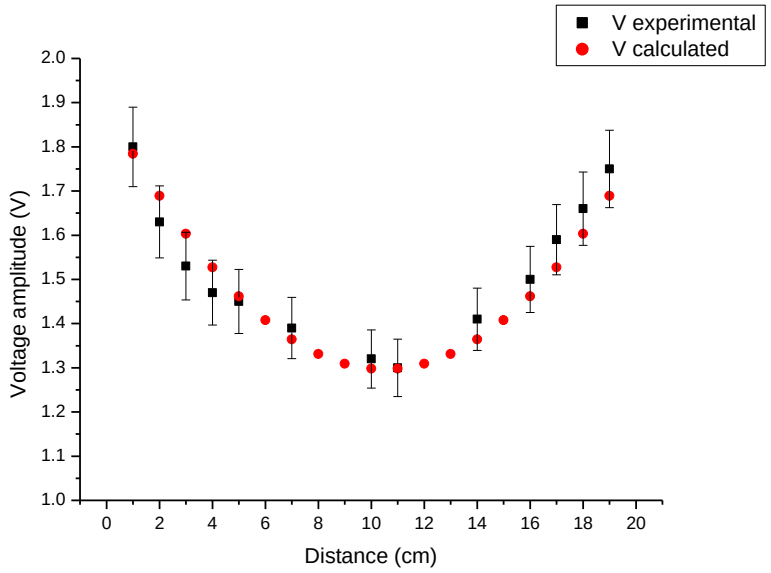

***Figure 4.11**: Comparison between the experimental (fig. 4.7) and calculated data (fig.4.10), taken 4 s after the application of a 5 s long electric pulse of 3 V.*

The comparison exhibited in Fig. 4.11 is the final confirm that an electrochromic film placed between two plates of conductive glass, a portion having a size of 1 cm x 1 cm and a thickness of 90 microns, can be treated by an electrical point of view, as the circuit represented in figure 4.9.

REFERENCES

[24] B. W. Faughnan, R. S. Crandall, i: J. I. Pankove (Ed.), topics in Applied Physics devices, Vol. 40, Springer-Verlag, New York, **1980**

[25] I.L. Skryabin , J.M.Bell, G.B. Smith "optimisation of conductivity of transparent conductor layers in electrochromic device", Paper presented at *BrisPhys'94, 11th Congress of the Australian Institute of Physics*, Brisbane, July **1994**.

[26] D.R. Macfarlane, J. Sun, M. Forsyth, J.M. Bell, L.A. Evans, I.L. Skryabin, Polymer electrolytes for electrochromic windows applications, *Solid State Ionics* 86-88, **1996,** 959-964

[27] I.L. Skryabin, J.M. Bell, G. Volgeman, "Twards a model of large area electrochromic device operation", in: Proceedings of the 3rd Symposium on Electrochromic Materials, International Electrochromic Society, 96-24, **1996**, p. 396

[28] I.L. Skryabin, J.M. Bell, in failure modes in sol-gel deposited electrochromic devices, *Solar Enargy Materials and Solar Cells* **1999**, 437-448

[29] R. Vergaz, D. Barrios, J.M. Sànchez-Pena, C. Pozo-Gonzalo, M. Salsamendi, J.A. Pomposo, impedance analysis and equivalent circuit of all-plastic viologen based electrochromic device *Displays* 29, **2008,** 401-407

[30] L. Sziràki, L. Bòbics Impedance study of electrochromism in anodic Ir oxide films 47 *Electrochimica Acta* **2002,** 2189-2197

[31] Th. Pauportè, R. Durand Impedance spectroscopy study in sputtered iridium oxide films *J. of Appl. Electrochemistry* 30, **2000,** 35-41

[32] J. Wang, J.M. Bell, I.L: Skryabin Kinetics of charge injection in sol-gel deposited WO_3 *Solar Energy Materials and Solar Cells* 56, **1999,** 465-475

[33] J. Garcia-Canadas, F. Fabregat-Santiago, J. Kapla, J. Bisquert, G. Garcia-Belmonte, I. Mora-Serò, M.O.M. Edwards "Dynamic behaviour of viologen-activated nanostructured TiO_2: correlation between kinetics of charging and coloration" *Electrochim. Acta* 49 **2004,** 745-752

[34] R. Vergaz, D. Barrios, J:M:S: Pena, C. Marcos, C. Pozo, J.A. Pomposo "Electro-optical analysis of PEDOT symmetrical electrochromic devices" *Solar Energy Materials and Solar Cells* 92, **2008**, 107-111

[35] A. Jin, W. Chen, Q. Zhu, Y. Yang, V.L. Volkov, G.S. Zakharova " Electrical and electrochemical characterization of poly(ethylene oxide)/V_2O_5 xerogel electrochromic films" *Solid State Ionics* 179, **2008,** 1256-1262

CONCLUSION

In the first part of this research the characterization of the electrooptical properties of a new kind of solid electrochromic film was performed. This film is obtainable by simply doping preformed solid thermoplastic polymers with electrochromic molecules and plasticizers. Some innovations in the preparation process and in properties make this film particularly suitable for the production of large-area devices. The effect of the concentration of the different components and the effect of the thickness of the cell on the absorption properties of the ECD under object of study was studied in order to explore and to optimize the electrochromic parameters.

Colouration/decolouration processes were complicated by the presence of a second redox step.

The graphs where the transmittance values obtained at 5 sec long voltage pulses of various amplitudes, show that the second reduction of viologen becomes important for lower values of the cell thickness, when the applied voltage pulse exceeds 1.8 V. Even if this value of pulse amplitude is applied for a time longer than 5 sec, transmittance data show that the second reduction of viologen doesn't occur, so colored neutral viologen is not formed. This behavior is not dependent on the hardness, that is the content of polymer, of the EC film.

The intensity of coloration reached by our device is expressed by the contrast ratio CR. The values of this parameter are high enough to allow the naked eye perception of the color changes occurring when the voltage is applied. We have obtained CR values that decrease when the hardness of the film is increased, at a fixed thickness of the cell, and increase when the thickness is increased, for a fixed value of hardness. For the harder devices (content of PVF equal to 45-

50%) it has been noticed a critical reduction of CR ratio, with values that don't exhibit a sensible variation when the thickness is changed.

Another important parameter that we have studied to better understand and characterize the operating functions of our ECD is the response time to the application and the switching off of an electric field (T_{on}, T_{off}). We have calculated both T_{on} and T_{off} at various voltage pulse amplitudes and for various cell thicknesses. Experimental data show that while T_{on} doesn't depend on the thickness of the EC film and on its hardness, T_{off} increases for more rigid and more thick films.

In the second part of this thesis the kinetic and the electric model which allowed us to interpret the experimental data are presented.

The model for the kinetic mechanism underlying the colouration process of a laminable electrochromic film, has been built up under the assumption that only the first step of the viologen reduction, producing the radical cation $V^{+\cdot}$, occurs. This condition is experimentally fulfilled for pulse lengths less than 5 sec and voltage pulse amplitudes lower than 2.6V. The solutions of the kinetic equations have been given in terms of a single exponential function in the bulk of the film at any voltage pulse amplitude. In the environment of the cathode a quadratic exponential term has had to be added for voltage pulse amplitudes equal or higher than 2.0V. These solutions have been found considering the important role of oxygen molecule as an intermediate agent for the electronic exchanges between the cathode and the viologen electrochromic species. Constant concentration of O_2^- across the whole sample accomplishes the single exponential behaviour at voltages lower than 2.0 V. For higher voltages O_2^- accumulates in the neighbouring of cathode with a concentration directly proportional to the duration of the pulse, and leading to a quadratic exponential contribution to the kinetic mechanism. Moreover it has been possible to measure the extension of the zone where the O_2^-

species accumulates at high voltages, analysing the colouration of a sample with a thickness ***l***=90 μ. It has been found to vary from 3 to 11 μ.

To find out under what restrictions, if any, our ECD device can be suitable for applications which require the employment of large electrochromic surfaces, a large EC device was studied by an electrical point of view from measurements of optical transmittance. A comparison of the transmittance measures of a small size sample (sample A: 1cm * 1cm) with those of the large size sample (sample B: 20cm * 1cm), but composed of the same EC mixture and having the same thickness, allowed us to obtain the trend of potential as a function of distance from the point of application of the same potential. By comparing these values with those obtained by a simulation process, in which the EC device was regarded as an electric circuit consisting of several elementary cells, they are found in agreement within an error of 5% . The elementary cell is a Randles circuit which has to be added to the resistance of the conductive glass. The studies by Vergaz et al. on our EC film support our conclusions. They confirm that our device behave as a Randles circuit up to voltages near 1.8V. Our experimental data show that the inner potential doesn't exceed the value of 1.8 Volt. The simulation process has provided a value of resistance of the conductive glass (Rc) of the same order of magnitude as the experimental one, certified by the manufacturer. The difference between the two values could be due to impurities that may be present or on the conductive glass, used for the construction of the device, or within the components of the EC mixture. These results can be used as inputs in future simulations of the operation of these devices in order to optimize the pulsed voltage signals that could enhance the uniformity of coloration as well as reduce the power consumption.

After all, what comes out from the kinetic and electric models adopted to interpret the experimental data, is that a critical value of the electric potential exists. When the applied voltage pulse amplitude exceeds this value, the operational functions of our ECD change. This value is

1.8 V and coincides with the value of the potential at which the second reduction of viologen starts to become important. From a kinetic point of view, when this value is exceeded an accumulation of oxygen in the neighbouring of the electrodes occurs. From an electrical point of view 1.8 V is the inner voltage (value of the potential inside the film) that doesn't have to be exceeded to allow the large area device to be represented as a circuit whose elementary cell is a Randless circuit.